

DEPARTAMENT OF  
CHEMISTRY

Tiago Martins Rodrigues  
BSc in Biotechnology

Ionic liquids assisted direct transesterification  
of microalgae for biodiesel production





# Ionic liquids assisted direct transesterification of microalgae for biodiesel production

**Tiago Martins Rodrigues**

BSc in Biotechnology

**Adviser:** Doctor Márcia Ventura

*Researcher, Chemistry Department, NOVA School of Science and Technology*

**Co-advisers:** Doctor Inês Matos

*Researcher, Chemistry Department, NOVA School of Science and Technology*

**Examination Committee:**

**Chair:** Professor Sofia Rocha Pauleta

**Rapporteurs:** Doctor Patrícia Reis

**Adviser:** Doctor Márcia Ventura



## **Ionic liquids assisted direct transesterification of microalgae for biodiesel production**

Copyright © Tiago Martins Rodrigues, NOVA School of Science and Technology, NOVA University Lisbon.

The NOVA School of Science and Technology and the NOVA University Lisbon have the right, perpetual and without geographical boundaries, to file and publish this dissertation through printed copies reproduced on paper or on digital form, or by any other means known or that may be invented, and to disseminate through scientific repositories and admit its copying and distribution for non-commercial, educational or research purposes, as long as credit is given to the author and editor.







## ACKNOWLEDGMENTS

I would like to express my deepest gratitude to all the people who contributed to the completion of this dissertation.

Firstly, I would like to thank my family for giving me the opportunity to complete this thesis. My family has been an important pillar in this journey as they have given me all their love, motivation and understanding to get through this challenging time.

Next, I would like to thank my supervisors Dr. Márcia Ventura and Dr. Inês Matos for their wise guidance, constant availability and encouragement throughout this process.

I would also like to express my gratitude to my laboratory and course colleagues, whose discussions and collaborations have enriched my academic experience and contributed to the progress of this project. In this regard, I would like to thank my colleague Daniela Agostinho and Dr. Zeljko Petrovski for their help.

I would additionally like to thank my girlfriend for her emotional support and kindness. Her presence and encouragement were a great comfort to me, and I am grateful to have her by my side.

The realization of this dissertation would not have been possible without the help and support of all these special people, and for this I express my most sincere thanks to them all. Each one has contributed in a unique way to my professional and emotional growth.







## ABSTRACT

The growing global demand for sustainable energy sources, coupled with the negative environmental impacts caused by the use of fossil fuels, has driven the development of renewable alternatives such as biodiesel. Biodiesel, produced from biological materials such as vegetable oils, animal fats and, more recently, microalgae, stands out as a promising solution for reducing dependence on fossil fuels and mitigating climate change. Microalgae, in particular, are seen as a highly efficient source due to their rapid growth, high lipid content, and ability to be cultivated in diverse environments without competing with agricultural areas destined for food production. This dissertation investigates the feasibility of producing biodiesel from microalgae through an integrated process of extraction and direct transesterification, assisted by ionic liquids. The main objective was to develop and characterize a di-anionic ionic liquid (DAIL), derived from sulfosuccinic acid, capable of simultaneously optimizing lipid extraction and the transesterification reaction, promoting the production of methyl esters (biodiesel) more efficiently. The performance of this ionic liquid was compared with that of traditional catalysts such as sulfuric acid ( $H_2SO_4$ ) and sodium hydroxide (NaOH), as well as with a commercial ionic liquid (1-ethyl-3-methylimidazolium ethylsulfate).

The experimental tests demonstrated that DAIL outperformed the commercial ionic liquid in the esterification of benzoic acid to methyl benzoate. Introducing a microwave pre-treatment to the algae enhanced the extraction yield but did not significantly improve the yield of FAMES. Slight differences in the FAME's profile were observed between the samples with and without pre-treatment. Further studies are needed to assess the potential of the proposed ionic liquid and its combination with microwave pre-treatment, particularly in addressing limitations of conventional biodiesel production methods, especially concerning process efficiency and sustainability.

**Keywords:** biodiesel, microalgae, ionic liquid, transesterification; one-pot reaction



## RESUMO

A crescente procura global de fontes de energia sustentáveis, associada aos impactos ambientais negativos causados pela utilização de combustíveis fósseis, tem impulsionado o desenvolvimento de alternativas renováveis como o biodiesel. O biodiesel, produzido a partir de materiais biológicos como óleos vegetais, gorduras animais e, mais recentemente, microalgas, destaca-se como uma solução promissora para reduzir a dependência dos combustíveis fósseis e mitigar as alterações climáticas.

As microalgas, em particular, são vistas como uma fonte altamente eficiente devido ao seu rápido crescimento, alto teor de lípidos e capacidade de serem cultivadas em diversos ambientes sem competir com áreas agrícolas destinadas à produção de alimentos. Esta dissertação investiga a viabilidade da produção de biodiesel a partir de microalgas através de um processo integrado de extração e transesterificação direta, assistido por líquidos iónicos. O principal objetivo foi desenvolver e caracterizar um líquido iónico di-aniónico (DAIL), derivado do ácido sulfosuccínico, capaz de otimizar simultaneamente a extração de lípidos e a reação de transesterificação, promovendo a produção de ésteres metílicos (biodiesel) de forma mais eficiente. O desempenho deste líquido iónico foi comparado com o de catalisadores tradicionais como o ácido sulfúrico ( $H_2SO_4$ ) e o hidróxido de sódio (NaOH), bem como com um líquido iónico comercial (etilsulfato de 1-etil-3-metilimidazólio).

Os testes experimentais demonstraram que o DAIL superou o líquido iónico comercial na esterificação do ácido benzoico em benzoato de metilo. A introdução de um pré-tratamento por micro-ondas nas algas aumentou o rendimento da extração, mas não melhorou significativamente o rendimento dos FAMES. Foram observadas ligeiras diferenças no perfil do FAME entre as amostras com e sem pré-tratamento. São necessários mais estudos para avaliar o potencial do líquido iónico proposto e a sua combinação com o pré-tratamento por micro-ondas, em

particular para resolver as limitações dos métodos convencionais de produção de biodiesel, especialmente no que diz respeito à eficiência e sustentabilidade do processo.

**Palavas chave:** biodiesel, microalga, líquido iónico, transesterificação

# INDEX

<b>1. INTRODUCTION.....</b>	<b>1</b>
1.1 Biodiesel.....	1
1.1.1 Biodiesel composition.....	2
1.2 Third generation of biodiesel.....	4
1.2.2 Pre-treatments for lipid extraction on algae.....	7
1.2.3 Transesterification reaction.....	9
1.2.4 Biodiesel purification.....	13
1.3 Ionic Liquids.....	14
1.3.2 Synthesis of Ionic liquids .....	16
1.3.3 Ionic liquids in pre-treatment.....	17
1.3.4 Ionic liquids in extraction .....	18
1.3.5 Ionic liquids in catalysis.....	20
1.3.5.1. Using Ionic Liquids as catalysts on transesterification reaction .....	21
1.3.6 One-pot transesterification reaction.....	24
<b>2. MATERIALS AND METHODS.....</b>	<b>27</b>
2.1 List of materials .....	27
2.2 Synthesis of the Dianionic Ionic Liquid (DAIL).....	28
2.2.1 Synthesis of the ionic liquid precursor .....	28
2.2.2 Synthesis of DAIL.....	28
2.2.3 Differential Scanning Calorimetry .....	31

2.2.4	Silver nitrate test.....	31
2.2.5	Nuclear magnetic resonance .....	31
2.2.6	FTIR-ATR .....	32
2.3	EMIM ETSO <sub>4</sub> Ionic Liquid .....	32
2.3.1	Nuclear Magnetic Resonance of EMIM ETSO <sub>4</sub> .....	33
2.4	GC-FID Analysis.....	33
2.5	Direct transesterification Assays .....	34
2.5.1	Testing the integrated catalysis and FAME's extraction process.....	35
2.6	Calculating the concentration of FAMEs .....	42
<b>3.</b>	<b>RESULTS AND DISCUSSION.....</b>	<b>47</b>
3.1	Characterization of the synthesized ionic liquid.....	47
3.1.1	Nuclear Magnetic Resonance of IL precursor.....	47
3.1.2	Nuclear Magnetic Resonance of DAIL.....	49
3.1.3	FTIR of DAIL .....	50
3.1.4	DSC of DAIL.....	52
3.2	Nuclear Magnetic Resonance of EMIM ETSO <sub>4</sub> .....	53
3.3	Optimization of one-pot reaction conditions.....	54
3.4	Extract's yield for samples without and with pre-treatment.....	56
<b>4.</b>	<b>CONCLUSION .....</b>	<b>63</b>
<b>5.</b>	<b>REFERENCES .....</b>	<b>64</b>
<b>6.</b>	<b>ANEXES.....</b>	<b>68</b>

## LIST OF FIGURES

Figure 1 - Different generations of biodiesel.....	2
Figure 2 - Third/fourth generation of biodiesel. ....	5
Figure 3- Transesterification reaction process. ....	9
Figure 4 - Intermediate step In transesterification .....	10
Figure 5-Chemical reaction of precursor [N <sub>4</sub> 1 2OH 2OH]Cl synthesis.....	28
Figure 6 - Structure of DAIL.....	29
Figure 7 - Chemical formula of N-Methyldiethanolamine (MDEA).....	29
Figure 8 - Chemical formula of 1-Chlorobutane. ....	30
Figure 9 - Chemical formula of sulfosuccinic acid. ....	31
Figure 10- Chemical formula of 1-Ethyl-3-Methylimidazolium Ethylsulphate [EMIM][ESO <sub>4</sub> ]. ...	33
Figure 11- Diagram of the main steps from the reaction to GC analysis.....	34
Figure 12 - Diagram of all the steps from pre-treatment to GC analysis.....	35
Figure 13 -Diagram of the transesterification reaction.....	36
Figure 14 - Diagram of the FAMEs extraction process with hexane. ....	37
Figure 15- Diagram of the transesterification reaction with benzoic acid, microalgae, catalyst, methanol and C14.....	39
Figure 16 - <sup>13</sup> H NMR spectrum of IL precursor. ....	48
Figure 17- <sup>13</sup> C NMR spectrum of IL precursor.....	48
Figure 18 - <sup>1</sup> H NMR spectrum of DAIL. ....	49
Figure 19 - <sup>13</sup> C NMR spectrum of DAIL.....	50
Figure 20- FTIR of sample DAIL.....	51
Figure 21- Termogram of the second heating cycle of the Ionic liquid DAIL. ....	52
Figure 22 - <sup>1</sup> H NMR spectrum of the Ionic liquid EMIM ETSO <sub>4</sub> . ....	53
Figure 23 - <sup>13</sup> C NMR spectrum of EMIM ETSO <sub>4</sub> . ....	54

Figure 24- FAMES' profile for samples without (above) and with (below) pre-treatment.....	58
Figure 25 - $^{13}\text{C}$ APT of IL precursor.....	68
Figure 26 - $^1\text{H}$ $^{13}\text{C}$ HSQC of IL precursor.....	69
Figure 27 - $^{13}\text{C}$ APT of DAIL.....	69
Figure 28- $^1\text{H}$ $^{13}\text{C}$ HSQC of DAIL.....	70
Figure 29 - $^1\text{H}$ $^{13}\text{C}$ HSQC of EMIM.....	71

## LIST OF TABLES

Table 1 - Activation energy and rate constants at 50°C a methanol to oil ratio of 6:1, and catalysis with sodium hydroxide .....	10
Table 2 - This table contains the most used Ionic liquids in transesterification reaction, their name, formula and key properties.....	23
Table 3 - It describes the different conditions used to optimise the reagents (without algae). .....	38
Table 4- Table with the names of each sample, their description and some important observations.. .....	40
Table 5- Table with the names of each sample, their description and some important observations.. .....	42
Table 6- Concentration of methyl benzoate obtained by transesterification of benzoic acid within each sample and the yield related to the initial benzoic acid mass.....	55
Table 7 - Mass extract and its respective percentage for samples B1 to B8. ....	56
Table 8 - Range of FAMES' concentrations (mg ester/g of extrate) for algae Chlorella found in literature.....	57
Table 9. Total determined FAMES content in the different samples.....	59
Table 10- FAMES concentration in mg of FAMES per g of extracted lipid and per g of algae)	61

## ACRONYMS

<b>DAIL</b>	Dianionic Ionic liquid
<b>MW</b>	Microwave
<b>IL</b>	Ionic liquid
<b>GC-FID</b>	Gas Chromatography - Flame Ionization Detector
<b>MDEA</b>	N-Methyldiethanolamine
<b>EMIM ETSO<sub>4</sub></b>	1-Ethyl-3-Methylimidazolium Ethylsulphate
<b>NMR</b>	Nuclear Magnetic Resonance
<b>FTIR ATR</b>	Fourier transform infrared - Attenuated total reflectance
<b>MB</b>	Methyl benzoate
<b>Y</b>	Yield
<b>FAME</b>	Fatty Acid Methyl Esters
<b>HPLC</b>	High-performance liquid chromatography



# 1.

# INTRODUCTION

## 1.1 Biodiesel

Over the years, energy demand has significantly increased alongside the global population. As a result, it has become essential to look for renewable "green energy" alternatives. One of these alternatives is the use of biodiesel instead of fossil fuels. Biodiesel is a renewable fuel produced from biological sources such as vegetable oils, animal fats, and recycled cooking grease. It primarily consists of fatty acid methyl esters (FAME), which are derived from the transesterification of oils and fats. This chemical process involves triglycerides found in oils or fats reacting with an alcohol, usually methanol, in the presence of a catalyst, producing biodiesel (methyl esters) and glycerol as a byproduct (Sharma, 2020; Atabani et al., 2012).

Biodiesel can be classified into four different generations as shown in figure 1. The first generation is based on biomass of first generation such as corn and other food crops, emitting fewer dangerous gases into the environment and being relatively cheap and simple to produce (Khan et al., 2019). However, its production was insufficient to meet demand, and it used food resources, leading to shortages and an increased ecological footprint. The second generation uses food waste as raw material, which has the primary advantage of utilizing waste products (Khan et al., 2019). Nevertheless, pre-processing food waste is highly expensive and requires advanced technology to convert biomass into biodiesel. The third generation, based on algae, has the advantage of being easy to grow without competing with food resources (Lam & Lee, 2012; Singh & Gu, 2010). However, algae have a low lipid content, require substantial resources for cultivation and the optimization of extraction methods. The fourth generation utilizes chemical processes, offering high performance and a greater capacity to eliminate carbon

dioxide (Khan et al., 2019). The disadvantages include the high cost of bioreactors and the need for significant investment in advanced technology research.

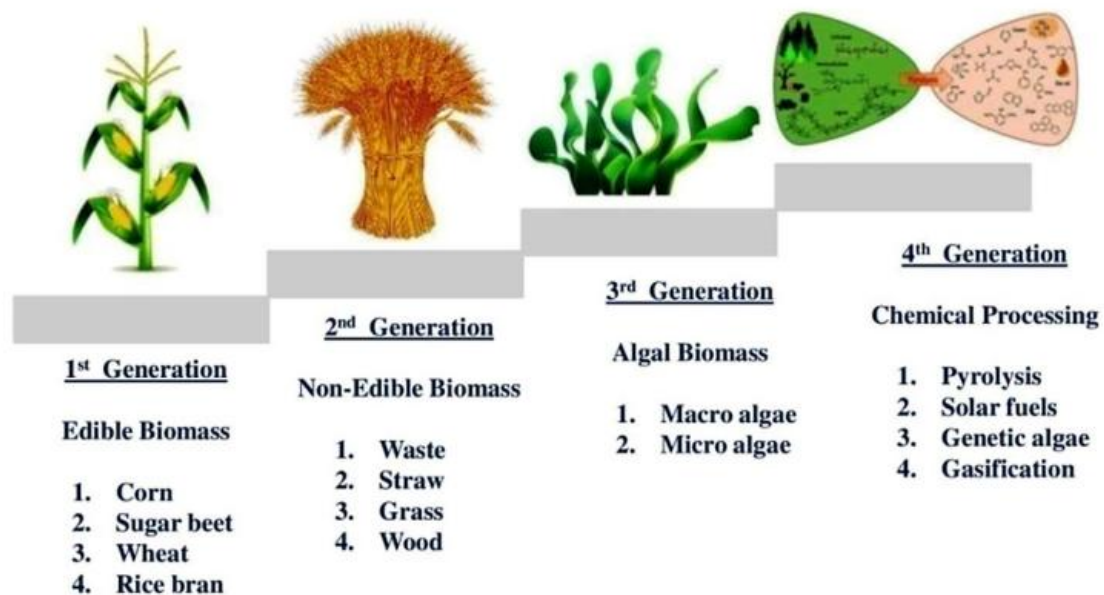


Figure 1 - Different generations of biodiesel. (Khan et al., 2019).

### 1.1.1 Biodiesel composition

The composition of biodiesel esters can vary depending on the feedstock used and the specific transesterification process. Methyl esters are the most common type of fatty acid alkyl esters in biodiesel (Knothe, 2010; Sharma et al., 2014). They are produced by reacting triglycerides with methanol in the transesterification process. Common methyl esters found in biodiesel include:

- Methyl palmitate (C16:0)
- Methyl stearate (C18:0)
- Methyl oleate (C18:1)
- Methyl linoleate (C18:2)
- Methyl linolenate (C18:3)
- Methyl arachidate (C20:0)

### 1.1.1.1 Characteristics of Biodiesel

Biodiesel has emerged as a promising alternative to conventional fossil fuels due to its renewable nature and potential to reduce greenhouse gas emissions. However, to ensure its suitability as a replacement for petroleum diesel, biodiesel must meet several critical quality criteria.

One of the most important parameters is viscosity, which affects the fuel's ability to atomize properly during injection into the combustion chamber. Proper viscosity ensures efficient combustion and minimizes the formation of engine deposits (Moser, 2009). Biodiesel typically has a higher viscosity than conventional diesel, which can pose challenges, especially in colder climates, where fuel flow properties become critical.

Another key characteristic is the cetane number (CN), which measures the fuel's ignition quality. A higher cetane number indicates shorter ignition delays, leading to more efficient combustion and lower emissions of hydrocarbons and carbon monoxide. Biodiesel generally has a higher cetane number than petroleum diesel due to its chemical structure, which enhances its combustion properties (Van Gerpen, 2005).

The water content in biodiesel must be kept to a minimum. Excessive water can lead to microbial growth, promote corrosion in the fuel system, and negatively impact the combustion process. Thus, maintaining a low water content is crucial for the long-term stability and performance of biodiesel (Knothe, 2001).

Oxidative stability is another vital factor, as biodiesel is prone to oxidation due to the presence of unsaturated fatty acids. Oxidation can lead to the formation of acids and sediments, which can clog filters and injectors. Antioxidants are often added to biodiesel to enhance its oxidative stability and extend its shelf life (Ramos et al., 2009).

The acid number is an indicator of the free fatty acids present in the biodiesel. A high acid number can lead to increased corrosion of engine components. Therefore, controlling the acid number is essential to ensure the longevity of engines using biodiesel (Oklahoma State University et al., 2020).

Another crucial quality parameter is the glycerol content. Both free and total glycerol must be minimized to avoid the formation of deposits within the fuel system. High levels of glycerol can cause problems such as injector fouling and poor combustion (Moser, 2009). The cloud point and pour point are critical for biodiesel's performance in colder temperatures. The cloud point is the temperature at which wax crystals begin to form, while the pour point is the lowest temperature at which the fuel can still flow. Biodiesel's performance in cold weather can be

enhanced by blending it with winterized diesel or by using additives that lower the cloud and pour points (Van Gerpen, 2005).

The calorific value of biodiesel, which measures the energy content of the fuel, is slightly lower than that of petroleum diesel. This means that more biodiesel is required to produce the same amount of energy, which can affect fuel economy (Knothe, 2001).

Finally, emissions are a significant consideration. Biodiesel combustion typically results in lower emissions of carbon dioxide (CO<sub>2</sub>), particulate matter (PM), and unburned hydrocarbons (HC) compared to conventional diesel. However, it may result in higher emissions of nitrogen oxides (NO<sub>x</sub>), which is a challenge that requires ongoing research and optimization of engine settings (Ramos et al., 2009).

## 1.2 Third generation of biodiesel

The third generation of biodiesel, as shown in figure 2, based on microalgae/macroalgae, has been immensely significant, and research into its possibilities continues to this day. Unlike the first generations, which relied on food crops like soybean or rapeseed, this newer generation focuses on non-food sources like algae. This shift reduces competition with food production, addressing concerns about food security and land use change (Lam & Lee, 2012; Singh & Gu, 2010; Milledge & Heaven, 2014). Biodiesel production starts with cultivating algae biomass. Algae are fast-growing marine organisms that can be grown in dedicated facilities. Next comes

oil extraction, where the oil is separated from the algae using techniques like mechanical pressing or solvent extraction (Lam & Lee, 2012; Milledge & Heaven, 2014).

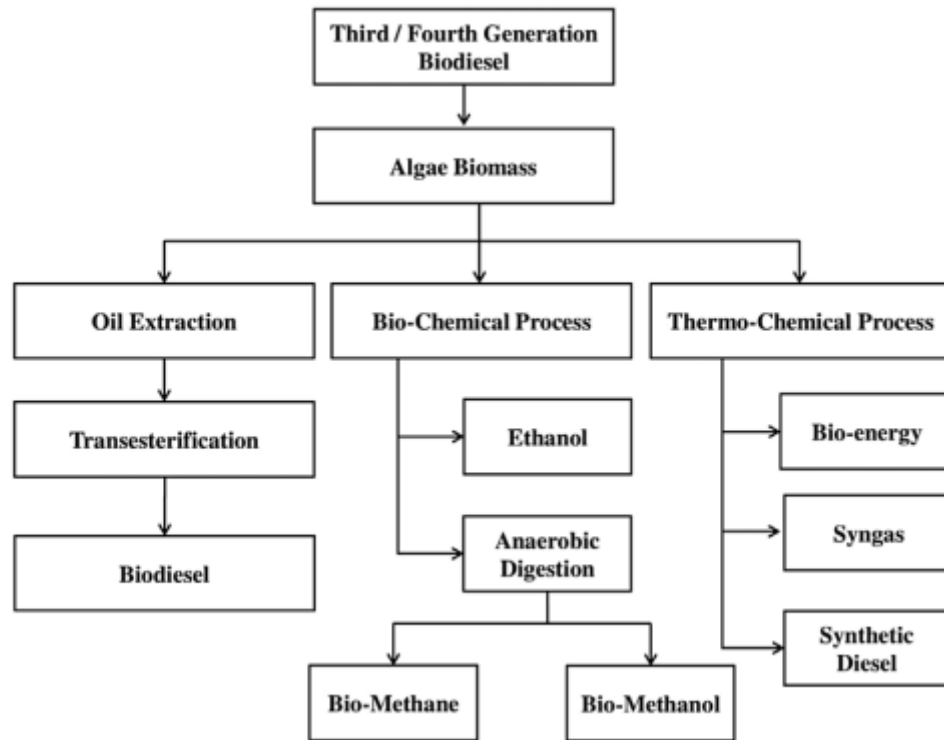


Figure 2 - Third/fourth generation of biodiesel. (Lam & Lee, 2012; Milledge & Heaven, 2014).

Microalgae, among the oldest living organisms, thrive primarily in water. They can be autotrophic, utilizing inorganic compounds for carbon, or heterotrophic, relying on organic compounds. Autotrophic microalgae can further be categorized into photoautotrophic, using light as an energy source, or chemoautotrophic, deriving energy from oxidizing organic compounds. Their simplicity of cell structure compared to plants enhances photosynthesis yield, while their marine habitat provides easy access to nutrients, CO<sub>2</sub>, and other compounds (Hannon et al., 2010; Borowitzka, 2018).

*Chlorella vulgaris*, a common microalgae, is widely researched for its potential applications. It's a green-pigmented eukaryotic microalga found in freshwater, easily cultivated in photoreactors requiring only water, carbon dioxide, light, and minimal minerals. This algae is rich in protein (43-58% of dry weight) and lipids (5-58% of dry weight, potentially higher under certain conditions) (Rumin et al., 2020; Borowitzka, 2018). Producing biodiesel from microalgae involves growing, harvesting, and drying them into a powder. Subsequent steps include cell disruption, oil extraction, and chemical transesterification. Cell disruption methods include

high-pressure homogenizers, autoclaving, and acid/base treatments, while lipid extraction methods involve solvent-based techniques like liquid-liquid extraction, often using hexane due to its efficiency (Hannon et al., 2010; Rumin et al., 2020).

Microalgae and certain microorganisms offer higher oil yields per unit of land compared to traditional oilseed crops, owing to their rapid growth and oil accumulation capacity. Biodiesel from third-generation feedstocks exhibits superior fuel properties, including higher cetane numbers, lower viscosity, and improved oxidative stability, leading to better engine performance, reduced emissions, and compatibility with existing infrastructure. Additionally, third-generation processes can yield valuable co-products such as protein-rich biomass, biofertilizers, and bioplastics, enhancing economic viability and sustainability. While the rapid growth of microalgae can reduce lipid content, ongoing research aims to optimize growth conditions and lipid content through cultivation techniques, genetic engineering, and extraction methods, thereby improving overall efficiency and scalability (Hannon et al., 2010; Rumin et al., 2020; Borowitzka, 2018).

#### **1.2.1.1 Microalgae Chlorella**

Chlorella is a genus of unicellular green algae belonging to the class Chlorophyceae. Known for its high growth rate and adaptability to various aquatic environments, Chlorella cells are spherical, about 2 to 10 micrometers in diameter, and have a vivid green color due to their chlorophyll content (Mata, Martins & Caetano, 2010).

The lipid composition of Chlorella is a critical factor in its viability as a biodiesel source. The main types of lipids found in Chlorella include triglycerides, which are the primary type of lipid used in biodiesel production, consisting of three fatty acid chains attached to a glycerol backbone; phospholipids, which are important components of cell membranes though not directly used in biodiesel; and glycolipids, which play a role in cell structure and function (Chisti, 2007).

The fatty acid profile of Chlorella significantly influences the quality and properties of the resulting biodiesel. Common fatty acids found in Chlorella include palmitic acid (C16:0), a saturated fatty acid that contributes to the stability and cetane number of biodiesel; oleic acid (C18:1), a monounsaturated fatty acid that improves the fluidity and cold flow properties of

biodiesel; and linoleic acid (C18:2), a polyunsaturated fatty acid that can enhance the oxidative stability of biodiesel (Griffiths & Harrison, 2009).

Chlorella offers several advantages as a biodiesel source: it has a high lipid yield, a rapid growth rate, and can contribute to sustainability by reducing reliance on fossil fuels and lowering greenhouse gas emissions (Patil, Tran & Giselrød, 2008). However, there are challenges that need to be addressed, such as the high production cost of algal biodiesel compared to conventional biodiesel, the need for efficient harvesting and lipid extraction methods to make the process economically viable, and the challenge of scaling up production while maintaining efficiency and cost-effectiveness (Pulz & Gross, 2004). Overall, Chlorella holds great potential as a sustainable source of biodiesel, but further research and technological advancements are necessary to overcome existing challenges (Mata, Martins & Caetano, 2010).

### **1.2.2 Pre-treatments for lipid extraction on algae**

Pre-treatment plays a crucial role in biodiesel production, as it prepares the feedstock for efficient conversion into biodiesel through transesterification. It involves a series of steps designed to remove impurities, improve accessibility to lipids, and optimize the conditions for the transesterification reaction (Encinar et al., 2012). Many feedstocks for biodiesel production, such as vegetable oils, animal fats, or waste cooking oil, contain impurities like water, free fatty acids (FFAs), phospholipids, and solids. These impurities can interfere with the transesterification reaction, reduce biodiesel yield, and lead to lower-quality biodiesel. Pre-treatment processes such as degumming, neutralization, and filtration are employed to remove these impurities and prepare a cleaner feedstock (Gavrilescu & Chisti, 2005). High levels of FFAs in the feedstock can hinder the transesterification reaction by consuming the catalyst and forming soap, which can lower biodiesel yield and quality. Pre-treatment methods such as acid or alkaline neutralization and esterification are used to reduce FFAs to acceptable levels before transesterification (Bokhari et al. 2015). Pre-treatment can improve the accessibility of triglycerides in the feedstock, making them more reactive during the transesterification process. Mechanical disruption, enzymatic hydrolysis, and solvent extraction are some techniques used to break down cell walls and release lipids from biomass, especially in unconventional feedstocks like microalgae or waste oils (Li et al. 2010). Some pre-treatment methods are designed to ensure compatibility with the catalyst used in the transesterification reaction. For example, acidic or

alkaline pre-treatment may be selected based on the type of catalyst (acid or base) employed in the transesterification step. Pre-treatment helps ensure the quality of the biodiesel produced by removing impurities and contaminants that could affect biodiesel properties and performance. Quality control tests conducted on the feedstock before and after pre-treatment help assess the suitability of the feedstock for biodiesel production and monitor the effectiveness of pre-treatment processes (Wang et al. 2023).

### 1.2.2.1 Microwave heating

Microwave heating involves the ability of molecules to absorb and transmit microwave radiation. This heating is achieved by the dipoles or ions of each molecule aligning and re-aligning with the oscillations of the magnetic field (López-Grimau et al., 2012). Each solvent has a different absorption capacity, which influences its heating efficiency. As shown in Table 2, methanol has a better ability to absorb microwaves than water, and water has a better ability to absorb microwaves than hexane (Zhang et al. 2023).

The effectiveness of microwave heating is particularly notable in the context of using ionic liquids. Ionic liquids, known for their unique properties such as low volatility and high thermal stability, have shown promising results when combined with microwave heating. This combination can be particularly advantageous in various chemical processes due to the efficient and uniform heating provided by microwaves (Fabre et al. 2021)

In the field of biodiesel production, the application of microwave heating in conjunction with ionic liquids has been explored to improve process efficiency. One of the significant challenges in biodiesel production from microalgae is the breakdown of the robust cell walls. Microwave heating can facilitate the disruption of these cell walls, making the intracellular lipids more accessible for extraction. The enhanced cell disruption, coupled with the catalytic properties of ionic liquids, can lead to a higher transesterification yield, which is the conversion of triglycerides into biodiesel (Kapooore et al. 2018).

Research indicates that the synergistic effect of microwave heating and ionic liquids not only accelerates the reaction rate but also improves the overall yield and purity of biodiesel. This is due to the localized superheating of the reaction mixture, which enhances mass transfer and reduces the reaction time. Moreover, the use of ionic liquids can provide a more

environmentally friendly and sustainable alternative to conventional catalysts, further promoting the efficiency and viability of biodiesel production processes (Yu et al. 2011).

### 1.2.3 Transesterification reaction

Transesterification is an alternative reaction to esterification. It occurs between an ester and an alcohol through the exchange of an alkoxy group, as shown in figure 3. A catalyst is usually added to the reaction, such as a base or an acid or an enzyme. The acids most used as catalysts are sulfuric acid and hydrochloric acid. The base most used as a catalyst is sodium hydroxide. The products of this reaction are a new ester and an alcohol (Ma & Hanna, 1999).

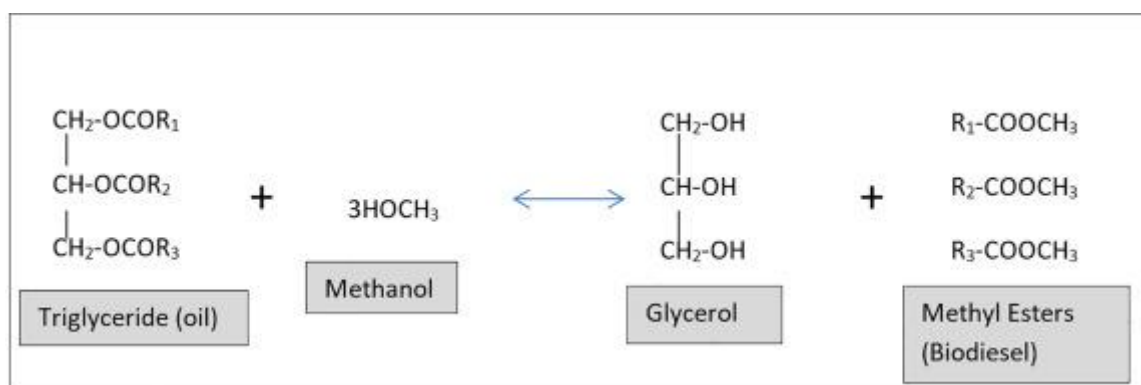


Figure 3- Transesterification reaction process. (Meher and Sagar, 2006).

The mechanism of catalytic transesterification described by Meher and Sagar is separated into two steps. The first step involves the protonation of the carbonyl group of the ester by the acid catalyst. In this step, the acid catalyst donates a proton to the oxygen atom of the carbonyl group of the ester, making it more susceptible to nucleophilic attack. The alcohol, acting as a nucleophile, attacks the carbonyl carbon of the protonated ester, resulting in the formation of an acyl intermediate. This intermediate is a reactive species with a broken carbon-oxygen bond and a new carbon-oxygen bond formed with the alcohol (Meher, Dharmagadda, and Naik, 2006).

In the second step, alkyl exchange occurs between the alcohol and the alkyl group of the acyl intermediate. The alcohol acts as a nucleophile, replacing the original alkyl group of the

acyl intermediate, resulting in the formation of the desired methyl or ethyl ester and regeneration of the acid catalyst (Meher and Sagar, 2006).

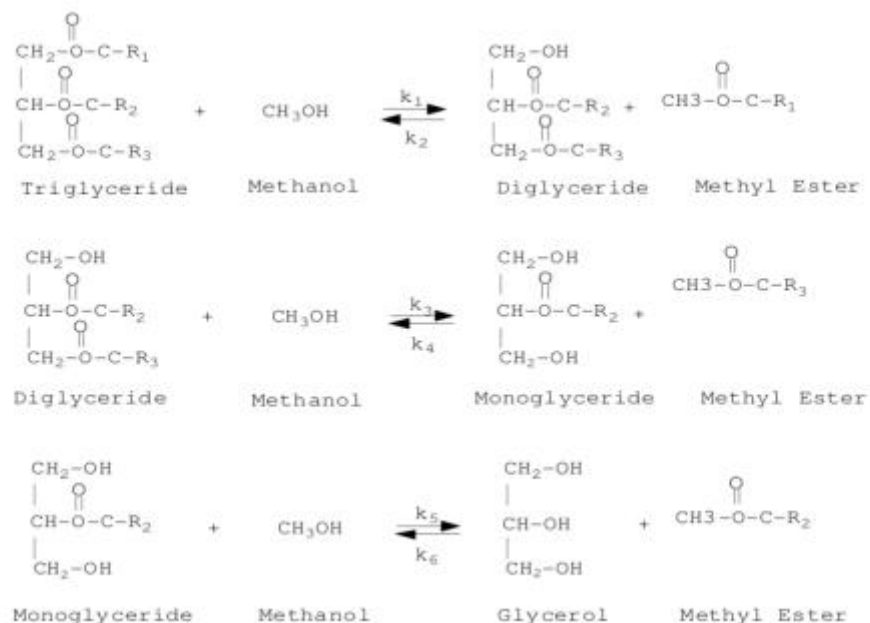


Figure 4 - Intermediate step in transesterification where  $k_1$  to  $k_6$  are reaction constants. (Meher and Sagar, 2006).

Table 1 - Activation energy and rate constants at 50°C a methanol to oil ratio of 6:1, and catalysis with sodium hydroxide (0.20 wt%). (Meher and Sagar, 2006).

Step	Rate Number	[l/(mol min)]	Activation Energie Number	[kJ/(mol K)]
First	$k_1$	0.050	$E_1$	54998.68
	$k_2$	0.110	$E_2$	41555.49
Second	$k_3$	0.215	$E_3$	83094.24
	$k_4$	1.228	$E_4$	61249.57
Third	$k_5$	0.242	$E_5$	26112.34
	$k_6$	0.007	$E_6$	40116.19

The kinetics of intermediate steps in transesterification were investigated by Nouredini and Zhu as shown in Figure 4 and Figure 5. The study determined kinetic parameters, including reaction constants ( $k$ ) and activation energies ( $E$ ), under specific conditions: a temperature of 50°C, a methanol to oil ratio of 6:1, and catalysis with sodium hydroxide (0.20 wt%). It was found that temperature plays a pivotal role in directing the reaction. Higher temperatures favored reactions with higher activation energies, while lower temperatures favored those with lower activation energies (Nouredini and Zhu, 1997).

The first two steps of the reaction were found to be favored by high temperatures due to the high activation energy in forward reactions ( $k_1$  and  $k_3$ ). However, the reaction of monoglycerides to glycerol exhibited a unique behavior. Although theoretically, a higher temperature would favor the reverse reaction due to its higher activation energy, higher concentrations

of monoglycerides offset this effect. The study also highlighted the optimal temperature for the production of methyl esters, with 60°C being identified as the optimal temperature. Furthermore, it was observed that mixing initially influenced the reaction. However, as methyl esters were formed, they acted as mutual solvents for the reactants, resulting in the formation of a single-phase system where the effect of mixing became insignificant (Noureddini and Zhu, 1997).

In contrast to homogeneous catalyst systems used in the study by Noureddini and Zhu, a heterogeneous system was employed in subsequent research. Calcium oxide derived from eggshells served as the catalyst, introducing additional complexities to the reaction mechanism. The use of a heterogeneous catalyst led to the occurrence of heat transport effects alongside the actual reaction effects, necessitating the consideration of both macro- and micro-kinetics. While macro-kinetics described mass and heat transportation processes, micro-kinetics delved into adsorption and desorption processes (Gaide et al., 2022).

A catalyst is important in transesterification reaction because it activates the carbonyl group of the triglycerides. This is essential because triglyceride esters are relatively inert and do not readily react with alcohols to form the desired esters. The catalyst facilitates the formation of reactive intermediates, such as acyl intermediates, which are essential for the transesterification reaction. These intermediates increase the reactivity of the triglycerides with the alcohol, leading to the formation of methyl or ethyl esters and glycerol (Lotero et al., 2005). By lowering the activation energy barrier, the catalyst accelerates the rate of the transesterification reaction. This results in faster conversion of triglycerides to esters and glycerol, leading to higher reaction efficiency (Leung, Wu, and Leung, 2010).

### 1.2.3.1 Catalysts in transesterification

Homogeneous catalysts, which include both acidic and basic catalysts, are dissolved in the reaction medium and provide uniform reaction conditions. Commonly used basic homogeneous catalysts in transesterification include sodium hydroxide (NaOH), potassium hydroxide (KOH), and sodium methoxide (NaOCH<sub>3</sub>). These catalysts are highly efficient and widely used in industrial biodiesel production due to their ability to achieve high reaction rates and conversion efficiencies (Ma & Hanna, 1999). Basic catalysts function by generating alkoxide ions from the alcohol, which then attack the carbonyl carbon of the triglyceride, leading to the formation of fatty acid alkyl esters and glycerol. However, homogeneous basic catalysts are

sensitive to free fatty acids and water in the feedstock, which can lead to soap formation and complicate the purification of biodiesel (Marchetti et al., 2007). Acidic homogeneous catalysts, such as sulfuric acid ( $\text{H}_2\text{SO}_4$ ) and hydrochloric acid (HCl), are also used in transesterification, particularly for feedstocks with high free fatty acid content. Acid catalysts can simultaneously catalyze esterification and transesterification reactions, converting free fatty acids into esters, thus minimizing soap formation (Canakci & Van Gerpen, 1999). However, acidic catalysts generally require longer reaction times and higher temperatures, and they are more corrosive than basic catalysts, posing challenges for reactor materials and maintenance.

Heterogeneous catalysts, which are in a different phase than the reactants, offer significant advantages in terms of ease of separation, catalyst recovery, and reusability. These catalysts include solid acids, solid bases, and supported catalysts. Solid base catalysts, such as calcium oxide (CaO), magnesium oxide (MgO), and hydrotalcites, have been extensively studied for transesterification. These catalysts are highly effective and can be easily separated from the reaction mixture, reducing the need for extensive purification (Sharma et al., 2011). However, the activity of solid base catalysts can be affected by the presence of water and free fatty acids in the feedstock, similar to homogeneous base catalysts. Solid acid catalysts, including ion-exchange resins, sulfonated carbon, and zeolites, are effective in catalyzing transesterification, especially for feedstocks with high free fatty acid content. These catalysts offer high thermal stability and can be used in continuous flow systems, enhancing process efficiency (Dias et al., 2008). The main limitation of solid acid catalysts is their generally lower activity compared to base catalysts, which may require higher reaction temperatures and longer times. Supported catalysts, where active catalytic species are dispersed on inert supports like silica, alumina, or activated carbon, provide high surface area and improved catalyst stability. These catalysts combine the advantages of homogeneous and heterogeneous systems, offering high activity and ease of separation. For example, potassium hydroxide supported on alumina has shown high efficiency in transesterification reactions (Jain et al., 2011). Enzymatic catalysts, particularly lipases, offer a green and sustainable alternative for transesterification. Lipases can catalyze the reaction at mild temperatures and pressures, and they are highly selective, reducing the formation of by-products (Bhandari et al., 2008). Enzymatic transesterification can also handle high free fatty acid feedstocks without soap formation. However, the high cost of enzymes and their potential deactivation by alcohols pose challenges for their widespread industrial application. Immobilization of lipases on solid supports can enhance their stability and reusability, making enzymatic catalysis more economically viable (Du et al., 2004).

## 1.2.4 Biodiesel purification

Extraction processes can be used as a downstream step in biodiesel production to separate the desired biodiesel (fatty acid methyl or ethyl esters) from the reaction mixture and any impurities or byproducts. After the transesterification reaction, the resulting mixture typically contains biodiesel (fatty acid methyl or ethyl esters), glycerol (a byproduct of the reaction), excess alcohol, catalyst, and possibly other impurities such as free fatty acids (Rombaut et al., 2015).

The first step in the extraction process is to separate the biodiesel from the glycerol and other components. This separation can be achieved through gravity settling, centrifugation, or other separation techniques (Yang et al., 2019). Glycerol, being denser than biodiesel, usually settles at the bottom of the container or can be separated by centrifugation (Tapanes et al., 2011).

Once the biodiesel is separated from the glycerol, it may undergo washing with water or other solvents to remove any remaining impurities, catalyst residues, or excess alcohol. Washing helps improve the purity and quality of the biodiesel product. In literature hexane is used for washing because it is a highly effective solvent for extracting lipids, including triglycerides found in vegetable oils, fats, and other lipid-rich materials. It has a strong affinity for non-polar compounds, making it particularly efficient for dissolving lipids while leaving polar impurities behind. It is relatively inexpensive compared to other solvents commonly used in extraction processes (Encinar et al., 2012).

Hexane is considered to have low acute toxicity to humans and the environment when used properly in controlled industrial settings (Gavrilescu & Chisti, 2005). It is classified as a volatile organic compound (VOC) and evaporates quickly at room temperature, minimizing its potential for environmental contamination. Hexane is volatile and easily evaporates from the extracted oil or other substances, leaving behind a relatively pure extract (Dunn et al., 1997). This facilitates the recovery and reuse of the solvent, reducing waste and minimizing environmental impact.

It is widely accepted and approved for use in extraction processes by regulatory agencies worldwide, including the US Food and Drug Administration (FDA) and the European Food Safety Authority (EFSA). Its regulatory status provides assurance of safety and compliance with industry standards.

Hexane's ability to dissolve lipids efficiently allows for high yields of oil extraction from oilseeds, such as soybeans, canola, and sunflower seeds (Encinar et al., 2012). This efficiency contributes to the economic viability of oilseed processing and biodiesel production industries.

After washing, the biodiesel is typically dried to remove any residual water or solvent. Drying can be achieved through evaporation or other drying methods (Encinar et al., 2012).

## 1.3 Ionic Liquids

Ionic liquids are typically composed of ions with a melting temperature below 100°C. They are versatile in chemical reactions, serving as solvents, catalysts, and reagents (Plechko and Seddon, 2008). Classified into three generations, the first generation primarily functioned as solvents (Rogers and Seddon, 2003). The second generation introduced specific chemical applications where functional groups on the ionic liquid cations play direct roles (Seddon, 2003). The third generation focused on reducing toxicity, making them suitable for pharmaceutical use (Bica and Rogers, 2010).

Ionic liquids are known for their high viscosity, which often exceeds that of conventional solvents, and their density is typically higher than that of water due to heavy ion composition. They possess excellent solvating capabilities, dissolving a wide range of materials including organic, inorganic, and polymeric compounds. Due to their ionic nature, they exhibit good electrical conductivity, beneficial for electrochemical applications. Another key feature is their tunable solubility, allowing adjustments by modifying the constituent ions to meet specific solvent needs. Most ionic liquids are non-flammable and chemically stable, offering safety advantages in industrial settings. Many formulations are designed to be less toxic than traditional solvents, although toxicity varies and requires specific evaluation. Additionally, their recyclability supports sustainable practices in chemical processes.

Room temperature ionic liquids (RTILs), a subset that remains liquid near or at room temperature (typically below 25°C), have gained prominence for their ease of handling and versatile applications across various fields.

Despite advantages such as a melting point below 100°C, Ionic liquids can be costly and may exhibit toxicity and low biodegradability (Zhao et al., 2012). Their synthesis involves combinations of different cations and anions, offering a myriad of possibilities for innovation (Wasserscheid and Welton, 2002). Widely used as catalysts, particularly in biodiesel production through transesterification processes, they have replaced corrosive conventional catalysts (Garcia et al., 2010). Their efficacy as catalysts stems from high activity, thermal stability, and the ability to combine different compounds effectively (Mehdi et al., 2010). Consequently, they are extensively researched and applied in various roles as solvents, catalysts, and co-catalysts, driving innovative catalytic systems (Rogers and Seddon, 2003). Identifying the specific contributions of individual cations or anions to catalytic activity remains a challenge (Wasserscheid and Welton, 2002).

#### 1.3.1.1 Dianionic and Dicationic Ionic Liquids

Dianionic ionic liquids contain one anion charged doubly and typically feature a two positive cation. These ILs are known for their ability to interact strongly with a range of substances due to the high charge density of the anions. This interaction can enhance their performance in various applications, such as in catalytic processes and separation technologies (Parker et al., 2021).

Dianionic ionic liquids are especially useful in applications requiring strong ionic interactions and high stability under specific conditions, such as in the transesterification reaction for biodiesel production. They can improve the efficiency of reactions by stabilizing intermediates and increasing reaction rates (Liu et al., 2022).

Dicationic ionic liquids, on the other hand, feature two positively charged cation and a single anion. These ILs offer unique properties due to their increased cationic charge density, which can influence solubility, viscosity, and thermal stability. The dicationic nature allows for the formation of complex structures and interactions, making them particularly useful in advanced chemical processes and materials science (Zhou et al., 2023).

An example of a monocationic ionic liquid is  $[\text{Py}_{1,1,1,2}][(\text{CF}_3\text{SO}_2)_2\text{N}]$ , where the monocationic cation is a combination of one pyrazolium ions, paired with the bis(trifluoromethanesulfonyl)imide anion (Miller et al., 2021). Dicationic ionic liquids are known for their high stability and can function as efficient solvents and catalysts. Their unique properties, such as enhanced electrochemical stability and tunable viscosity, make them suitable for

applications in electrochemical devices and high-performance separation processes (Chen et al., 2022).

Both dianionic and dicationic ionic liquids have demonstrated significant advantages in various industrial and research applications. Dianionic ionic liquids often excel in environments that require strong ionic interactions and stability, making them ideal for catalytic applications and complex chemical processes (Parker et al., 2021). Dicationic ionic liquids, with their unique structural attributes, offer enhanced stability and versatility, contributing to innovations in materials science and electrochemical technologies (Zhou et al., 2023).

### 1.3.2 Synthesis of Ionic liquids

The synthesis of ionic liquids involves a systematic approach to combining cations and anions to create solvents and materials with tailored chemical properties. These compounds, consisting entirely of ions, offer unique advantages such as low volatility, high thermal stability, and versatile solvation capabilities, making them valuable in various scientific and industrial applications (Freemantle, 2010; Plechkova & Seddon, 2008).

The synthesis process begins with the selection of suitable cations and anions. Cations commonly used include derivatives of quaternary ammonium, imidazolium, pyrrolidinium, or phosphonium, chosen for their stability and compatibility with desired applications. Anions are typically derived from halides, sulfates, acetates, or other organic or inorganic sources (Wasserscheid & Keim, 2000; Rogers et al., 2017).

The selected cations and anions are combined through a neutralization reaction under controlled conditions. This step aims to achieve a balanced ratio of ions to ensure the desired physical and chemical properties of the resulting ionic liquid. The reaction is often conducted in solvents that facilitate ion exchange and promote the formation of stable molecular structures (Wasserscheid & Welton, 2003; Earle & Seddon, 2000).

Post-synthesis, purification techniques such as solvent extraction, chromatography, or recrystallization are employed to remove any remaining impurities and isolate the pure ionic liquid. Characterization techniques, including NMR spectroscopy, DSC, IR spectroscopy, and MS, are

then used to confirm the chemical composition, purity, and structural integrity of the synthesized compound (Welton, 1999; Armand et al., 2009).

The choice of solvent during synthesis plays a critical role in the efficiency and purity of the neutralization reaction. Solvents should be inert, non-reactive with the cations and anions, and compatible with subsequent purification steps (Hallett & Welton, 2011; Stark et al., 2005). Controlling temperature and other reaction parameters such as pH and pressure is crucial to optimizing the synthesis process. These parameters influence the yield, purity, and properties of the final ionic liquid product (Rogers et al., 2015).

### **1.3.3 Ionic liquids in pre-treatment**

The pre-treatment of biomass is a critical step in the conversion of lignocellulosic materials into biofuels and other value-added products. Traditional pre-treatment methods, such as acid or alkaline hydrolysis, often suffer from high energy consumption, harsh conditions, and the generation of inhibitory by-products. Ionic liquids offer a novel approach by dissolving lignocellulosic components at relatively mild conditions, thereby reducing the need for high temperatures and pressures.

Ionic liquids act as excellent solvents for both cellulose and hemicellulose, breaking down the complex structure of lignocellulosic biomass through several mechanisms. The strong ionic interactions in ILs effectively disrupt the hydrogen bonds within the cellulose and hemicellulose networks, leading to the breakdown of crystalline structures and enhancing the accessibility of enzymes and chemicals to the biomass (Hallett & Welton, 2011).

ILs also solubilize lignin, a major barrier to enzymatic hydrolysis. By dissolving lignin, ILs facilitate the removal of this structural component, increasing the surface area of cellulose and hemicellulose for subsequent enzymatic attack (Zhao et al., 2016). The ability of ILs to swell biomass fibers and disrupt their crystalline structure significantly reduces the recalcitrance of lignocellulosic materials. This swelling effect increases the substrate's surface area, improving the efficiency of enzymatic hydrolysis and fermentation processes (Sun et al., 2017).

The use of ionic liquids in pre-treatment offers several advantages over conventional methods:

ILs operate effectively under mild conditions of temperature and pressure, reducing the energy requirements and enhancing process sustainability (Rogers et al., 2007). Many ionic

liquids are recyclable and can be reused multiple times without significant loss of catalytic activity, making them economically and environmentally viable for large-scale applications (Zhang et al., 2014). The tunable nature of ILs allows for the selective solvation of specific biomass components, minimizing the formation of inhibitory by-products and enhancing the yield of fermentable sugars (Wang et al., 2013).

Numerous studies have demonstrated the effectiveness of ionic liquids in biomass pre-treatment:

**Cellulose and Hemicellulose Dissolution:** Research has shown that ILs such as 1-ethyl-3-methylimidazolium acetate ([C<sub>2</sub>mim][OAc]) and 1-butyl-3-methylimidazolium chloride ([C<sub>4</sub>mim][Cl]) can dissolve cellulose and hemicellulose at ambient temperatures, significantly enhancing the efficiency of enzymatic hydrolysis (Liu et al., 2014).

**Lignin Removal:** Studies using ILs like 1-ethyl-3-methylimidazolium chloride ([C<sub>2</sub>mim][Cl]) have demonstrated effective lignin removal from biomass, facilitating the conversion of cellulose to glucose with high yields (Liu et al., 2007).

### 1.3.4 Ionic liquids in extraction

Ionic liquids are composed entirely of ions, which contribute to their distinctive characteristics. Their negligible vapor pressure reduces the risk of solvent loss and environmental contamination, while their high thermal stability allows for their use in a wide range of temperatures. The ability to tailor the cation and anion components of ILs enables the design of solvents with specific properties suited to extraction tasks (Plechkova & Seddon, 2008). This versatility is crucial for optimizing extraction efficiency and selectivity.

One of the primary applications of ionic liquids is in the extraction of metal ions from aqueous solutions. Traditional solvent extraction methods often suffer from inefficiencies and environmental concerns. Ionic liquids, however, provide a greener alternative. For example, ILs such as 1-butyl-3-methylimidazolium hexafluorophosphate ([BMIM][PF<sub>6</sub>]) have been used to extract metal ions like copper and nickel from aqueous solutions with high efficiency and selectivity (Visser et al., 2001). The ionic liquid phase can selectively dissolve and transport metal ions, often forming stable complexes that facilitate easy recovery of the metals.

Ionic liquids also show great promise in the extraction of organic compounds, particularly in the pharmaceutical and biotechnological industries. The extraction of bioactive compounds from natural sources, such as plant materials, can be significantly enhanced using ILs. For

instance, ILs like 1-ethyl-3-methylimidazolium acetate ([EMIM][OAc]) have been effectively used to extract alkaloids, flavonoids, and other valuable phytochemicals from plant matrices (Zhao et al., 2010). The high solubility of these compounds in ILs, coupled with the ability to recycle the ionic liquid, makes this approach both efficient and sustainable.

In the field of environmental remediation, ionic liquids offer innovative solutions for the extraction and removal of pollutants from contaminated environments. ILs can be employed to extract a wide range of contaminants, including heavy metals, pesticides, and organic pollutants, from soil and water. For example, studies have demonstrated the use of ILs in the extraction of heavy metals from industrial effluents and contaminated soils, showing improved efficiency over conventional extraction methods (Galan et al., 2010). The use of ILs minimizes the generation of secondary waste and reduces the environmental footprint of the extraction process. The extraction mechanisms of ionic liquids are influenced by their ability to form strong interactions with target solutes, such as hydrogen bonding,  $\pi - \pi$  interactions, and electrostatic interactions. The tunability of ILs allows for the optimization of these interactions to enhance extraction efficiency. Additionally, the hydrophobic or hydrophilic nature of the IL can be adjusted to favor the partitioning of specific solutes into the ionic liquid phase (Wasserscheid & Welton, 2003).

Ionic liquids have been successfully employed in the extraction of lipids from various sources, including microalgae, plant materials, and animal tissues. For instance, the extraction of lipids from microalgae, a promising feedstock for biofuel production, has been significantly improved using ILs. Traditional solvent extraction methods often face challenges such as high energy consumption and the use of toxic solvents. Ionic liquids, such as 1-ethyl-3-methylimidazolium hexafluorophosphate ([EMIM][PF<sub>6</sub>]), have demonstrated higher lipid extraction efficiencies with lower energy requirements and reduced environmental impact (Li et al., 2014). In the context of plant materials, ILs have been used to extract essential oils and fatty acids from seeds and leaves. The use of ILs in these processes not only enhances extraction yields but also allows for the selective extraction of specific lipid fractions, which is particularly advantageous for the pharmaceutical and food industries (Moniruzzaman et al., 2010). Similarly, in animal tissues, ILs have facilitated the extraction of lipids, including triglycerides and phospholipids, with improved efficiency and purity compared to conventional solvents (Fujita et al., 2007). The mechanisms underlying lipid extraction by ionic liquids are influenced by the strong interactions between ILs and lipid molecules. These interactions include hydrogen bonding, van der Waals forces, and electrostatic interactions, which facilitate the solubilization and transfer of lipids into the ionic liquid phase. The tunability of ILs allows for the optimization of these

interactions to maximize extraction efficiency. For example, the choice of IL with specific functional groups can enhance the solubility of lipid classes, thereby improving extraction selectivity (Ventura et al., 2017).

### 1.3.5 Ionic liquids in catalysis

Ionic liquids possess several intrinsic properties that make them ideal for catalytic applications. Their negligible vapor pressure minimizes the loss of solvents and reduces volatile organic compound (VOC) emissions, contributing to greener chemical processes. The tunability of ionic liquids, achieved by varying the combination of cations and anions, allows for the optimization of solubility, acidity, and hydrophobicity, which can be tailored to specific catalytic reactions (Plechkova & Seddon, 2008). Additionally, the high ionic strength and unique solvation properties of ILs can stabilize reactive intermediates and transition states, thus enhancing catalytic efficiency (Welton, 1999). In homogeneous catalysis, ionic liquids serve as both solvents and catalysts, or as media for dissolved catalysts. Their ability to dissolve a wide range of metal complexes and organocatalysts makes them versatile media for various catalytic reactions. For example, the use of ILs in transition metal-catalyzed reactions, such as hydrogenation and hydroformylation, has demonstrated improved reaction rates and selectivities compared to traditional solvents (Wasserscheid & Welton, 2003). A notable example is the use of 1-butyl-3-methylimidazolium hexafluorophosphate ([BMIM][PF<sub>6</sub>]) in the rhodium-catalyzed hydroformylation of olefins, which not only enhances reaction rates but also facilitates the recycling of the rhodium catalyst (Chauvin et al., 1995). In heterogeneous catalysis, ionic liquids can be used to immobilize catalysts on solid supports, thereby combining the benefits of both homogeneous and heterogeneous systems. ILs can stabilize nanoparticles and prevent their agglomeration, thus maintaining high catalytic activity and selectivity. For instance, the immobilization of palladium nanoparticles in ionic liquids has been shown to be effective for the Heck and Suzuki coupling reactions, offering high yields and excellent recyclability of the catalyst (Dupont & Scholten, 2010). Ionic liquids also find applications in biocatalysis, where they provide a unique environment for enzyme-catalyzed reactions. The ability of ILs to dissolve both polar and non-polar substrates, coupled with their non-volatile nature, makes them ideal media for biocatalysis. Enzymes often exhibit enhanced stability and activity in ILs, leading to improved reaction rates and product yields. For example, the use of ILs in lipase-catalyzed esterifications and transesterifications has been widely reported, showing significant improvements

in enzyme performance compared to conventional solvents (Kragl et al., 2002). The catalytic activity of ionic liquids is influenced by their ability to form strong interactions with both substrates and catalysts. Hydrogen bonding,  $\pi$ - $\pi$  interactions, and electrostatic interactions between the IL and the catalytic species can enhance the reactivity and selectivity of the catalytic process. The tunability of ILs allows for the optimization of these interactions, thereby facilitating the design of more efficient catalytic systems (Wasserscheid & Welton, 2003).

### 1.3.5.1. Using Ionic Liquids as catalysts on transesterification reaction

Ionic Liquids (ILs) offer a multitude of advantages owing to their adaptable characteristics. By selecting different combinations of cations and anions, the physicochemical properties of ILs can be tailored to match specific reaction requirements, including solubility, polarity, and acidity/basicity. This tunability allows for the optimization of reaction conditions to enhance the efficiency and selectivity of the transesterification process (Liu et al., 2015; Wei et al., 2017; Anastas & Warner, 1998).

ILs play a significant role in influencing the kinetics of transesterification reactions by modifying the activation energy and reaction pathway. Their presence facilitates the accessibility of reactants to active sites on the catalyst surface, thereby improving reaction rates (Wei et al., 2017). Moreover, ILs stabilize reaction intermediates and transition states, reducing the overall energy barrier for the reaction (Anastas & Warner, 1998).

In addition to serving as solvents and catalysts, ILs can immobilize catalysts either by dissolving them in the IL or anchoring them onto the IL matrix. This immobilization enhances the stability, recyclability, and ease of separation of catalysts from the reaction mixture (Mikkola & Salmi, 2012). Immobilized IL-based catalysts have demonstrated excellent catalytic activity and selectivity in transesterification reactions (Tavakkoli & Mulligan, 2013). ILs are often lauded as green solvents due to their low volatility, non-flammability, and negligible vapor pressure. This contributes to improved process safety, reduced solvent loss, and emissions (Holbrey et al., 2002). Furthermore, ILs are recyclable and can be recovered and reused in subsequent reaction cycles, minimizing waste generation and environmental impact (Gutowski et al., 2003).

Notably, ILs exhibit compatibility with a wide range of feedstocks used in biodiesel production, such as various vegetable oils, animal fats, and waste cooking oils. They effectively

dissolve these feedstocks and promote transesterification reactions without requiring additional cosolvents or pretreatment steps (Tan et al., 2008). This compatibility streamlines the biodiesel production process and broadens the range of potential feedstocks that can be utilized (Pinkert et al., 2009).

While much of the research on IL-catalyzed transesterification has focused on laboratory-scale studies, there is a burgeoning interest in scaling up these processes for industrial applications. Several studies have demonstrated the feasibility of using ILs in large-scale biodiesel production, underscoring their potential for commercialization (Zhao et al., 2005). However, challenges such as cost-effectiveness, scalability, and regulatory considerations need to be addressed to facilitate widespread adoption (Gutowski et al., 2003).

Table 2 shows the ionic liquids most used in the transesterification reaction and their properties.

Table 2 - This table contains the most used Ionic liquids in transesterification reaction, their name, formula and key properties. (Chen & Zhang, 2022; Liu et al., 2022; Ranu & Jana, 2005; Xie & Zhao, 2013).

<b>Ionic Liquid</b>	<b>Formula</b>	<b>Key Properties</b>
1-Butyl-3-methylimidazolium Hexafluorophosphate	[BMIM][PF <sub>6</sub> ]	High thermal stability, good solubility for organic compounds
1-Butyl-3-methylimidazolium Tetrafluoroborate	[BMIM][BF <sub>4</sub> ]	High ability to solubilize alcohols and fatty acids
1-Butyl-3-methylimidazolium Chloride	[BMIM][Cl]	Efficient in catalyzing transesterification, hygroscopic
1-Ethyl-3-methylimidazolium Ethylsulfate	[EMIM][EtSO <sub>4</sub> ]	Low toxicity, recyclable, sustainable
1-Ethyl-3-methylimidazolium Acetate	[EMIM][OAc]	Effective at low temperatures, dissolves a wide range of compounds
1-Hexyl-3-methylimidazolium Hexafluorophosphate	[HMIM][PF <sub>6</sub> ]	High affinity for non-polar organic compounds, facilitates reaction with triglycerides
Tetrabutylammonium Hydroxide	[TBA][OH]	Strong base, high ester conversion
1-Butyl-3-methylimidazolium Methylsulfate	[BMIM][MeSO <sub>4</sub> ]	High efficiency in transesterification, regenerable and reusable
Choline Hydroxide	[Ch][OH]	Biodegradable, less toxic, "green" option
1-Ethyl-3-methylimidazolium Hydrogen Sulfate	[EMIM][HSO <sub>4</sub> ]	Acidic ionic liquid, promotes transesterification under severe conditions with high yield

### 1.3.6 One-pot transesterification reaction

A one-pot transesterification reaction refers to a process where all the necessary reactants and catalysts are combined and reacted in a single reaction vessel or reactor system, without the need for intermediate steps or additional processing. This approach streamlines the biodiesel production process by reducing the number of process steps, minimizing the use of solvents, and simplifying the overall reaction setup (Leung et al., 2010).

In a typical one-pot transesterification reaction for biodiesel production, the triglyceride feedstock (such as vegetable oil or animal fat), alcohol (typically methanol or ethanol), and catalyst (usually a base such as sodium hydroxide or potassium hydroxide) are mixed together in a single reactor vessel. The reaction is then allowed to proceed under controlled conditions, such as temperature and pressure, to convert the triglycerides into fatty acid alkyl esters (biodiesel) and glycerol (Noureddini & Zhu, 1997). There are some advantages of one-pot transesterification like operational simplicity, increased efficiency, cost-effectiveness and higher yields (Meher et al., 2006; Kaieda et al., 2001).





## 2. MATERIALS AND METHODS

### 2.1 List of materials

i) reagents used in the synthesis of IL.

- N-Methyldiethanolamine from Thermo Scientific with a purity of over 98%
- 1-chlorobutane from Sigma-Aldrich with a purity of 99%
- Amberlite™ IRN-78, Ion exchange resin from Thermo Scientific
- Diethyl ether from Honeywell with a purity of over 99.8%
- Deuterium oxide from Eurisotop 99,9%
- Dimethyl sulfoxide-d<sub>6</sub> from Eurisotop with a purity of over 99.8%
- Sulfosuccinic acid solution 70% in H<sub>2</sub>O from Sigma-Aldrich
- Silver nitrate, 99%

ii) in the transesterification reaction including extraction;

- Hexane from LABCHEM, 98,5%
- NaCl from Sigma-Aldrich, 99%
- Microalgae used was *Chlorella vulgaris* soft from Allmicroalgae
- Benzoic acid from Sigma-Aldrich, 99.8%
- Methanol from Honeywell, 99%
- Panreac hydrochloric acid, 37%
- Sigma-Aldrich n-hexane, 99%
- Sigma-Aldrich undecane, 99%
- Nonadecane from Sigma-Aldrich, 99%
- Tetradecane from Sigma-Aldrich, 99%
- Sulfuric acid Fluka 95%-97%

iii) in the pre-treatment tests.

- Sigma-Aldrich n-hexane 99%

## 2.2 Synthesis of the Dianionic Ionic Liquid (DAIL)

### 2.2.1 Synthesis of the ionic liquid precursor

The ionic liquid precursor was synthesized using N-Methyldiethanolamine (MDEA) and the alkylating agent 1-chlorobutane. This reaction was carried out with four equivalents of 1-chlorobutane. The solvent used in this reaction was hexane. This reaction took place in a pressure tube for 3 days with magnetic stirring and a temperature of 90°C. The excess hexane was decanted and IL was then washed with diethyl ether to remove the excess alkylating agent, subsequently, the solvent was decanted, and the excess was evaporated on a rotavapor. In the end, the ionic liquid precursor was placed in the vacuum line at 40°C for 4 days. The yield of this reaction was between 95 and 99%. The physical state of this ionic liquid is liquid with viscous properties, and it shows a white colour. After drying, an  $^1\text{H}$  NMR and  $^{13}\text{C}$  NMR was carried out using deuterium oxide as solvent.

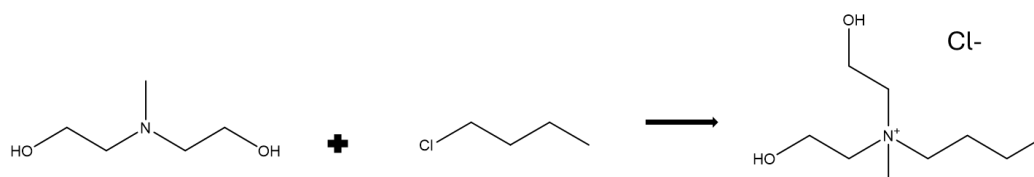


Figure 5-Chemical reaction of precursor  $[\text{N}_{4,1,2\text{OH},2\text{OH}}]\text{Cl}$  synthesis.

### 2.2.2 Synthesis of DAIL

The synthesized  $[\text{N}_{4,1,2\text{OH},2\text{OH}}]\text{Cl}$  was used as a precursor for the synthesis of the proposed ionic liquid (DAIL). In this synthesis, an anion exchange occurred in an ion exchange column where the Cl ion was exchanged with OH. This column contained ionic resin. In this reaction, a stoichiometry of 2 equivalents of my precursor ionic liquid to 1 equivalent of my sulfosuccinic acid was used. The solvent for this reaction was Milli-Q water. The water was added to activate the resin in the column and initiate the reaction. After the ionic liquid passed through the column and exchanged anions, it was stirred into a container with sulfosuccinic acid. The reaction ended when the pH was approximately 7. The water resulting from the reaction was then evaporated using a rotavapor and placed under vacuum. Finally, NMR was

conducted to characterize the DAIL. The chemical formula is  $[N_{4,1,2OH} 2OH]_2[COOCH_2CHSO_3HCOO]$  as shown in figure 6.

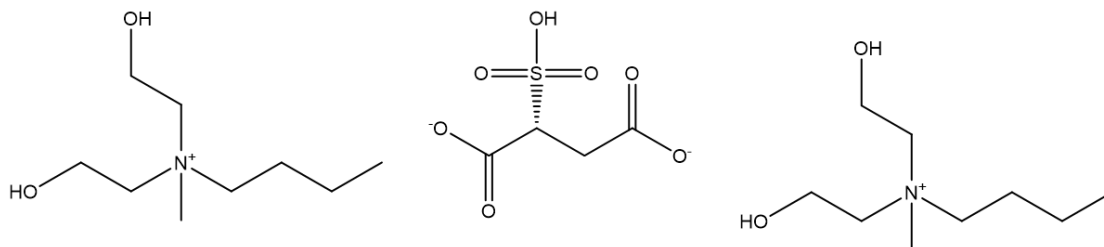


Figure 6 - Structure of DAIL.

### 2.2.2.1 Compounds used in the synthesis of DAIL Ionic Liquid

These compounds were used to synthesise the ionic liquid in this dissertation.

N-Methyldiethanolamine (MDEA) is a neutral compound classified within the ethanolamines. It is a tertiary amine characterized by a nitrogen atom bonded to a methyl group and two ethoxy groups, as depicted in Figure 7. Typically, colourless or yellow, MDEA has an odor reminiscent of ammonia and exhibits solubility in water. Its versatile applications span across pharmaceuticals, water treatment, fabric treatment, gas purification, and coatings (Hallett & Welton, 2011).

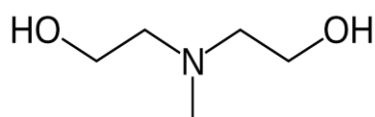


Figure 7 - Chemical formula of N-Methyldiethanolamine (MDEA). (Sigma-Aldrich)

1-Chlorobutane is an organic compound that belongs to the haloalkanes. The structure of this compound as shown in figure 8 has a carbon chain with a chlorine atom attached to the first carbon of the chain. This compound is colourless at room temperature with a strong smell. It

is not very soluble in water and its vapours are heavier than air (Plechkova & Seddon, 2008).

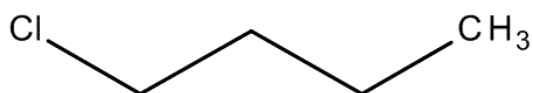


Figure 8 - Chemical formula of 1-Chlorobutane. (Sigma-Aldrich)

Sulfosuccinic acid is a chemical compound belonging to the group of coumarin derivatives. The structure of this compound as shown in figure 9 features a carbon chain attached to a sulfur atom with 2 carboxylic groups and a thiol attached to 2 oxygens (Biosynth, 2024). In esterification reactions, SSA acts as an effective catalyst by facilitating the conversion of carboxylic acids and alcohols into esters. The presence of sulfonic acid groups enhances the acidity of SSA, promoting the protonation of carbonyl groups and thereby accelerating the esterification process (Zhao et al., 2016). SSA is also utilized in acid-catalysed hydrolysis reactions where it catalyses the cleavage of bonds through protonation, leading to the breakdown of complex molecules into simpler compounds. This application finds utility in industries ranging from pharmaceuticals to petrochemicals, where controlled hydrolysis is crucial for product synthesis and purification (Hu et al., 2018). Furthermore, SSA plays a pivotal role in polymerization processes, particularly in the formation of polyester resins. Its acidic groups initiate polymerization reactions by facilitating the condensation of monomers, thereby contributing to the formation of high molecular weight polymers with desired properties (Sun et al., 2017). The catalytic activity of SSA is attributed to its ability to donate protons to substrates, thereby lowering the activation energy of chemical reactions. This protonation process enhances the

reactivity of organic molecules and promotes the formation of desired products under milder reaction conditions (Wang et al., 2019).

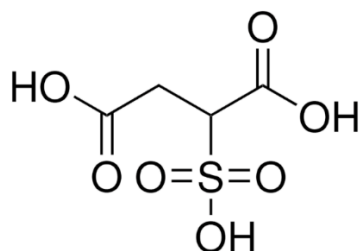


Figure 9 - Chemical formula of sulfosuccinic acid. (Sigma-Aldrich)

### 2.2.3 Differential Scanning Calorimetry

Calorimetry is a technique for measuring the thermal properties of a material and for establishing a connection between temperature and the physical properties of each substance. Differential Scanning Calorimetry (DSC) was used to understand the behaviour of the ionic liquid for a range of temperature over time. The program used variations of 10°C per minute in each cycle. The used temperature range was -90°C to 160°C. There were performed 6 cycles, 3 cycles of cooling and 3 of heating. The used sample purge flow was 50.00 mL/min and the flange temperature was -90°C. The gas used was N<sub>2</sub>.

### 2.2.4 Silver nitrate test

The possible presence of chlorine in the final compound was determined using the silver nitrate test. For this purpose, the compound produced was dissolved in 1mL of a 0.01M solution of silver nitrate. If no silver chloride precipitate formed, it was concluded that chlorine was not present in the compound produced.

### 2.2.5 Nuclear magnetic resonance

#### 2.2.5.1 Nuclear magnetic resonance of IL precursor

Nuclear magnetic resonance (NMR) spectra were obtained via Bruker ARX400 400MHz at 298K, analysed with MestreNova. The <sup>1</sup>H and <sup>13</sup>C spectra were acquired in deuterium oxide.

### 2.2.5.2 Nuclear Magnetic resonance of the DAIL

Nuclear magnetic resonance (NMR) spectra were obtained via Bruker ARX400 400MHz at 298K, analysed with MestreNova. The  $^1\text{H}$  and  $^{13}\text{C}$  spectra were acquired in deuterium oxide. Deuterated solvents were acquired from Eurisotop.

### 2.2.6 FTIR-ATR

In addition to NMR characterisation, FTIR-ATR was also carried out on the DAIL ionic liquid. A small portion of ionic liquid was added for FTIR-ATR analysis. The background was then corrected to eliminate interference from the gases and the analysis instrument itself. The spectral range was between  $4000\text{ cm}^{-1}$  (wavenumber) and  $400\text{ cm}^{-1}$ . This experiment was carried out at room temperature.

## 2.3 EMIM ETSO<sub>4</sub> Ionic Liquid

1-Ethyl-3-Methylimidazolium Ethylsulphate [EMIM] [ETSO<sub>4</sub>] is an ionic liquid that was used in this dissertation to compare it with our synthesized ionic liquid. [EMIM ETSO<sub>4</sub>] was used in one-pot transesterification reaction. This ionic liquid has many applications in areas such as chemistry and electrochemistry due to its unique properties, such as low volatility, high thermal stability, and tunable solvation properties. These characteristics make it useful in applications like catalysis, separation processes, and as electrolytes in batteries and supercapacitors.

The properties of low volatility and high thermal stability of ionic liquids like 1-Ethyl-3-Methylimidazolium Ethylsulphate are widely recognized, making them ideal for various industrial and laboratory applications (Plechova & Seddon, 2008). Additionally, their tunable solvation properties and role as electrolytes in electrochemical devices have been extensively studied (MacFarlane et al., 2014).

In the field of catalysis and separation processes, ionic liquids have shown significant promise due to their unique solvation characteristics and ability to dissolve a wide range of compounds, thus facilitating various chemical reactions and separations (Zhou & Bian, 2013; Wasserscheid & Welton, 2008).

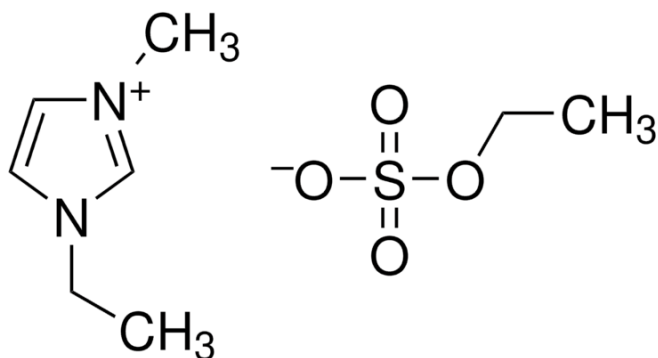


Figure 10- Chemical formula of 1-Ethyl-3-Methylimidazolium Ethylsulphate [EMIM][ETSO<sub>4</sub>]. (Sigma-Aldrich)

### 2.3.1 Nuclear Magnetic Resonance of [EMIM ETSO<sub>4</sub>]

A <sup>1</sup>H NMR was carried out to see if the ionic liquid was pure or not. Nuclear Magnetic Resonance (NMR) spectra were obtained via Bruker ARX400 400MHz at 298K, analysed with MestreNova. The NMR was carried out by the FCT-NOVA analysis laboratories.

## 2.4 GC-FID Analysis

The gas chromatograph with flame ionization detector (GC-FID) Agilent 6890 is used for the separation and identification of volatile organic compounds. Configuration includes a front inlet with Split/Splitless mode and Electronic Pneumatic Control (EPC), along with a front-facing FID detector. The VF5ms column is 30 meters long, with an internal diameter of 250 μm and a film thickness of 0.25 μm. Helium is used as the carrier gas.

Operational conditions are:

- Injector at 250°C with split mode and a pressure of 11.56 psi, split ratio 10:1.
- FID detector at 250°C, with hydrogen flow at 30 mL/min and air flow at 300 mL/min, flame and electrometer turned on.
- Pre-washes and post-washes with 8.00 μL of solvent over 5 cycles.
- Sample fill volume is 2.00 μL, injected at a speed of 20.00 μL/s.
- Pre-injection and post-injection dwell times are 1 second and 3 seconds, respectively.

Temperature programming of the oven:

- Starts at 40°C with a 1-minute hold time.
- Ramps up at 10°C/min to 150°C, holds for 15 minutes.
- Ramps at 5°C/min to 250°C, no hold time.
- Ramps at 10°C/min to 320°C, holds for 15 minutes.

The total heating program time was 69 minutes. Mobile phase flow rate was 1 mL/min, with automatic stop after 69 minutes. Chromatogram data was recorded and stored. After analysis, the integrations of the areas of each compound were corrected manually. A commercial standard with a complex of methyl esters was analysed along with samples. The GC analysis was carried out by the FCT-NOVA analysis laboratories.

## 2.5 Direct transesterification Assays

The integrated process for obtaining biodiesel addressed in this study involved, as first approach the simultaneous extraction and transesterification of triglycerides and free fatty acids contained in algal biomass oil. The fatty acid esters (FAMEs) obtained in this way were then removed from the reaction medium by extraction with hexane. The scheme of the general procedure is described in the figure 11.

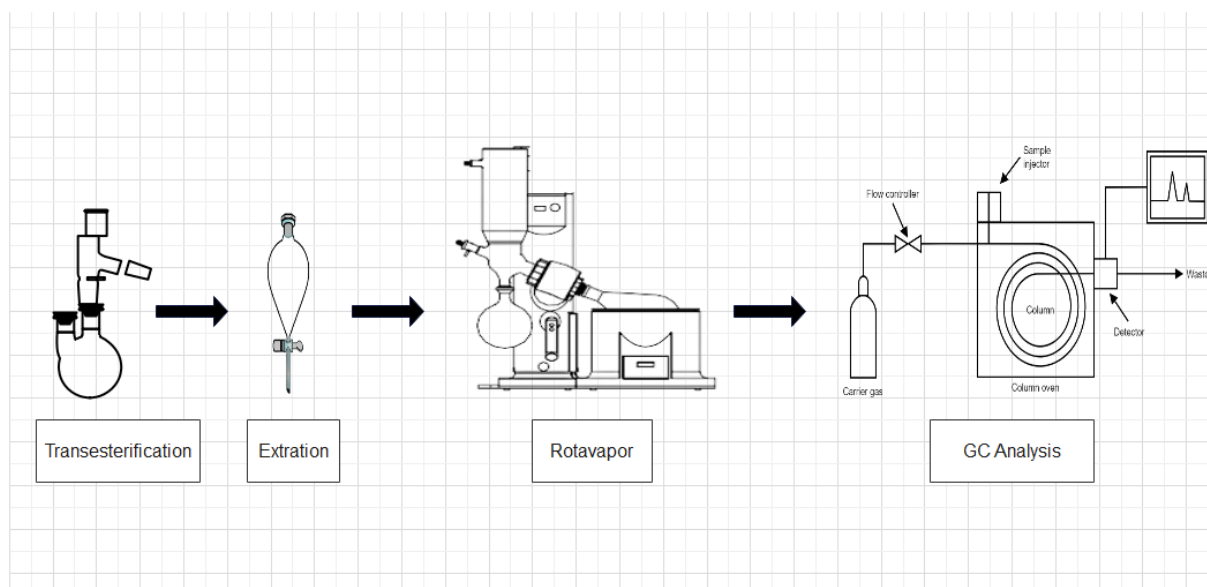


Figure 11- Diagram of the main steps from the reaction to GC analysis.

The first phase of this work was focused on the need to evaluate the overall efficiency of the process, considering the efficiency in the catalysis and FAMEs extraction steps. For this purpose, catalytic tests for the esterification of benzoic acid were carried out using traditionally used catalysts such as  $H_2SO_4$ , NaOH, HCl, or the combination of  $H_2SO_4$  and NaOH. These results were compared with those obtained under the same conditions for the two ILs tested (DAIL and [EMIM ETSO<sub>4</sub>] or the two ILs in combination with an acid or base. The tetradecane (C14) standard was used to assess any losses in the extraction step. The nonane (C9) standard was used as an internal standard for the determination of FAME by GC. These tests were initially conducted without algae. The introduction of algae was subsequently carried out for the trials with better results. As no FAMEs' peaks of interest were observed on the chromatograms obtained from these samples, a decision was made to implement a pre-treatment using microwave irradiation, either assisted or not by DAIL. A schematic diagram illustrating this second approach is depicted in Figure 12.

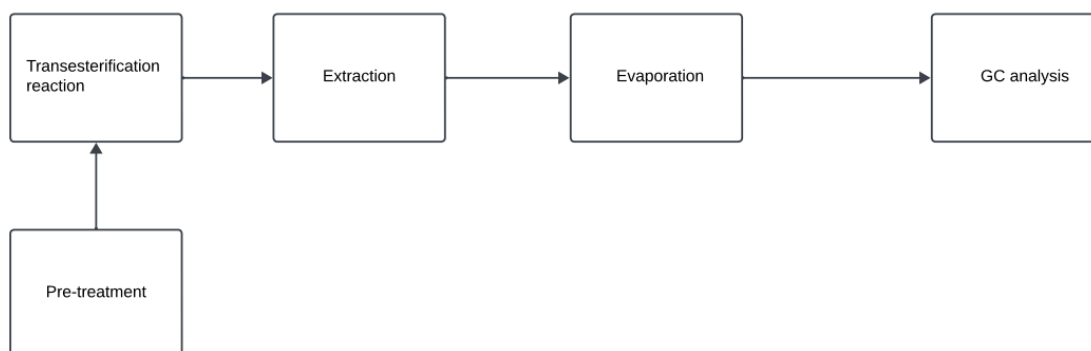


Figure 12 - Diagram of all the steps from pre-treatment to GC analysis.

## 2.5.1 Testing the integrated catalysis and FAME's extraction process

### 2.5.1.1 Optimizing Catalysis conditions

The integrated system, which involves catalysis followed by FAME's extraction (as depicted in Figure 12), was tested using two ILs as catalysts, along with traditional catalysts, in esterification reactions. Variables such as catalyst quantity, temperature, and sequential use of two catalysts were also investigated (table 3). Catalytic efficiency was assessed by determining the yield of

benzoic acid esterification into methyl benzoate. Additionally, the efficiency of the extraction process was evaluated by monitoring the recovered amount of inert C14 at the end of the process. The conditions that yielded the best benzoic acid esterification yields were then applied in the presence of algae. In this scenario, the amount of extract was determined for various assays, along with the corresponding chromatograms obtained. In general, the standard procedure for the catalytic reaction was to weight/measure all the components of the reaction and add them to a round-bottomed flask (for complete information on the used amounts for the different assays, please see table 3). The temperature of this reaction was controlled by a thermopar associated to the heating system. A cooling system was associated to the balloon to avoid solvent evaporation. The reaction was magnetically stirred for the time proposed for each test (see table 3). Once the reaction was complete, the flask was allowed to cool to room temperature before proceeding with the extraction. Benzoic acid was used because it was a fatty acid that stood out in the complex chromatograms of algae extracts.

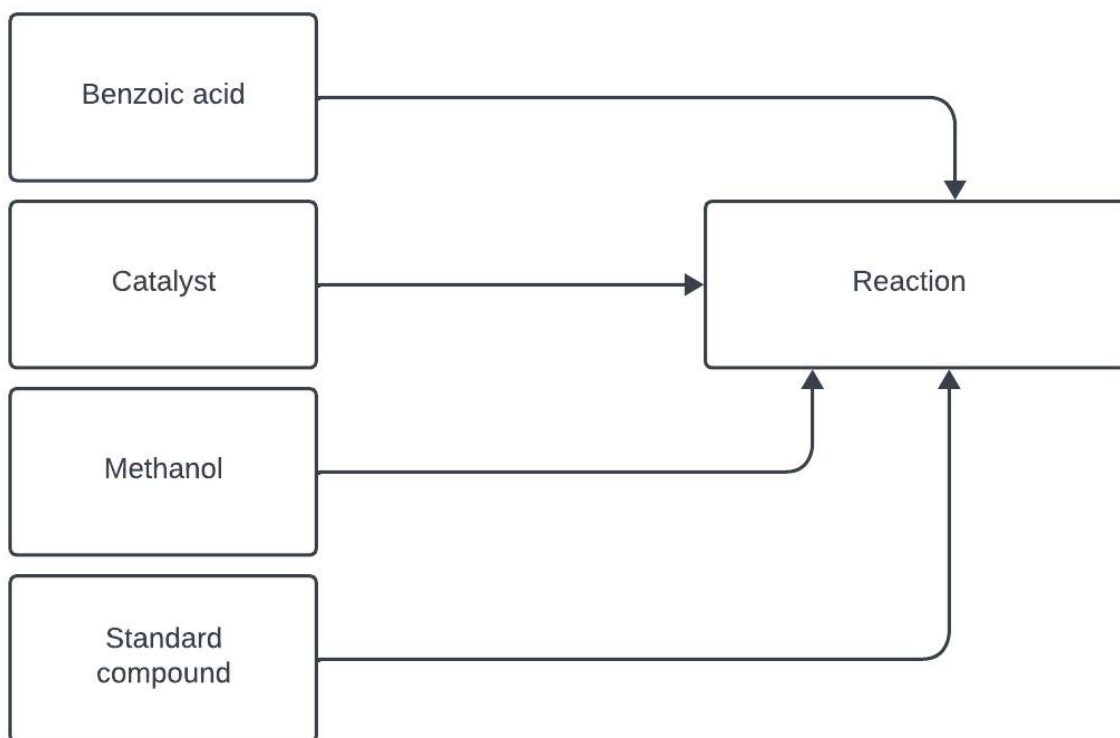


Figure 13 -Diagram of the transesterification reaction with benzoic acid, catalyst, methanol and C14.

Extraction with hexane as shown in figure 14 was carried out in the first tests with a total volume of 30 mL. In addition to the hexane, sodium chloride was added at a concentration of 20% for

better separation/visualization of the phases. The extraction was carried out in batches of 10mL each time to achieve improved extraction efficiency.

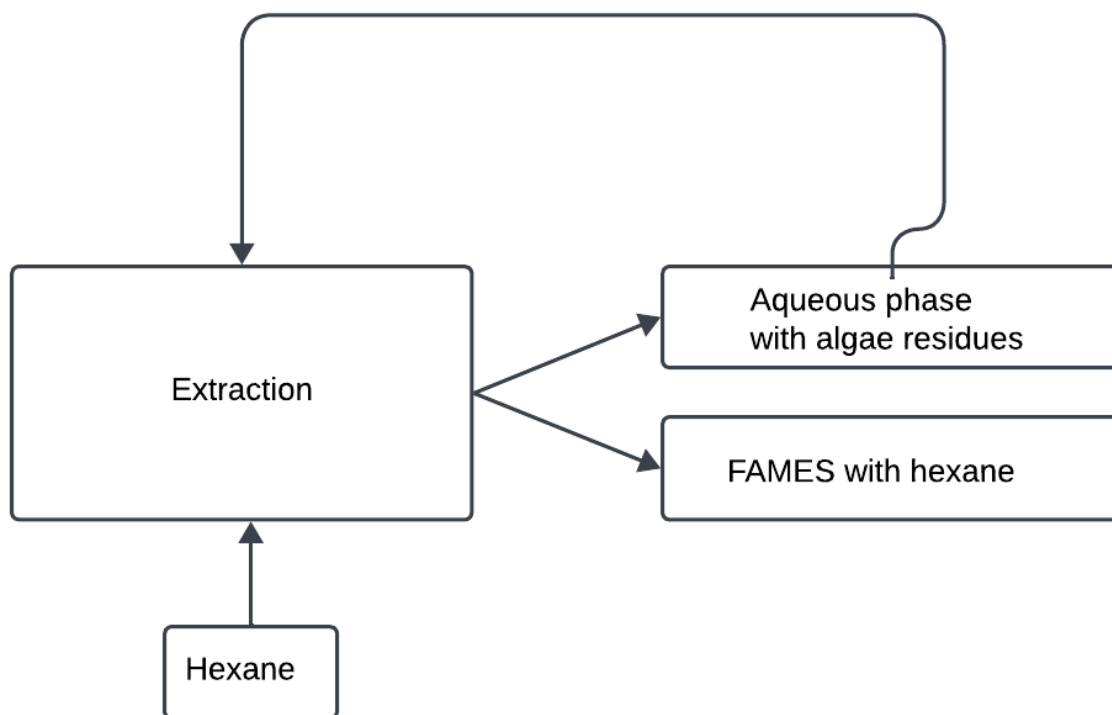


Figure 14 - Diagram of the FAMES extraction process with hexane.

Table 3 describes the conditions used in the different performed assays and some observations about that sample. As previously referred, the used catalysts were  $H_2SO_4$ , NaOH, DAIL  $[N_{4.1} 2OH_{2.0H}]_2[COOCH_2CHSO_3HCOO]$ ,  $[EMIM ETSO_4]$  and HCl. Temperature variation and reaction duration were also tested. The temperature ranged from 60°C to 70°C. The time taken for each reaction was 24 hours. The volume of methanol used in all the assays was of 10 mL and for those assays with algae, the used Chlorella mass was 0.1 g.

Table 3 - It describes the different conditions used to optimise the reagents (without algae). This table also describes each component used, such as benzoic acid, standard compounds, time, catalysts, solvent and temperature. Volume of used methanol was 10 mL; mass of used Benzoic acid was 1 mg. Volume of used C14 and C9 was 1 uL. The reaction time was 24 hours.

	TEMPERATURE (°C)	H <sub>2</sub> SO <sub>4</sub> (uL)	[EMIM ETSO <sub>4</sub> ] (mg)	DAIL (mg)	NaOH (uL)	HCl (uL)	Observations
A1	60	-	-	-	-	-	-
A2	60	22	-	-	200	-	2 steps reaction
A3	60	-	-	-	200	-	-
A4	60	-	-	100	-	-	-
A5	60	22	-	-	-	-	-
A6	60	-	100	-	-	-	-
A7	60	-	-	-	-	2	-
A8	60	22	-	100	-	-	2 steps reaction
A9	70	-	-	100	-	-	It has a temperature of 70°C
A10	60	-	-	100	-	2	2 steps reaction

### 2.5.1.2 Optimizing one-pot reaction

The optimized conditions for the catalysis of benzoic acid transesterification were applied to the one pot transesterification of lipids from algae.

For the assays performed using the algae, the solution after reaction was decanted and supernatant processed as described before. The residue was also extracted with fresh hexane (10 mL) and the extracted added to the one obtained from supernatant. The organic phase containing hexane and FAMES was dehydrated using sodium sulphate, filtered and introduced into a previously weighed round bottom balloon. The balloon containing the FAMES was taken to the rotavator to dry and then weighed after drying. Then 1.5mL of hexane is added, filtered, and after the internal standard, 1 uL nonadecane added. The samples were then taken to the analysis laboratory for GC analysis.

Once the ideal conditions had been found, the reactions with the algae began. Instead of benzoic acid, the tests were carried out with algae as shown in figure 15. The procedure was the same as in chapter 2.5.1.1.

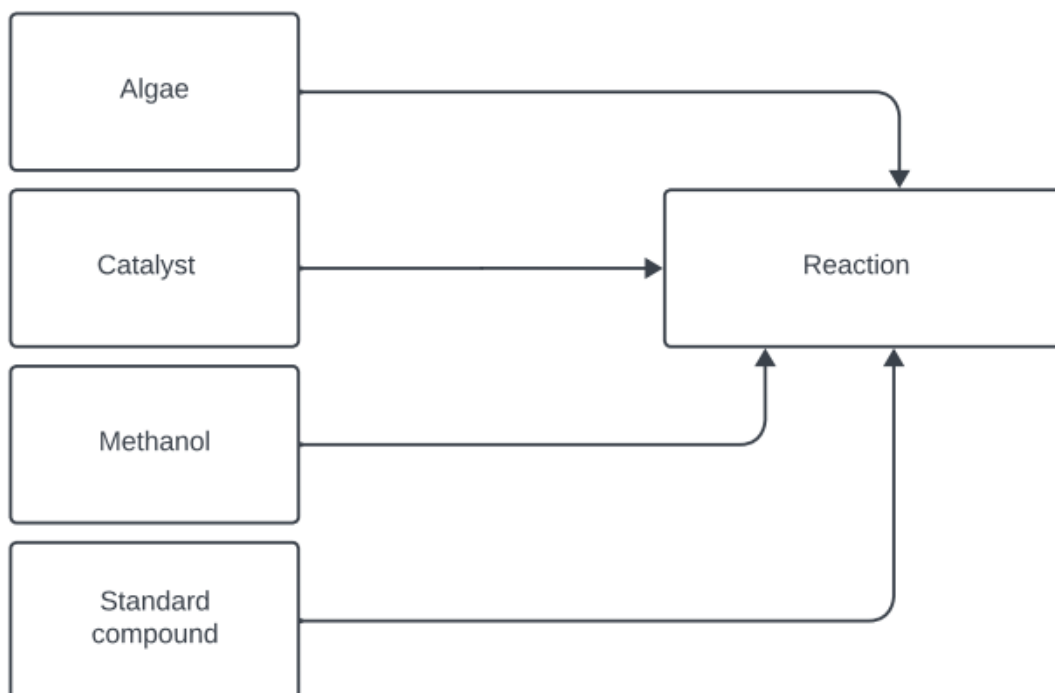


Figure 15- Diagram of the transesterification reaction with benzoic acid, microalgae, catalyst, methanol and C14.

After conditions have been optimized, assays were carried out with the introduction of algae biomass, a more complex matrix than benzoic acid. Despite the presence of algae, benzoic acid was continuously added to the reaction mixture to assess whether the extraction yield for this isolated component remained consistent with previous assays.

Samples B1 to B4 have H<sub>2</sub>SO<sub>4</sub> and DAIL [N<sub>4</sub> 1 2OH 2OH]<sub>2</sub>[COOCH<sub>2</sub>CHSO<sub>3</sub>HCOO] as catalysts. The volume of methanol used was 10 mL. The mass of benzoic acid used was 1 mg. The volumes of standards C14 and C9 were 1uL. The temperature used was 60°C. The reaction time was 24 hours except for sample B4, which was 48 hours. In sample B2 and B4 to B8, the extraction process was changed from 30 mL of hexane to 50mL. B2 and B4 to B8 the extraction was done with 50mL of hexane. Samples B1 and B3 still used 30 mL of hexane. The sample description and their observations are shown in table 4.

Table 4- Table with the names of each sample, their description and some important observations. This table contains the samples referring to the essays with algae. The samples B1 to B4 don't have pre-treatment. Volume of used methanol was 10 mL; mass of used Benzoic acid was 1 mg. Volume of used C14 and C9 was 1 uL. Temperature used was 60°C. Time used was 24 hours except B4 was 48 hours.

Samples	Sample de- scription	DAIL (mg)	H <sub>2</sub> SO <sub>4</sub> (uL) [C]=100ppm	Observa- tions
<b>B1</b>	Sample with H <sub>2</sub> SO <sub>4</sub>	-	22	-
<b>B2</b>	Sample with H <sub>2</sub> SO <sub>4</sub>	-	22	Different extraction pro- cess*
<b>B3</b>	Sample with DAIL	100	-	-
<b>B4</b>	Sample with DAIL/H <sub>2</sub> SO <sub>4</sub>	100	22	-

\* The extraction process was changed to 50 mL instead of 30 mL. This was applied to B2 and B4 to B8.

Note: Sample B1 and B3 used a different extraction process 30 mL (see the text above table 4).

The absence of peaks of interest in the chromatograms obtained in the various assays conducted in the presence of algae (see results section) led to the necessity of addressing the utilization of a pre-treatment prior to the transesterification reaction. The pre-treatment was carried out by microwave (MW) action, and in some cases, with the combined action of the IL. These assays were performed solely with the DAIL. The solvent used in the pre-treatment was methanol for all samples.

The description for samples with pre-treatment is shown in table 5.

After the first two microwave tests, it was tried the approach of adding the ionic liquid before the pre-treatment took place. As the ionic liquid has properties that can also weaken the cell wall, these tests were carried out. The aim was to try to increase the efficiency of the pre-treatment using the properties of the ionic liquid.

Table 5 describes the conditions used in the different performed assays. As previously referred, the used catalysts were  $H_2SO_4$  and DAIL  $[N_{4,1,2OH,2OH}]_2[COOCH_2CHSO_3HCOO]$ . Temperature variation and reaction duration were also tested. The temperature was  $60^\circ C$ . The time taken for each reaction was 24 hours. The volume of methanol used in all the assays was of 10 mL and for those assays with algae, the used Chlorella mass was 0.1 g.

Table 5- Table with the names of each sample, their description and some important observations. This table contains the samples referring to the essays with algae. These samples have pre-treatment. MW conditions are 5 minutes, 60°C and 750W.

Sample	DAIL (mg)	H <sub>2</sub> SO <sub>4</sub> (uL) [C]=100ppm	Observations:
B5	100	-	DAIL added during pre-treatment
B6	100	-	DAIL added after pre-treatment
B7	100	22	DAIL added during pre-treatment and H <sub>2</sub> SO <sub>4</sub> added after pretreatment
B8	100	22	DAIL and H <sub>2</sub> SO <sub>4</sub> added after pre-treatment.

## 2.6 Calculating the concentration of FAMES

The FAMES were determined using an GC (see 2.2 GC-FID Analysis), after which each chromatogram was analysed and compared with a standard chromatogram containing all the esters (see appendix). The FAMES were determined using an GC (see 2.2 GC-FID Analysis), after which each chromatogram was analysed and compared with the used mix standard's chromatogram containing all the esters (see appendix). The standard mix is from Supelco: Mix 37 FAMES supelco 47885-U. The composition is:

- Methyl butyrate 400  $\mu$  g/mL
- Methyl hexanoate 400  $\mu$  g/mL
- Methyl octanoate 400  $\mu$  g/mL
- Methyl decanoate 400  $\mu$  g/mL
- Methyl undecanoate 200  $\mu$  g/mL
- Methyl laurate 400  $\mu$  g/mL

- Methyl tridecanoate 200  $\mu$  g/mL
- Methyl myristate 400  $\mu$  g/mL
- Methyl myristoleate 200  $\mu$  g/mL
- Methyl pentadecanoate 200  $\mu$  g/mL
- Methyl cis-10-pentadecenoate 200  $\mu$  g/mL
- Methyl palmitate 600  $\mu$  g/mL
- Methyl palmitoleate 200  $\mu$  g/mL
- Methyl heptadecanoate 200  $\mu$  g/mL
- cis-10-Heptadecenoic acid methyl ester 200  $\mu$  g/mL
- Methyl stearate 400  $\mu$  g/mL
- trans-9-Elaidic acid methyl ester 200  $\mu$  g/mL
- cis-9-Oleic acid methyl ester 400  $\mu$  g/mL
- Methyl linolelaidate 200  $\mu$  g/mL
- Methyl linoleate 200  $\mu$  g/mL
- Methyl arachidate 400  $\mu$  g/mL
- Methyl  $\gamma$ -linolenate 200  $\mu$  g/mL
- Methyl cis-11-eicosenoate  $\leq$  200  $\mu$  g/mL
- Methyl linolenate 200  $\mu$  g/mL
- Methyl heneicosanoate 200  $\mu$  g/mL
- cis-11,14-Eicosadienoic acid methyl ester 200  $\mu$  g/mL
- Methyl behenate 400  $\mu$  g/mL
- cis-8,11,14-Eicosatrienoic acid methyl ester 200  $\mu$  g/mL
- Methyl erucate 200  $\mu$  g/mL
- cis-11,14,17-Eicosatrienoic acid methyl ester 200  $\mu$  g/mL
- cis-5,8,11,14-Eicosatetraenoic acid methyl ester 200  $\mu$  g/mL
- Methyl tricosanoate 200  $\mu$  g/mL
- cis-13,16-Docosadienoic acid methyl ester 200  $\mu$  g/mL
- Methyl lignocerate 400  $\mu$  g/mL
- cis-5,8,11,14,17-Eicosapentaenoic acid methyl ester 200  $\mu$  g/mL
- Methyl nervonate 200  $\mu$  g/mL
- cis-4,7,10,13,16,19-Docosahexaenoic acid methyl ester 200  $\mu$  g/mL

The retention times for each ester are shown below in table 6.

Table 6 - Retention times in minutes for each ester. Suska-Malawska et al. (2022)

Compound	Retention Time [min]
C6:0	3.18 ± 0.008
C8:0	4.69 ± 0.004
C10:0	6.14 ± 0.005
C12:0	7.45 ± 0.018
C13:0	8.03 ± 0.006
C14:0	8.68 ± 0.008
C15:0	9.39 ± 0.034
C16:1	10.14 ± 0.011
C16:0	10.37 ± 0.015
C17:1	11.28 ± 0.015
C17:0	11.54 ± 0.015
C18 unsat mix	12.84 ± 0.046
C18:0	13.22 ± 0.022
C22:0	27.49 ± 0.006

The FAMES present in each sample chromatogram were identified by comparison of the retention times in both sample and standard chromatograms and, areas integrated. The concentrations were determined based on the Internal Standard Method (NASCIMENTO, Ronaldo Ferreira do et al), according to Eq 1. and Eq.2.

The internal standard method in chromatography is a technique used to improve the precision and accuracy of analytical quantifications. This method is useful for correcting variations in the injected volume, detector response or other variables that may affect the analysis. The technique consists of adding a substance of known concentration, the internal standard, to all samples and standards prior to chromatographic analysis. The internal standard must have equivalent properties to the analyte, but with a different retention time. After analysis, the ratio between the peak areas of the analyte and the internal standard is calculated.

$$\frac{y_A}{y_{PI}} = F \left( \frac{C_A}{C_{PI}} \right) \quad (\text{Eq.1})$$

Being,

$$F = \frac{CA}{CPI} \text{ (Eq.2)}$$

In which:

yA: The analytical signal of the sample

yPI: The analytical signal of the internal standard

F: The adjustment factor or the proportionality constant

CA: The concentration of the analyte in the sample

CPI: The concentration of the internal standard in the sample



## 3. RESULTS AND DISCUSSION

### 3.1 Characterization of the synthesized ionic liquid

The elucidation of the chemical structure of DAIL and its precursors was performed by  $^1\text{H}$ - and  $^{13}\text{C}$  – NMR and FTIR-ATR.

#### 3.1.1 Nuclear Magnetic Resonance of IL precursor

Figures 16 and 17 illustrate the  $^1\text{H}$ -NMR and  $^{13}\text{C}$ -NMR spectra of the precursor ionic liquid.

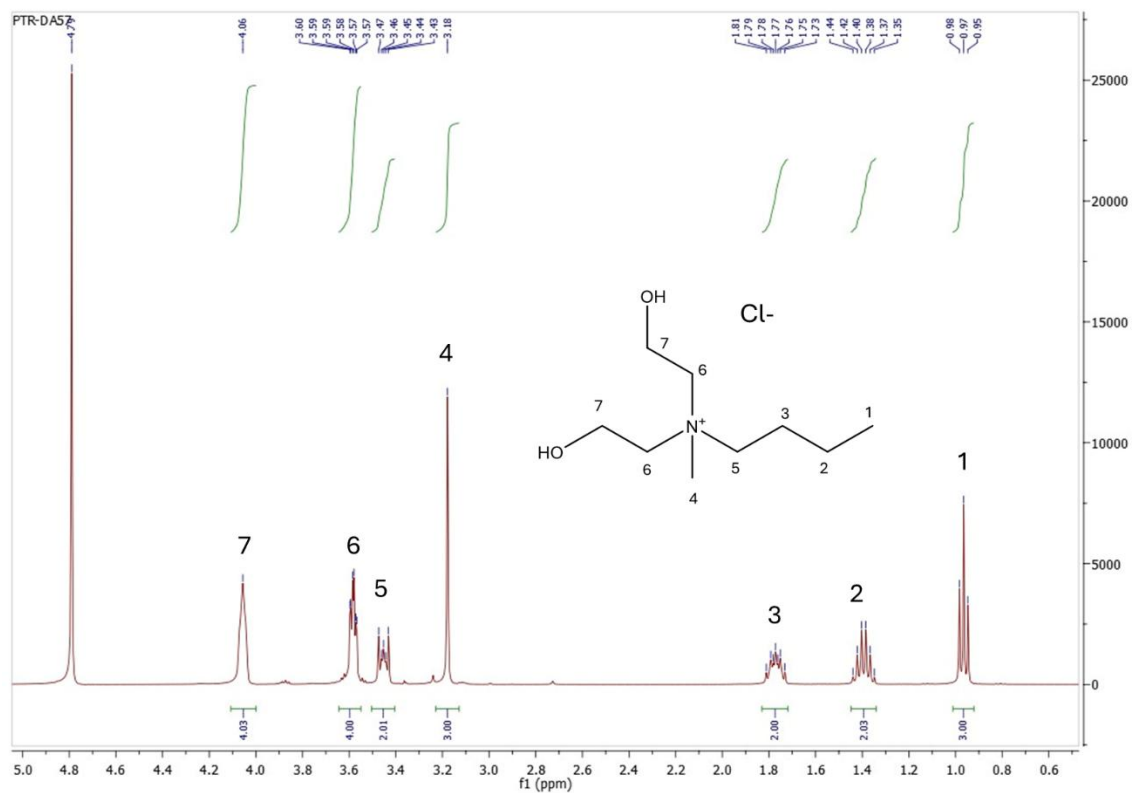


Figure 16 -  $^1\text{H}$  NMR spectrum of IL precursor.

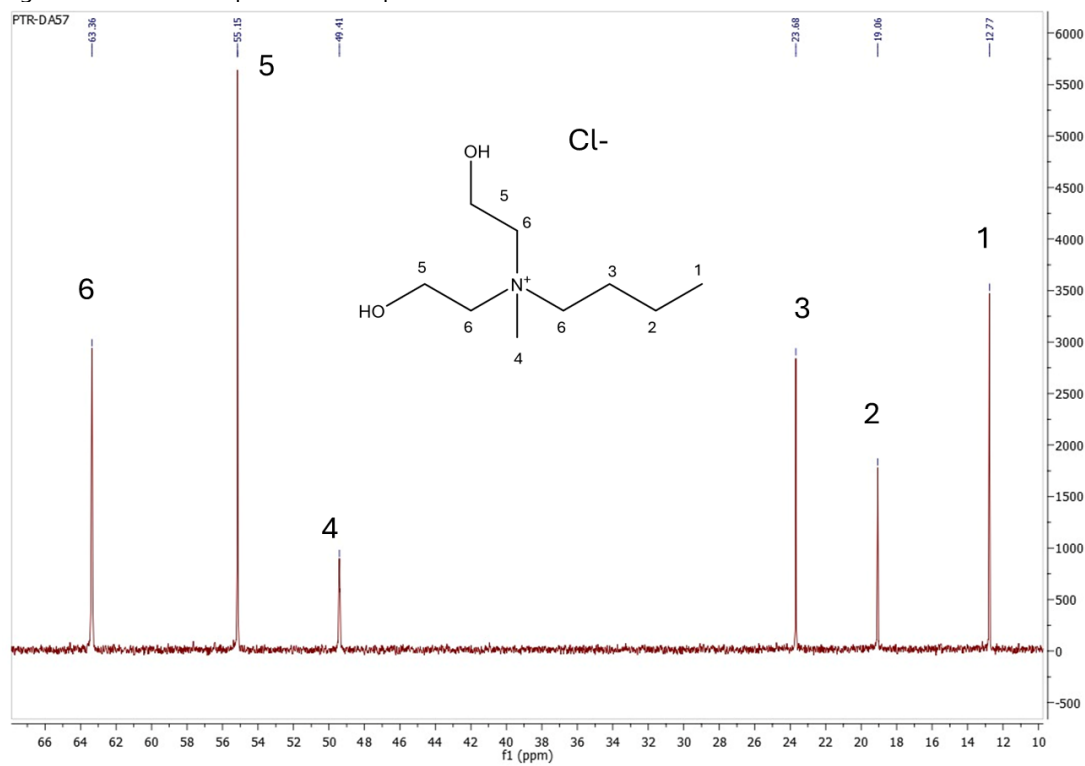


Figure 17-  $^{13}\text{C}$  NMR spectrum of IL precursor.

$^{13}\text{C}$  NMR ( $\text{D}_2\text{O}$ , 100 MHz)  $\delta$ : 12.77 ( $\text{C}_\alpha\text{H}_2\text{CH}_2\text{CH}_2\text{CH}_2\text{N}$ ), 19.06 ( $\text{CH}_3\text{C}_\alpha\text{H}_2\text{CH}_2\text{CH}_2\text{N}$ ), 23.68 ( $\text{CH}_3\text{CH}_2\text{C}_\alpha\text{H}_2\text{CH}_2\text{N}$ ), 49.41 ( $\text{NCH}_3$ ), 55.15 ( $\text{N}(\text{CH}_2\text{CH}_2\text{OH})_2$ ), 63.36 ( $\text{CH}_3\text{CH}_2\text{CH}_2\text{C}_\alpha\text{H}_2\text{N}$ ,  $\text{N}(\text{CH}_2\text{CH}_2\text{OH})_2$ ) ppm.

### 3.1.2 Nuclear Magnetic Resonance of DAIL

Figure 18 and 19 illustrates the  $^1\text{H}$ -NMR and  $^{13}\text{C}$ -NMR spectrum of DAIL where all expected signals from cation and anion as well as respective integration was observed. The cation-anion (2:1) proportion is confirmed.

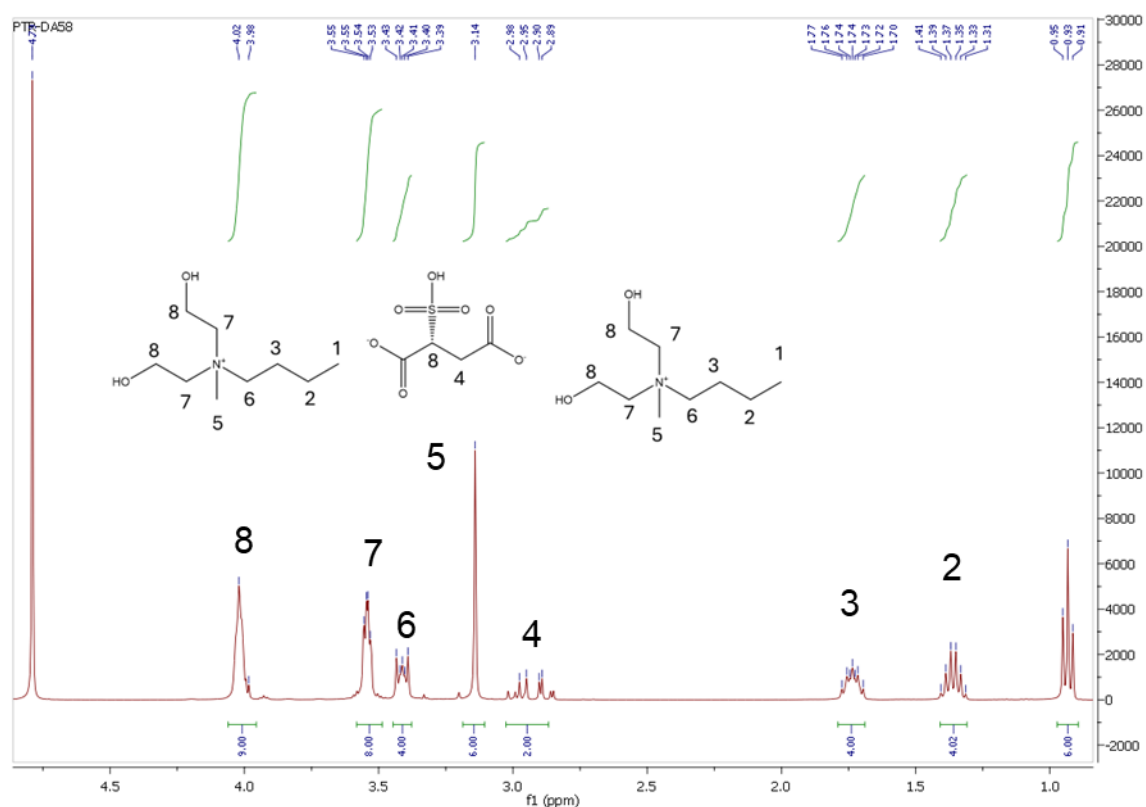


Figure 18 -  $^1\text{H}$  NMR spectrum of DAIL.

$^1\text{H}$  NMR ( $\text{D}_2\text{O}$ , 400 MHz)  $\delta$ : 0.93 (t, 6H,  $J = 8$  Hz,  $2(\text{CH}_3\text{CH}_2\text{CH}_2\text{CH}_2\text{N})$ ), 1.36 (sxt, 4H,  $J = 8$  Hz  $2(\text{CH}_3\text{CH}_2\text{CH}_2\text{CH}_2\text{N})$ ), 1.70-1.77 (m, 4H,  $2(\text{CH}_3\text{CH}_2\text{CH}_2\text{CH}_2\text{N})$ ), 2.89-2.98 (m, 2H, ( $\text{OOCCHSO}_3\text{HCH}_2\text{COO}$ )), 3.14 (s, 6H,  $2(\text{NCH}_3)$ ), 3.39-3.43 (m, 4H,  $2(\text{CH}_3\text{CH}_2\text{CH}_2\text{CH}_2\text{N})$ ), 3.53-3.55 (m, 8H,  $2(\text{N}(\text{CH}_2\text{CH}_2\text{OH})_2)$ ), 3.98-4.02 (m, 9H,  $2(\text{N}(\text{CH}_2\text{CH}_2\text{OH})_2)$ , ( $\text{OOCCHSO}_3\text{HCH}_2\text{COO}$ )) ppm.

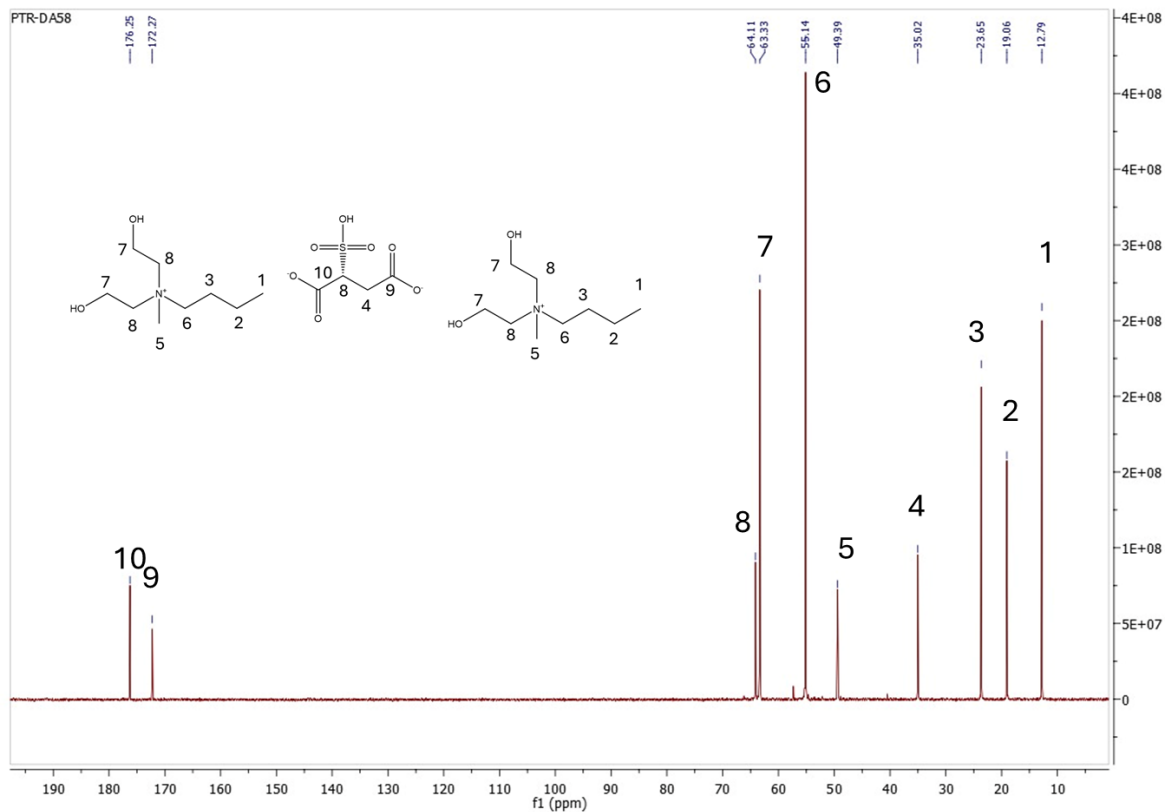


Figure 19 -  $^{13}\text{C}$  NMR spectrum of DAIL.

$^{13}\text{C}$  NMR ( $\text{D}_2\text{O}$ , 100 MHz)  $\delta$  : 12.79 ( $2(\text{CH}_3\text{CH}_2\text{CH}_2\text{CH}_2\text{N})$ ), 19.06 ( $2(\text{CH}_3\text{CH}_2\text{CH}_2\text{CH}_2\text{N})$ ), 23.65 ( $2(\text{CH}_3\text{CH}_2\text{CH}_2\text{CH}_2\text{N})$ ), 35.02 ( $\text{OOCCHSO}_3\text{HCH}_2\text{COO}$ ), 49.39 ( $2(\text{NCH}_3)$ ), 55.14 ( $2(\text{N}(\text{CH}_2\text{CH}_2\text{OH})_2)$ ), 63.33 ( $2(\text{CH}_3\text{CH}_2\text{CH}_2\text{CH}_2\text{N})$ ,  $2(\text{N}(\text{CH}_2\text{CH}_2\text{OH})_2)$ ), 64.11 ( $\text{OOCCHSO}_3\text{HCH}_2\text{COO}$ ), 172.27 ( $\text{OOCCHSO}_3\text{HCH}_2\text{COO}$ ), 176.25 ( $\text{OOCCHSO}_3\text{HCH}_2\text{COO}$ ) ppm.

### 3.1.3 FTIR of DAIL

The FTIR graph presented shows absorbance as a function of molecular vibration frequency. The frequency is represented on the horizontal axis in  $\text{cm}^{-1}$ , while the absorbance is represented on the vertical axis in arbitrary units. The graph has several peaks, each corresponding to a specific vibration frequency of a functional group in the molecule.

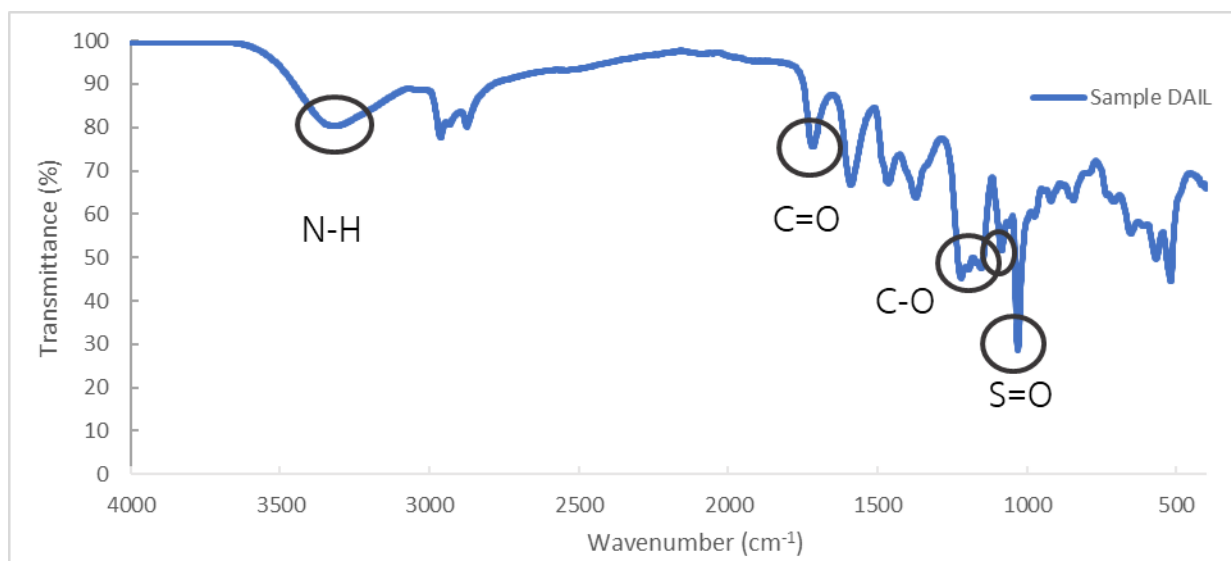


Figure 20- FTIR of sample DAIL.

The broad peak around  $3300\text{ cm}^{-1}$  might be due to N-H stretching vibrations. However, due to the broadness, it could also be due to residual water vapor from the atmosphere or during sample preparation. The peak around  $1750\text{ cm}^{-1}$  could be indicative of a C=O stretching vibration, suggesting the presence of a carbonyl group. The peaks at  $1030$  and  $1226\text{ cm}^{-1}$  represent the S=O (asym) and S=O (sym) bonds of the sulfonic acid group, respectively. Other peaks in the  $1200\text{-}1300\text{ cm}^{-1}$  region could be due to C-O stretching vibrations from various functional groups.

### 3.1.4 DSC of DAIL

The DSC graph presented on Figure 21 shows the variation in heat flow as a function of temperature.

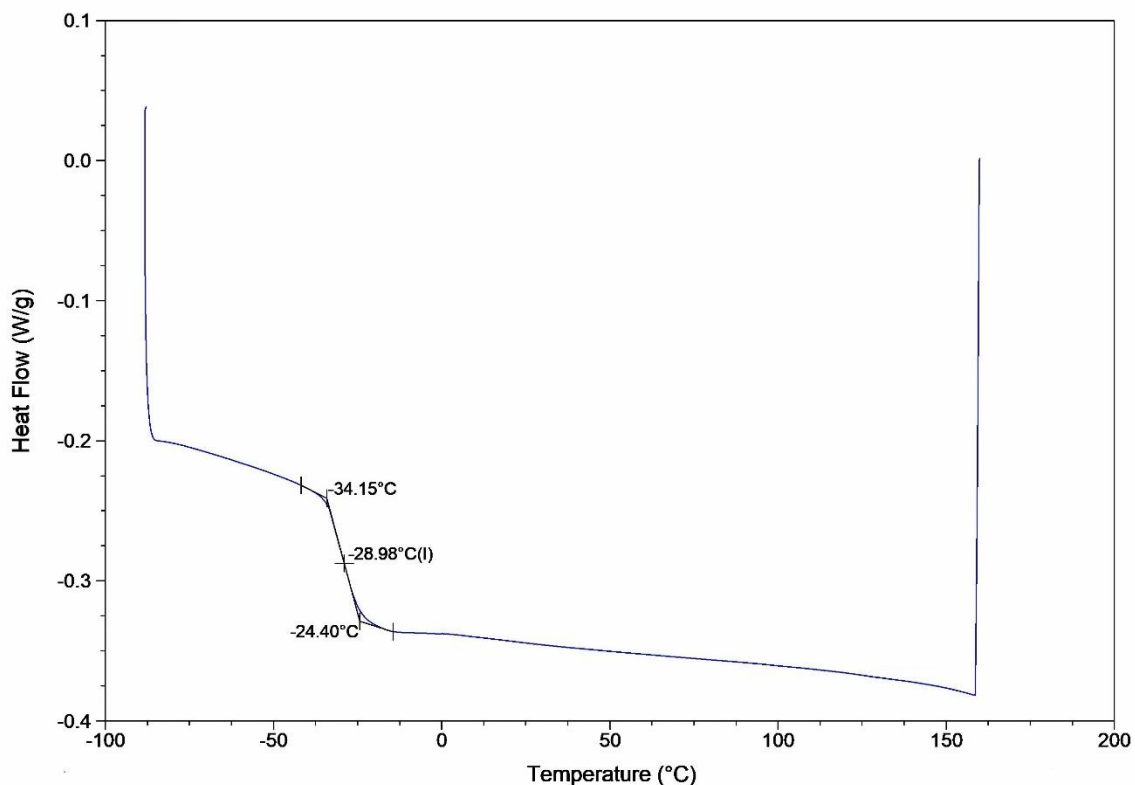


Figure 21- Thermogram of the second heating cycle of the Ionic liquid DAIL where the Tg is 28,98°C.

Of the 6 cycles carried out, 3 heating cycles and 3 cooling cycles, there was no variation beyond the Tg mentioned in the thermogram in figure 21. In the first cycle occur the release of water. No other thermal events were observed, so only the thermogram of the 2nd heating cycle, from which the Tg was calculated is being showed. The value for the Tg is 28.98°C.

## 3.2 Nuclear Magnetic Resonance of [EMIM ETSO<sub>4</sub>]

Figure 22 and Figure 23 illustrate the <sup>1</sup>H-NMR and <sup>13</sup>C-NMR of EMIM ETSO<sub>4</sub> where all expected signals from cation and anion as well as respective integration was observed.

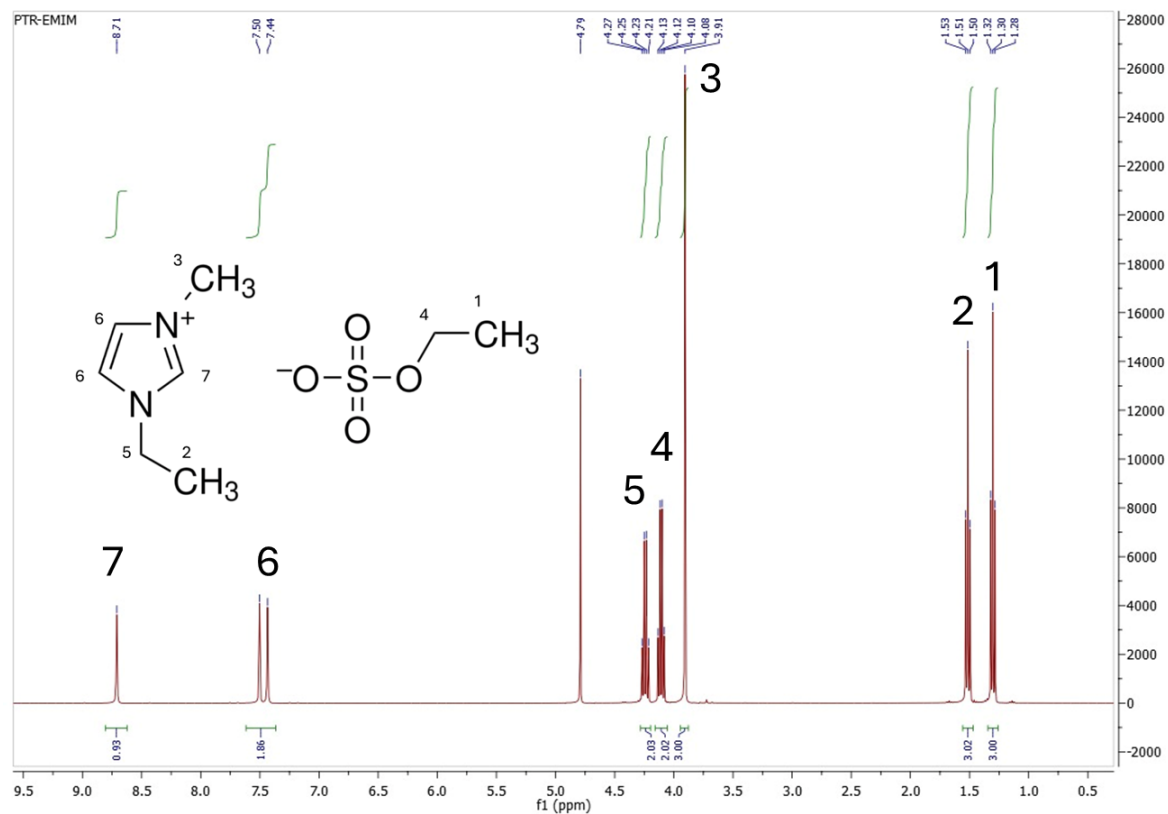


Figure 22 - <sup>1</sup>H NMR spectrum of the Ionic liquid [EMIM ETSO<sub>4</sub>].

<sup>1</sup>H NMR (D<sub>2</sub>O, 400 MHz)  $\delta$  : 1.30 (t, 3H,  $J = 8$  Hz, (CH<sub>3</sub>CH<sub>2</sub>O)), 1.51 (t, 3H,  $J = 6$  Hz, (CH<sub>3</sub>CH<sub>2</sub>N)), 3.91 (s, 3H, (CH<sub>3</sub>N)), 4.11 (q, 2H,  $J = 6.67$  Hz CH<sub>3</sub>CH<sub>2</sub>O)), 4.24 (q, 2H,  $J = 8$  Hz (CH<sub>3</sub>,CH<sub>2</sub>,N)), 7.47 (d, 2H, (NCHCHN)) 8.71 (s,1H, (NCHN)) ppm.

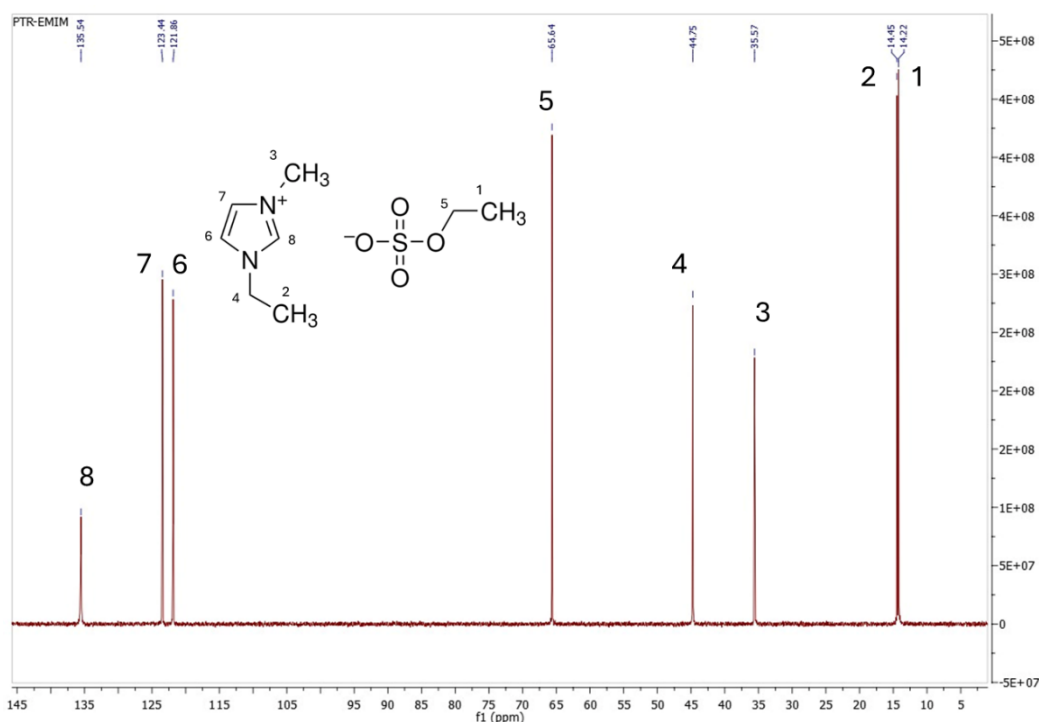


Figure 23 -  $^{13}\text{C}$  NMR spectrum of [EMIM][ETSO<sub>4</sub>].

$^{13}\text{C}$  NMR ( $\text{D}_2\text{O}$ , 100 MHz)  $\delta$ : 14.22 ( $\text{C}_\text{H}_3\text{C}_\text{H}_2\text{O}$ ); 14.45 ( $\text{C}_\text{H}_3\text{C}_\text{H}_2\text{N}$ ); 35.57 ( $\text{C}_\text{H}_3\text{N}$ ); 44.75 ( $\text{C}_\text{H}_3\text{C}_\text{H}_2\text{N}$ ); 65.64 ( $\text{C}_\text{H}_3\text{C}_\text{H}_2\text{O}$ ); 121.86 ( $\text{NCHCHN}$ ); 123.44 ( $\text{NCHCHN}$ ); 135.54 ( $\text{NCHN}$ ) ppm.

### 3.3 Optimization of one-pot reaction conditions

The capacity of used ILs as catalysts was tested for the esterification of benzoic acid to methyl benzoate. Once extraction with hexane was performed after the reaction, the extraction yield was also monitored using the inert tetradecane (C14). Nonane (C9) added as internal standard allowed for the determination of yield methyl benzoate yield for each sample. The results are shown in the table 6, indicating the concentration and yield of each sample. This table is referring to samples without algae.

The recovery of C14 ranged from 20.0% to 69.1% of the initially introduced amount, with an average recovery rate of 29%. This low extraction efficiency may be due to the lower effectiveness of n-hexane compared to other solvents, such as the traditionally used chloroform system.

Table 7- Concentration of methyl benzoate obtained by transesterification of benzoic acid within each sample and the yield related to the initial benzoic acid mass (1mg).

Sample	MB (mg) Y (%)
A1	MB =0,163 Y = 14,7
A2	MB =0,586 Y =52,5
A3	MB =0,456 Y =40,9
A4	MB =0,357 Y =32,0
A5	MB =0,898 Y =80,5
A6	MB =0,262 Y =23,5
A7	MB =0,356 Y =32,0
A8	MB =0,711 Y =63,8
A9	MB =0,310 Y =27,8
A10	MB =0,308 Y =27,6

From table 7 it can be observed that the ILs DAIL (A4) and [EMIM ETSO<sub>4</sub>] (A6) have some catalytic effect since the obtained yields are higher than the one obtained for the non-catalysed reaction (A1) for the reaction. The synthesised ionic liquid DAIL has higher yields than the ionic liquid EMIM ETSO<sub>4</sub>.

Whenever the traditional catalysts are combined with the ionic liquid, the yield decreased by comparison with that of the traditional catalysts. Temperature of reaction appears to have no effect on the yield of the reaction.

Based on the results, the reaction conditions were applied to the reaction in the presence of algae, but it presented some challenges. Under these circumstances, it was not possible to

analyse most of the composition of the extract, as the chromatograms showed a very low peak Intensities in the samples, whether acid or DAIL was used (chromatograms in the appendix). This very low peak Intensities was attributed to an inefficient extraction in the absence of pre-treatment. As a result, it was decided to apply a microwave-based pre-treatment.

### 3.4 Extract's yield for samples without and with pre-treatment

The extracted oil mass for samples without (B1-B4) and with (B5-B8) a pre-treatment and, its yield related to the initial mass of used algae are shown in table 8.

Table 8 - Mass extract and its respective percentage for samples B1 to B8.

Sample	Extracted Mass (g)	Extracted mass (%) (1)
B1	0,011	11,2
B2	0,022	20,3
B3	0,002	2.0
B4	0,014	14,4
B5	0,024	23,9
B6	0,020	20,4
B7	0,033	33,1
B8	0,060	59,4

(1) Percentage of extracted mass related to the mass of used algae (0.1g).

The values obtained for the extracted mass vary between 2.0% and 59.4% depending on the conditions used in the overall process of obtaining FAMEs. Typical values of extracted mass for chlorella in one-pot reactions are 5- 58% (Mata, T. M. et al). The samples with pre-treatment (B5 to B8) are the ones with high extraction yields . The use of H<sub>2</sub>SO<sub>4</sub> In B7 and B8 samples with pre-treatment have higher values than the others. This suggests that these values, particularly for samples B7 to B8, are being inflated by the extraction of other compounds than lipids. It is possible that the H<sub>2</sub>SO<sub>4</sub> acid is an "aggressive" catalyst and ends up hydrolysing various

compounds after the cell wall has been damaged and is permeable by the pre-treatment. Despite this, the pre-treated samples have the highest yields compared to the untreated ones.

According to the literature, the esters most found in the algae *Chlorella vulgaris* are C16 and C18 (Converti et al. (2009), Mata et al. (2010), Rodolfi et al. (2009), Griffiths & Harrison (2009)). Typical FAMES and their concentration values (mg/g lipid extract) for chlorella algae are (Griffiths & Harrison (2009), Converti et al. (2009), Rodolfi et al. (2009), Takagi et al. (2000); Mata et al. (2010); Li et al. (2011) Gouveia & Oliveira (2009)) are presented in Table 9.

Table 9 - Range of FAMES' concentrations (mg ester/g of extrate) for algae Chlorella found in literature.

<b>Esters</b>	<b>Values (mg/g of lipid's extrate)</b>	<b>References</b>
C14:0	1.0 - 2.5	Converti et al. (2009), Mata et al. (2010)
C16:1	0.5 - 2.0	Converti et al. (2009), Rodolfi et al. (2009)
C16:0	5.0 - 15.0	Converti et al. (2009), Mata et al. (2010), Gouveia & Oliveira (2009)
C18:3 cis	2.0 - 10.0	Gouveia & Oliveira (2009), Rodolfi et al. (2009)
C18:2 cis	10.0 - 30.0	Mata et al. (2010), Rodolfi et al. (2009), Griffiths & Harrison (2009)
C18:1 trans	0.5 - 2.0	Converti et al. (2009), Rodolfi et al. (2009), Griffiths & Harrison (2009)
C18:0	0.5 - 2.0	Converti et al. (2009), Gouveia & Oliveira (2009)
C20:5	5.0 - 15.0	Mata et al. (2010), Gouveia & Oliveira (2009), Griffiths & Harrison (2009)
C22:6	5.0 - 15.0	Mata et al. (2010), Gouveia & Oliveira (2009)

Figure 24 shows the profile of FAMES as a percentage of the total identified methyl esters in each sample. The profiles for samples without (top) and with (bottom) pretreatment display slight differences. A broader distribution of FAMES is observed in the pretreated samples, with

a higher prevalence of esters with C20-C24 chains. Conversely, lauric acid methyl ester was detected only in samples without pretreatment, while C18 fatty acid methyl esters are more prominent both quantitatively and qualitatively in these untreated samples.

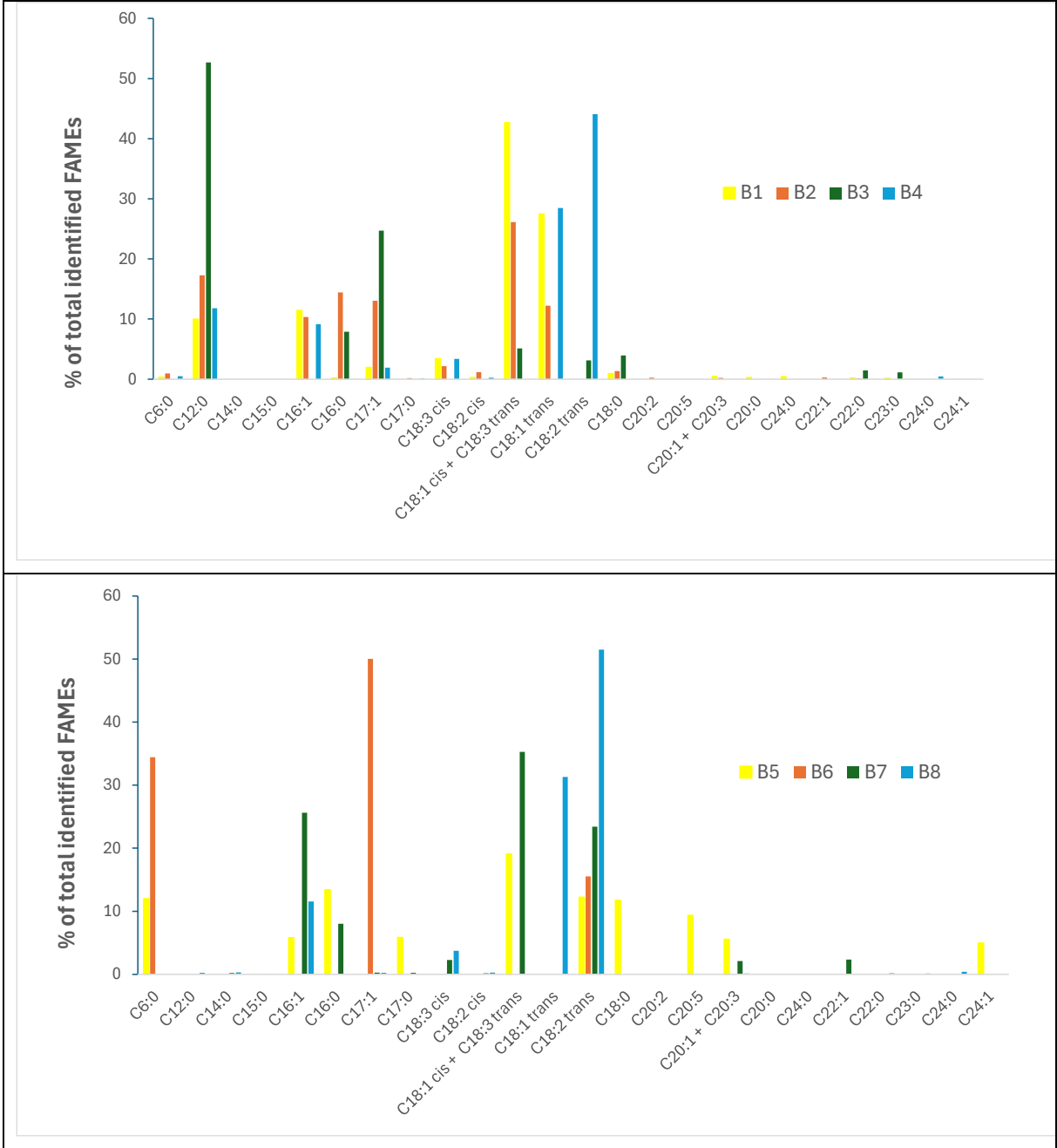


Figure 24- FAMES' profile for samples without (above) and with (below) pre-treatment.

The total amount of identified FAMES in each sample ranged from 0.006 mg in sample B6 to 3.9 mg in sample B2, indicating that the different procedures influenced the extraction and/or transesterification efficiency. The representativity of FAMES in each sample, shown in Table 10, was calculated as the ratio of total identified FAMES to the mass of lipid extract obtained for the various samples. The data suggest that, although greater masses are extracted when pretreatment is applied, the amount of FAMES is significantly lower. This is also observed in samples B7 and B8, where H<sub>2</sub>SO<sub>4</sub> is used, compared to samples B1 and B4, implying that fatty acid degradation may have occurred during pretreatment or that other compounds are being preferentially extracted.

Table 10. Total determined FAMES content in the different samples

Sample	Extract mass (g)	Mass of total determined FAMES (mg)	% FAMES in the extract
B1	0,011	1,466	13,0
B2	0,023	3,895	16,6
B3	0,002	0,111	5,5
B4	0,014	0,940	6,5
B5	0,024	0,019	0,08
B6	0,020	0,006	0,03
B7	0,033	0,614	1,9
B8	0,059	0,721	1,2

In Table 11 are presented the values for the concentration of major FAMES usually found in *Chlorella* microalgae. The concentration was determined based on the amount of extract and on the used amount of used dried algae. After analysing Table 10, the results obtained on the extraction and quantification of FAMES from algae were significantly influenced by the different procedures applied to the samples. Specific samples used H<sub>2</sub>SO<sub>4</sub>, DAIL or a combination of both as catalysts, which had a direct impact on the concentrations of FAMES. Pre-treatment has also an important role on the FAMES extracted. For example, the concentration of C16:1 was significantly higher in B1 and B2 (14,9 and 17,2 respectively) than in the samples that used the ionic liquid as a catalyst, such as B5 and B6, which showed very low or non-detectable

values. This suggests that  $\text{H}_2\text{SO}_4$  was more efficient at both promote the extraction and transesterification of specific FAMEs compared to DAIL. This fact can be observed for instance in samples B7 and B8, which used a combination of  $\text{H}_2\text{SO}_4$  and DAIL, showed different concentrations.

The linoleic acid isomer methyl ester (C18:2 trans) had a higher concentration in B7 and B8 than in B5 and B6, suggesting that  $\text{H}_2\text{SO}_4$  enhanced the catalysis of transesterification of this compound. The combination of  $\text{H}_2\text{SO}_4$  and DAIL may create a synergistic effect, enhancing the catalytic activity and facilitating the transesterification of fatty acids.

Sample B1, which was subjected to a different extraction process from the others, showed unique results compared to the other samples, such as the high values of C12:0 (lauric acid) and C16:1 (palmitoleic acid). This suggests that the old extraction method used in B1 was particularly efficient at extracting these FAMEs. The impact of the extraction method is as important as the catalyst used, since the integrity and efficiency of the extraction can be altered by small variations in the process. As discussed above, samples B5 to B8, which were subjected to a microwave pre-treatment, showed different FAMEs compositions compared to the untreated samples. The microwave seems to have influenced the extraction of certain FAMEs, such as C18:3 cis, which was detected in lower concentrations in B7 and B8, possibly due to thermal degradation during pre-treatment. Pre-treatment with microwaves has been shown to be an important factor affecting the integrity of FAMEs, especially those most sensitive to thermal degradation. Therefore, adjustments to the microwave pre-treatment should be considered for future work.

Table 11- FAMES concentration in mg of FAMES per g of extracted lipid and per g of algae)

Esther/Sample	Concentration							
	(mg of FAME/g of extracted lipid)							
	(mg of FAME/g of algae)							
	B1	B2	B3	B4	B5	B6	B7	B8
<i>C14:0</i>	-	-	-	-	-	-	0,03	0,03
							0,01	0,02
<i>C16:1</i>	14,9	17,2	-	5,9	0,04	-	4,7	1,4
	1,68	4,02	-	0,8	0,01	-	1,5	0,8
<i>C16:0</i>	0,269	24	4,3	-	0,1	-	1,4	-
	0,03	5,6	0,08	-	0,002	-	0,4	-
<i>C17:1</i>	2,51	21,7	13,6	1,2	-	0,1	0,04	0,02
	0,283	5,1	0,27	0,17	-	0,03	0,01	0,01
<i>C17:0</i>	-	0,27	-	0,05	0,04	-	0,04	-
		0,06	-	0,007	0,01	-	0,01	-
<i>C18:3 cis</i>	13,1	3,6	-	2,2	-	-	0,04	0,4
	1,48	0,84	-	0,31	-	-	0,01	0,2
<i>C18:2 cis</i>	0,9	1,9	-	0,14	-	-	0,02	0,03
	0,102	0,45	-	0,02	-	-	0,009	0,01
<i>C18:1 cis + C18:3 trans</i>	154	43,5	2,8	-	0,1	-	6,5	-
	17,3	10,2	0,05	-	0,03	-	2,1	-
<i>C18:1 trans</i>	100	20,3	-	18,6	-	-	-	3,8
	11,3	4,7	-	2,6	-	-	-	2,2
<i>C18:2 trans</i>	-	-	1,7	28,8	0,09	0,04	4,3	6,2
			0,03	4,1	0,02	0,009	1,4	3,7
<i>C18:0</i>	3,3	2,2	2,1	-	0,09	-	-	-
	0,372	0,51	0,04	-	0,02	-	-	-
<i>C20:5</i>	-	-	-	-	0,07	-	-	-
					0,01	-	-	-
<i>C20:2</i>	-	0,37	-	-	-	-	-	-
		0,08	-	-	-	-	-	-
<i>C20:1 + C20:3</i>	1,6	0,33	-	-	0,04	-	0,3	0,01
	0,182	0,07	-	-	0,01	-	0,1	0,008
<i>C20:0</i>	0,97	-	-	-	-	-	-	-
	0,11	-	-	-	-	-	-	-
<i>C22:0</i>	0,66	0,2	-	0,11	-	-	-	0,02
	0,0744	0,04	-	0,016	-	-	-	0,01
<i>C22:1</i>	-	0,4	-	-	-	-	0,4	0,01
		0,1	-	-	-	-	0,1	0,005



## 4. CONCLUSION

In this dissertation It was attempted the use of an Ionic liquid derived from sulfosuccinic acid in biodiesel production from microalgae. The synthesized dianionic ionic liquid (DAIL) proved to be more effective In catalysing the transesterification reaction, than the commercial ionic liquid (1-Ethyl-3-methylimidazolium ethyl sulfate). The highest extraction yields were obtained with pretreatment, particularly in samples using  $H_2SO_4$ , which likely promoted the extraction of additional non-lipid compounds due to its aggressive catalytic nature. However, despite higher extraction yields, the amount of FAMES in pretreated samples was lower, suggesting potential degradation of fatty acids or preferential extraction of other substances. The data also indicate that  $H_2SO_4$  is more effective in promoting the extraction and transesterification of specific FAMES, such as C18:2 trans (linoleic acid isomer), compared to DAIL (ionic liquid). The combination of  $H_2SO_4$  and DAIL showed a synergistic effect, enhancing the transesterification process. Microwave pretreatment also had an impact on FAME composition with broader range of methyl fatty acids extracted but with low concentrations, possibly due to thermal degradation. Future studies should focus on optimizing the pre-treatment and extraction procedures.

## 5. REFERENCES

1. ASTM D6751-20. (2020). *Standard Specification for Biodiesel Fuel Blend Stock (B100) for Middle Distillate Fuels*.
2. Bokhari, A., Chuah, L. F., Yusup, S., et al. (2015). Microwave-assisted methyl esters synthesis of *Kapok (Ceiba pentandra)* seed oil: parametric and optimization study. *Biofuel Research Journal*, 2(3), 281-287. DOI: 10.18331/BRJ2015.2.3.6.
3. Borowitzka, M. A., & Moheimani, N. R. (2013). Sustainable biofuels from algae. *Mitigation and Adaptation Strategies for Global Change*, 18, 13-25.
4. Canakci, M., & Van Gerpen, J. (2001). Biodiesel production from oils and fats with high free fatty acids. *Transactions of the ASAE*, 44(6), 1429-1436.
5. Chen, X., & Zhang, J. (2022). Recent advances in dicationic ionic liquids: Synthesis, properties, and applications. *Chemical Engineering Journal*, 437, 135292. <https://doi.org/10.1016/j.cej.2021.135292>.
6. Chisti, Y. (2007). Biodiesel from microalgae. *Biotechnology Advances*, 25(3), 294-306.
7. Converti, A., Casazza, A. A., Ortiz, E. Y., Perego, P., & Del Borghi, M. (2009). Effect of temperature and nitrogen concentration on the growth and lipid content of *Nannochloropsis oculata* and *Chlorella vulgaris* for biodiesel production. *Chemical Engineering and Processing: Process Intensification*, 48(6), 1146-1151. <https://doi.org/10.1016/j.cep.2009.03.006>.
8. Demirbas, A. (2009). Progress and recent trends in biodiesel fuels. *Energy Conversion and Management*, 50(1), 14-34.
9. Encinar, J. M., González, J. F., & Rodríguez-Reinares, A. (2005). Biodiesel from used frying oil. Variables affecting the yields and characteristics of the biodiesel. *Industrial & Engineering Chemistry Research*, 44(15), 5491-5499.
10. Freedman, B. E. H. P., Pryde, E. H., & Mounts, T. L. (1984). Variables affecting the yields of fatty esters from transesterified vegetable oils. *Journal of the American Oil Chemists' Society*, 61, 1638-1643.
11. Gaide, I., Makareviciene, V., & Sendzikiene, E. (2022). Effectiveness of eggshells as natural heterogeneous catalysts for transesterification of rapeseed oil with methanol. *Catalysts*, 12(3), 246. <https://doi.org/10.3390/catal12030246>.

12. Goering, C. E., Schwab, A. W., Daugherty, M. J., Pryde, E. H., & Heakin, A. J. (1982). Fuel properties of eleven vegetable oils. *Transactions of the ASAE*, 25(6), 1472-1483.
13. Gouveia, L., & Oliveira, A. C. (2009). Microalgae as a raw material for biofuels production. *Journal of Industrial Microbiology and Biotechnology*, 36(2), 269-274. <https://doi.org/10.1007/s10295-008-0495-6>.
14. Griffiths, M. J., & Harrison, S. T. L. (2009). Lipid productivity as a key characteristic for choosing algal species for biodiesel production. *Journal of Applied Phycology*, 21(5), 493-507. <https://doi.org/10.1007/s10811-008-9392-7>.
15. Hu, S., Luo, X., Wan, C., & Li, Y. (2012). Characterization of crude glycerol from biodiesel plants. *Journal of Agricultural and Food Chemistry*, 60(23), 5915-5921.
16. Kaieda, M., Samukawa, T., Kondo, A., & Fukuda, H. (2001). Effect of methanol and water contents on production of biodiesel fuel from plant oil catalyzed by various lipases in a solvent-free system. *Journal of Bioscience and Bioengineering*, 91(1), 12-15.
17. Knothe, G. (2001). Historical perspectives on vegetable oil-based diesel fuels. *Inform*, 12(11), 1103-1107.
18. Knothe, G. (2005). *The biodiesel handbook*.
19. Knothe, G. (2005). Dependence of biodiesel fuel properties on the structure of fatty acid alkyl esters. *Fuel Processing Technology*, 86(10), 1059-1070.
20. Leung, D. Y., Wu, X., & Leung, M. K. H. (2010). A review on biodiesel production using catalyzed transesterification. *Applied Energy*, 87(4), 1083-1095.
21. Liu, C. F., Sun, R. C., Zhang, A. P., Ren, J. L., Wang, X. A., Qin, M. H., Chao, Z. N., & Luo, W. (2007). Homogeneous modification of sugarcane bagasse cellulose with succinic anhydride using an ionic liquid as reaction medium. *Carbohydrate Research*, 342(7), 919-926. <https://doi.org/10.1016/j.carres.2007.02.006>.
22. Liu, S., Yang, Z., Zhang, J., Wang, Q., & Zhang, X. (2022). Recent advances in supported acid/base ionic liquids as catalysts for biodiesel production. *Frontiers in Bioengineering and Biotechnology*, 10, 915055. doi:10.3389/fbioe.2022.915055.
23. Lotero, E., Liu, Y., Lopez, D. E., Suwannakarn, K., Bruce, D. A., & Goodwin, J. G. (2005). Synthesis of biodiesel via acid catalysis. *Industrial & Engineering Chemistry Research*, 44(14), 5353-5363.
24. Ma, F., & Hanna, M. A. (1999). Biodiesel production: a review. *Bioresource Technology*, 70(1), 1-15.

25. Mata, T. M., Martins, A. A., & Caetano, N. S. (2010). Microalgae for biodiesel production and other applications: a review. *Renewable and Sustainable Energy Reviews*, 14(1), 217-232. DOI: 10.1016/j.rser.2009.07.020.
26. Meher, L. C., Dharmagadda, V. S., & Naik, S. N. (2006). Optimization of alkali-catalyzed transesterification of *Pongamia pinnata* oil for production of biodiesel. *Bioresource Technology*, 97(12), 1392-1397.
27. Moser, B. R. (2009). Biodiesel production, properties, and feedstocks. *In Vitro Cellular & Developmental Biology - Plant*, 45(3), 229-266.
28. Nascimento, R. F. do, Lima, A. C. A. de, Barbosa, P. G. A., & Silva, V. P. A. da. (2018). *Cromatografia gasosa: aspectos teóricos e práticos*. Fortaleza: Imprensa Universitária. Disponível em: <http://repositorio.ufc.br/handle/riufc/39260>.
29. Nouredini, H., & Zhu, D. (1997). Kinetics of transesterification of soybean oil. *Journal of the American Oil Chemists' Society*, 74, 1457-1463.
30. Oklahoma State University. (2020). *Biodiesel Glossary*. Oklahoma State University Extension Service. Disponível em: <https://extension.okstate.edu>.
31. Ramos, M. J., Fernández, C. M., Casas, A., Rodríguez, L., & Pérez, Á. (2009). Influence of fatty acid composition of raw materials on biodiesel properties. *Bioresource Technology*, 100(1), 261-268. <http://dx.doi.org/10.1016/j.biortech.2008.06.039>.
32. Rezende, M. J. C., et al. (2021). Biodiesel: an overview II. *Journal of the Brazilian Chemical Society*, 32, 1301-1344.
33. Rodolfi, L., Zittelli, G. C., Bassi, N., Padovani, G., Biondi, N., Bonini, G., & Tredici, M. R. (2009). Microalgae for oil: Strain selection, induction of lipid synthesis and outdoor mass cultivation in a low-cost photobioreactor. *Biotechnology and Bioengineering*, 102(1), 100-112. <https://doi.org/10.1002/bit.22033>.
34. Takagi, M., Watanabe, K., Yamaberi, K., & Yoshida, T. (2000). Limited feeding of potassium nitrate for intracellular lipid and triglyceride accumulation of *Nannochloris sp.* UTEX LB1999. *Applied Microbiology and Biotechnology*, 54(1), 112-117. doi: 10.1007/s002530000333.
35. Yu, D., Wang, C., Yin, Y., Zhang, A., Gao, G., & Fang, X. (2011). A synergistic effect of microwave irradiation and ionic liquids on enzyme-catalyzed biodiesel production. *Green Chemistry*, 13, 1869-1875. DOI: 10.1039/C1GC15114B
36. Suska-Malawska, M., Kot, M., Gręzak, A., Mętrak, M., Muhiddin, K., & Szymczak, K. (2022). Potential impact of Holocene climate changes on camel breeding practices of

Neolithic pastoralists in the Central Asian drylands: A preliminary assessment. *The Holocene*, 32(12), 095968362211142. <https://doi.org/10.1177/09596836221114289>

## 6. ANEXES

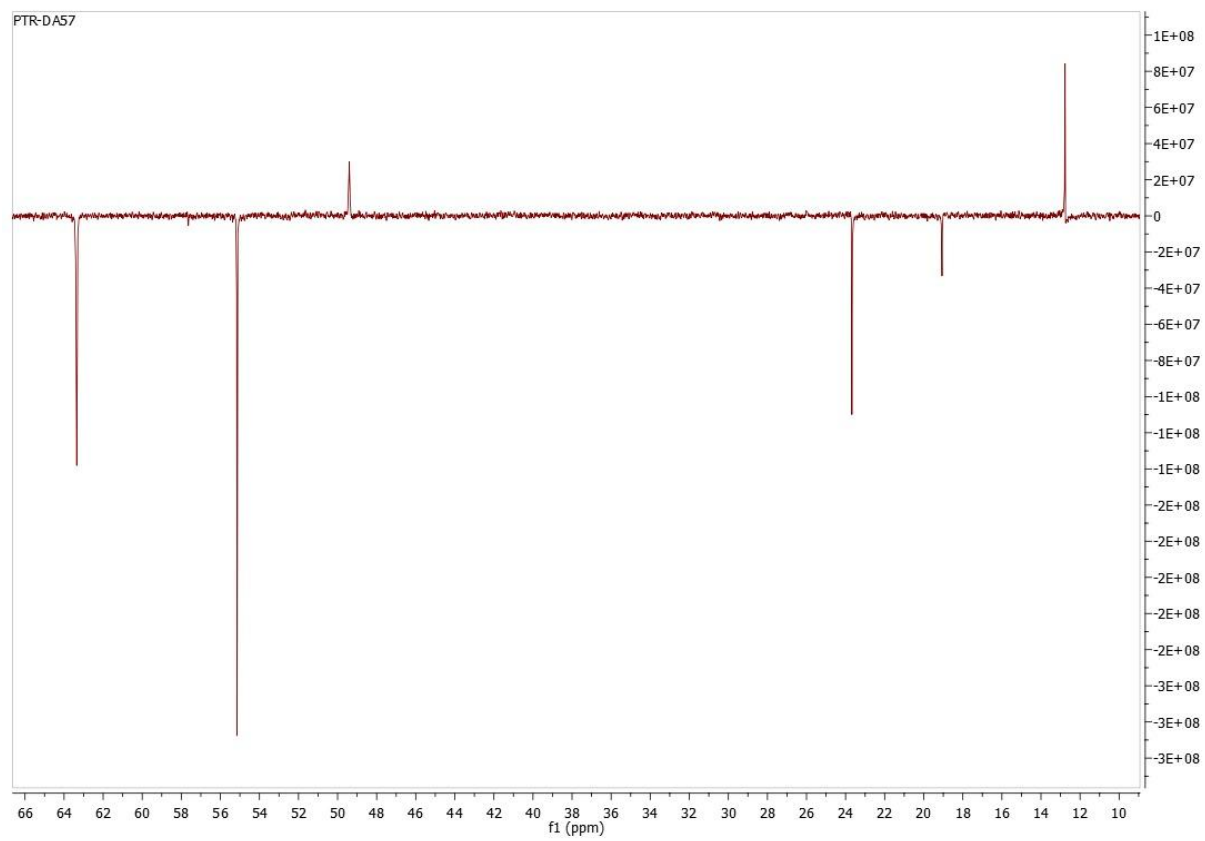


Figure 25 -  $^{13}\text{C}$  APT of IL precursor.

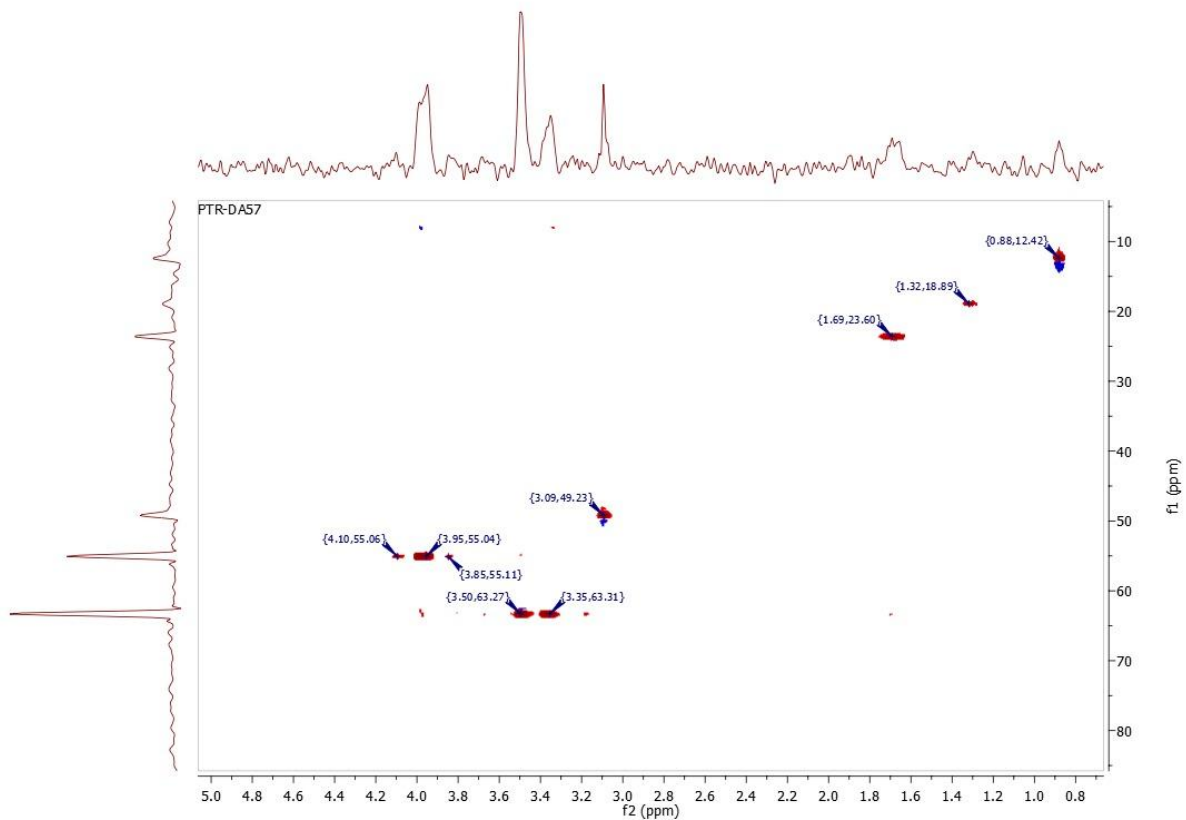


Figure 26 -  $^1\text{H}$   $^{13}\text{C}$  HSQC of IL precursor.

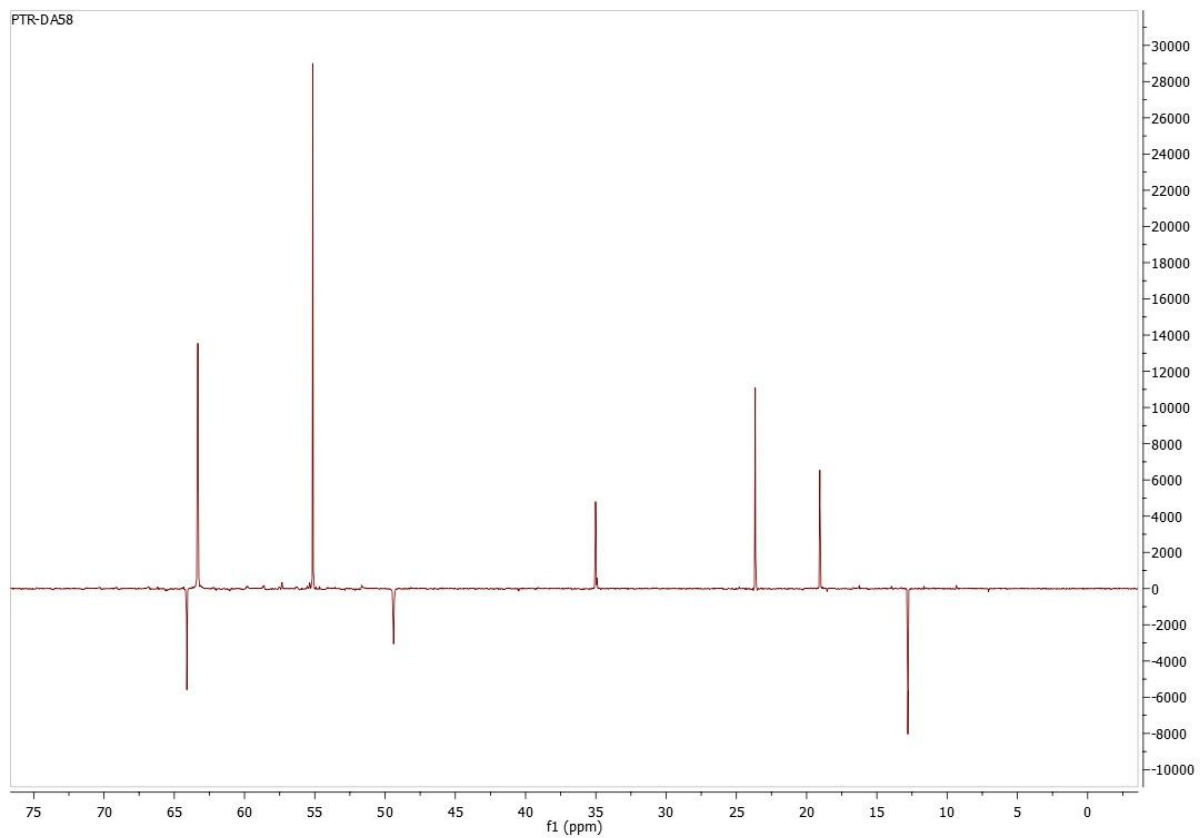


Figure 27 -  $^{13}\text{C}$  APT of DAIL.

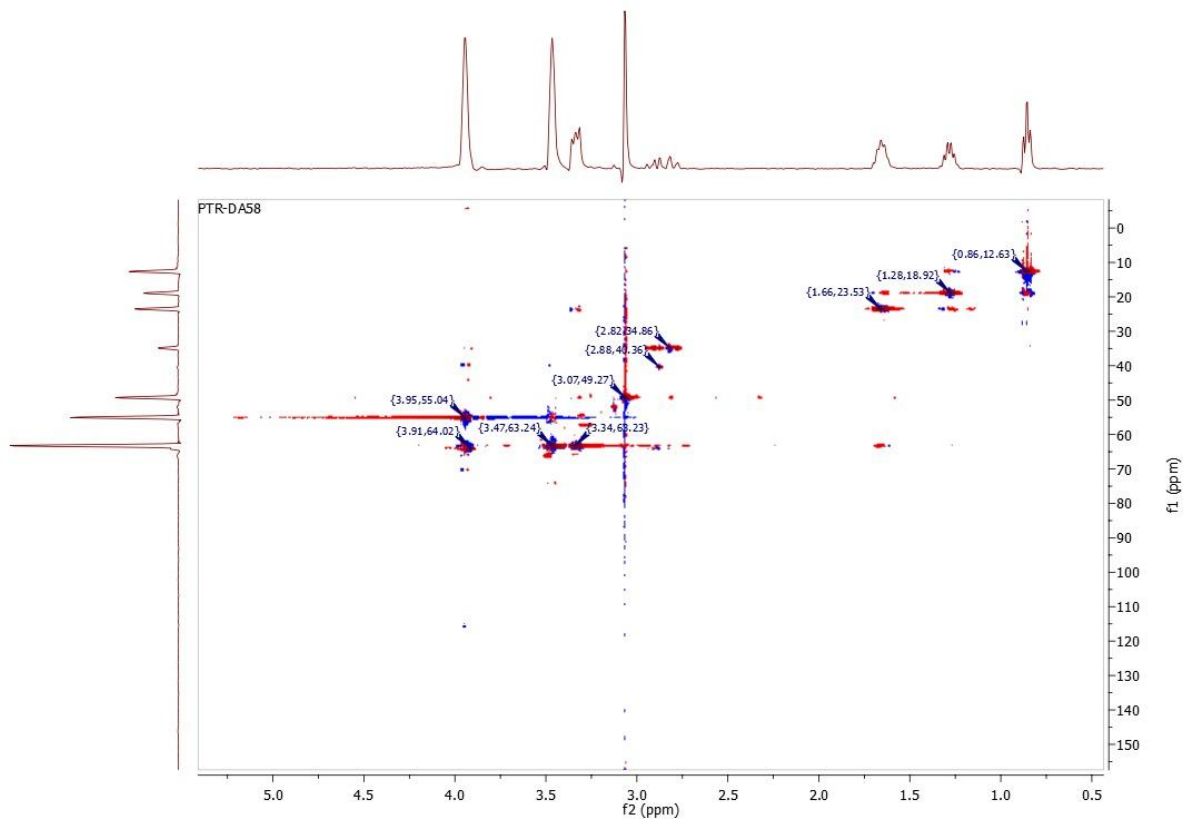


Figure 28-  $^1\text{H}$   $^{13}\text{C}$  HSQC of DAIL.

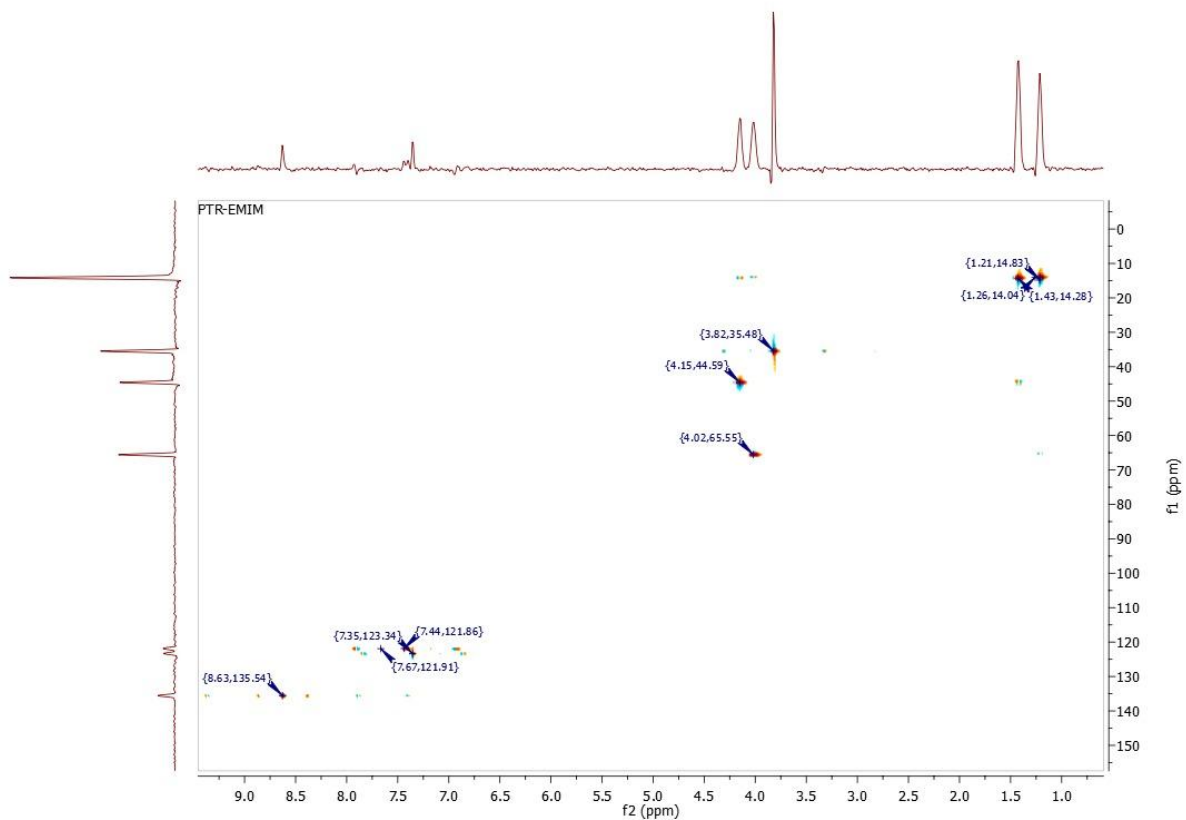


Figure 29 -  $^1\text{H}$   $^{13}\text{C}$  HSQC of EMIM.

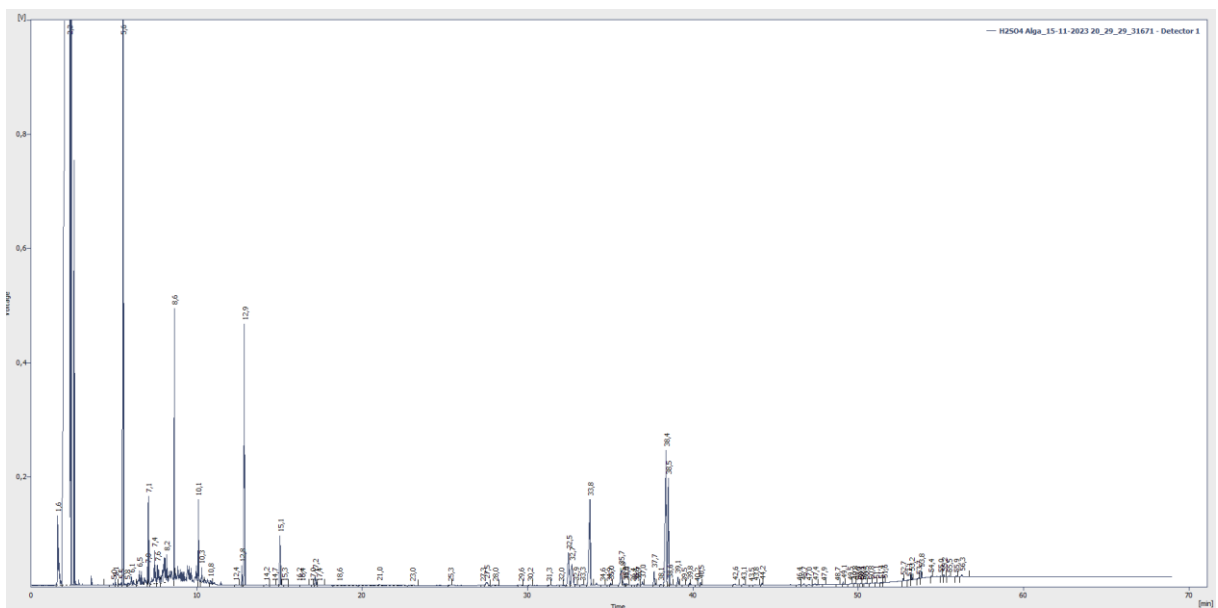
Below are the chromatograms of sample A4.



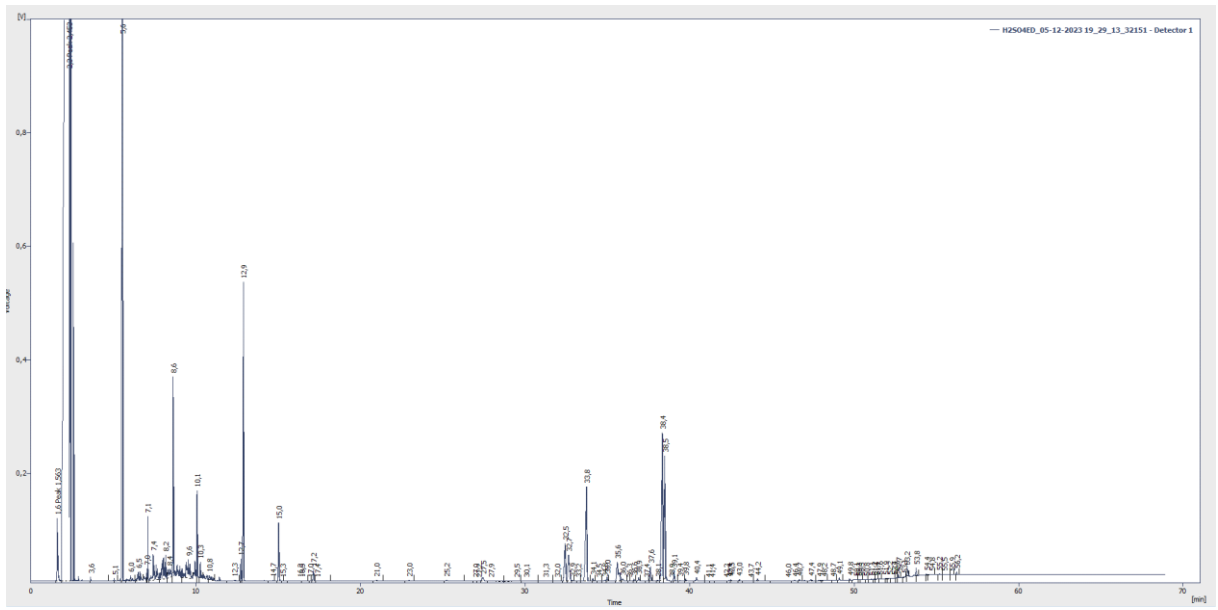
Below are the chromatograms of sample A5.



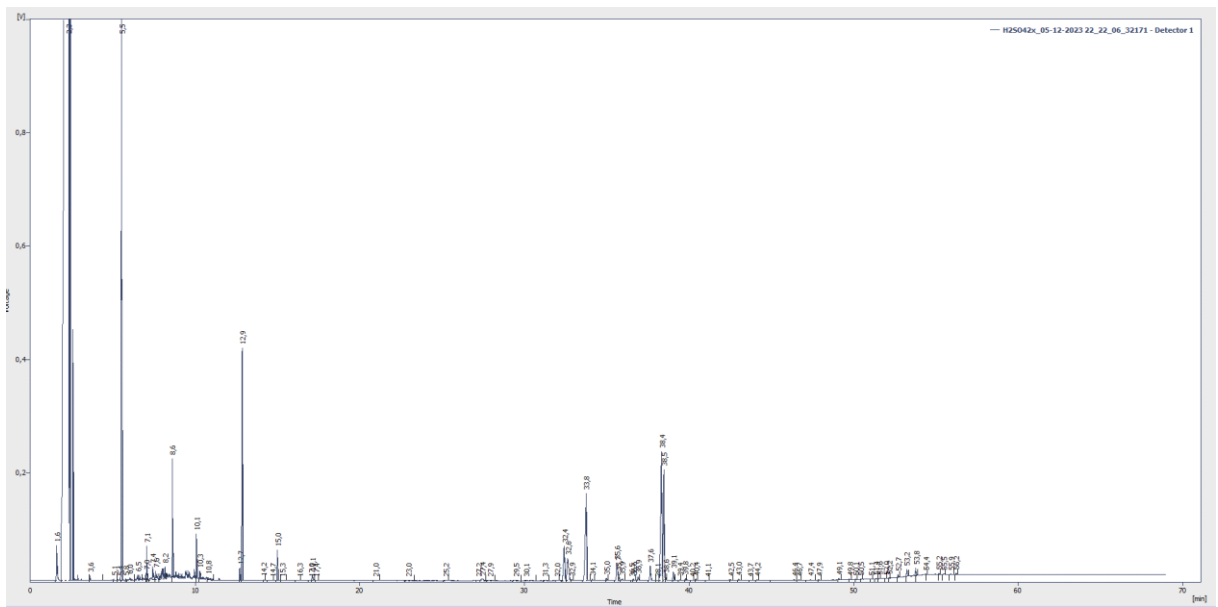
Below are the chromatograms of sample B1.



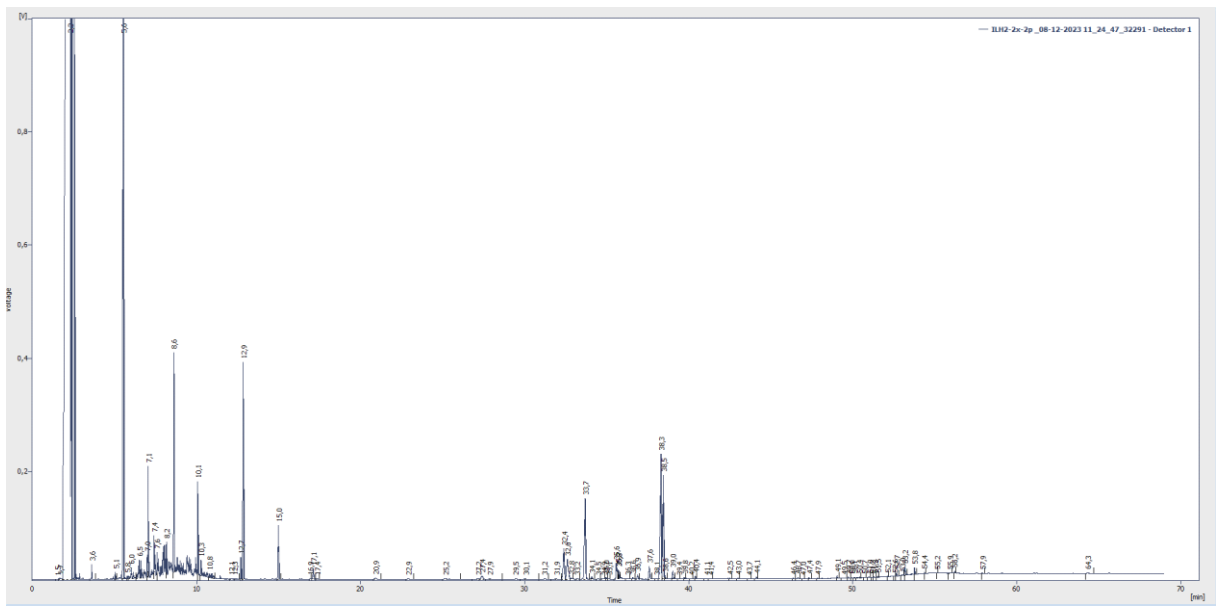
Below are the chromatograms of sample B2.



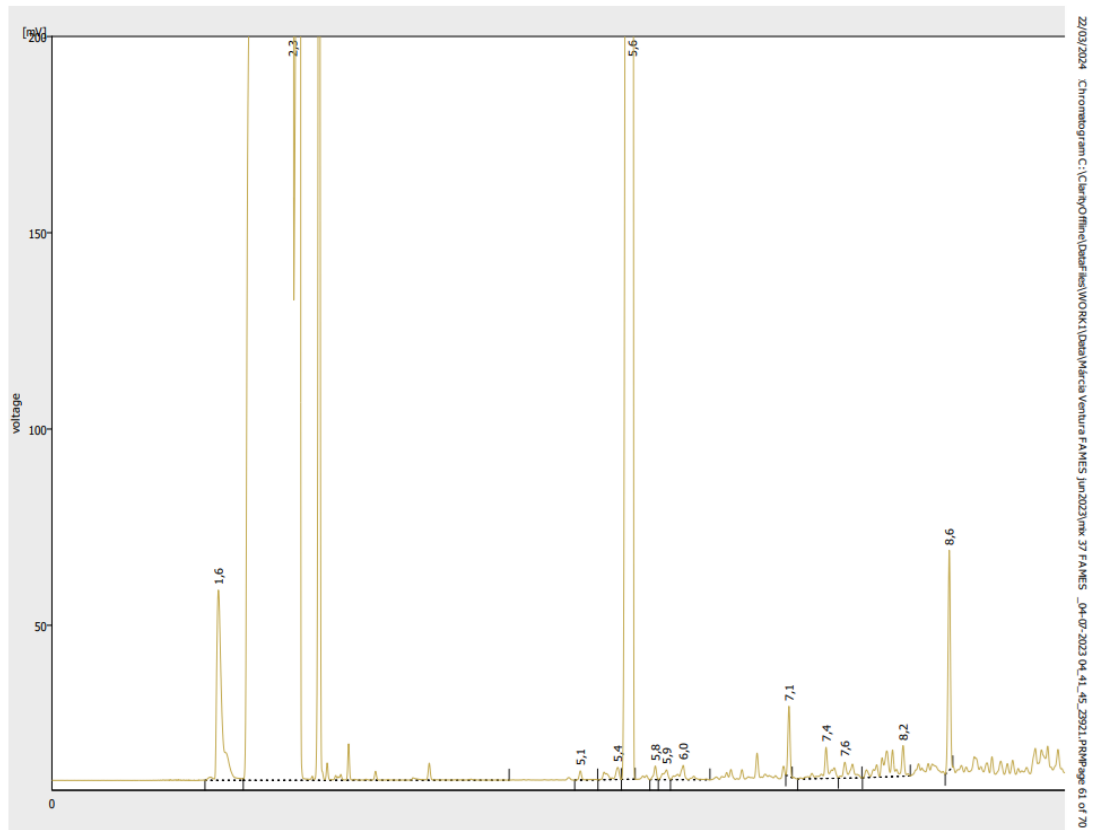
Below are the chromatograms of sample B3.

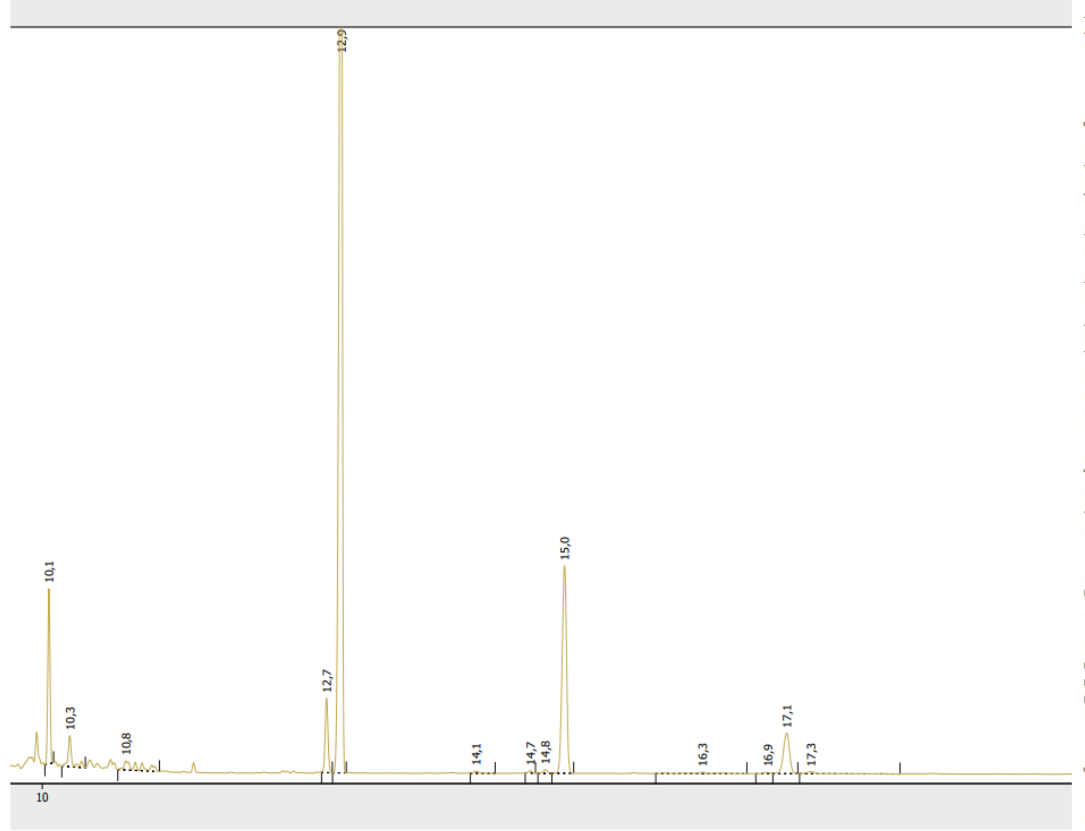


Below are the chromatograms of sample B4.

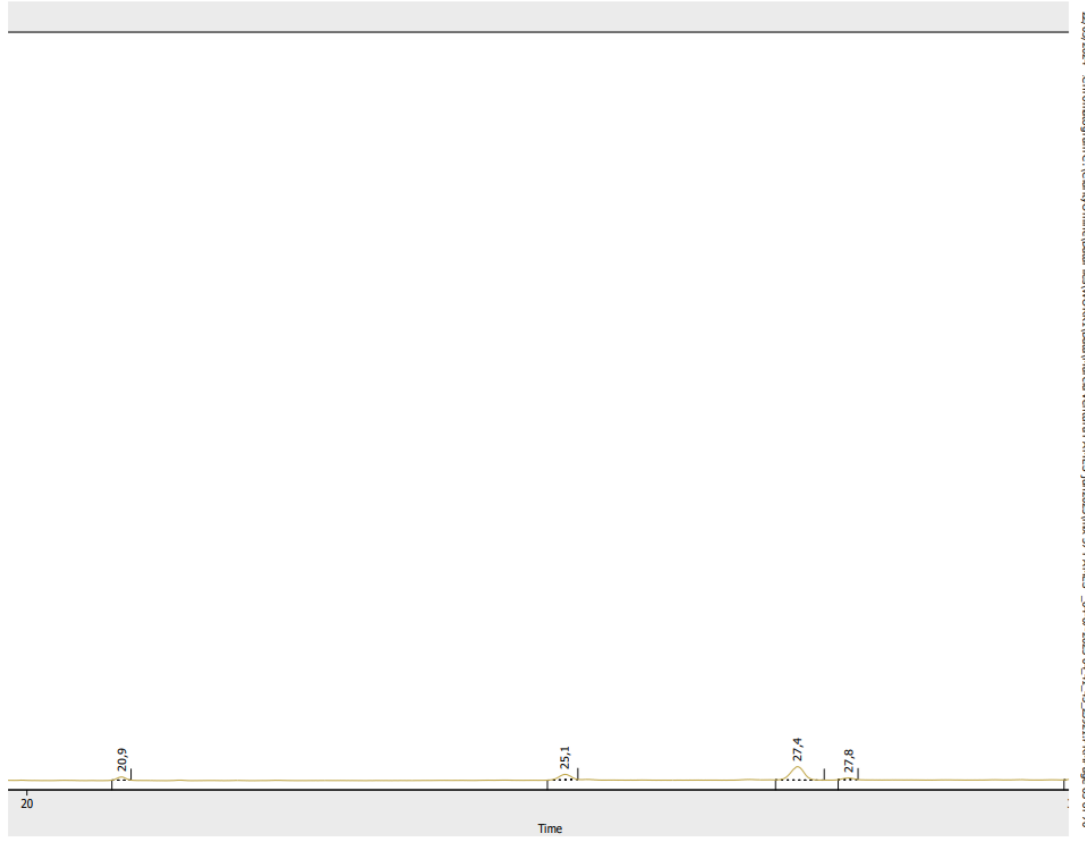


Below are the chromatograms of sample B5.

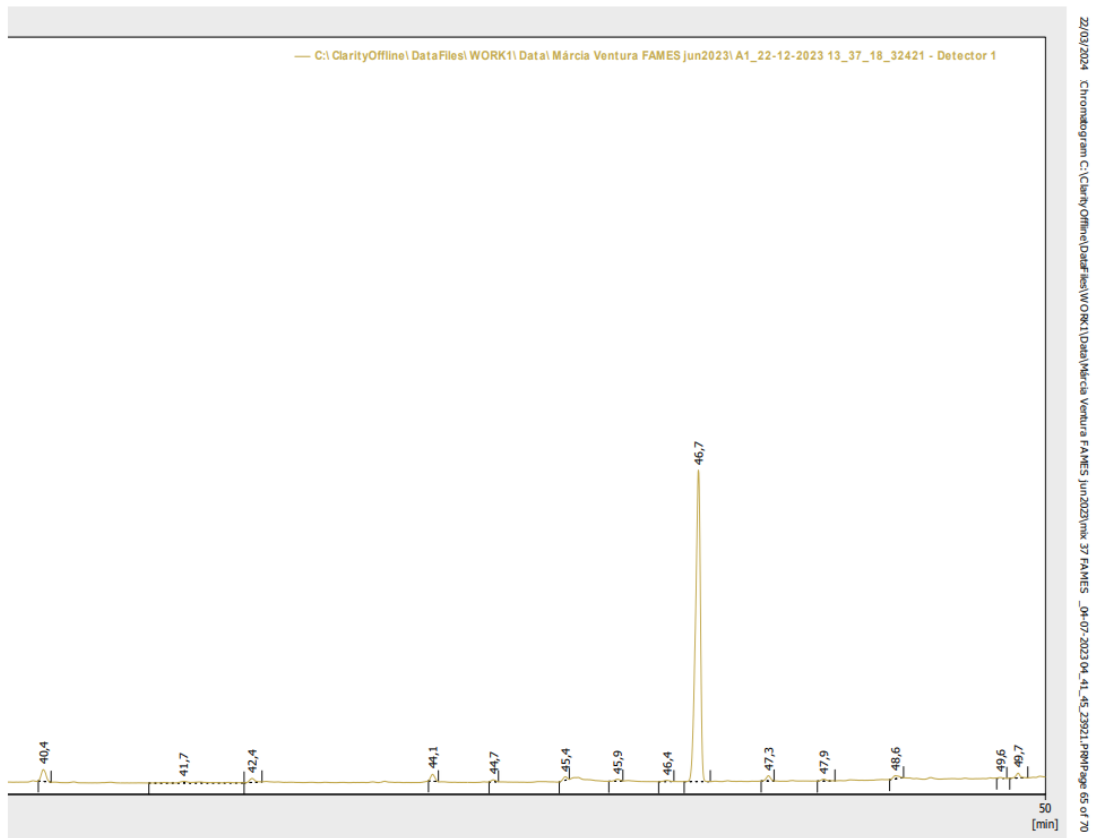
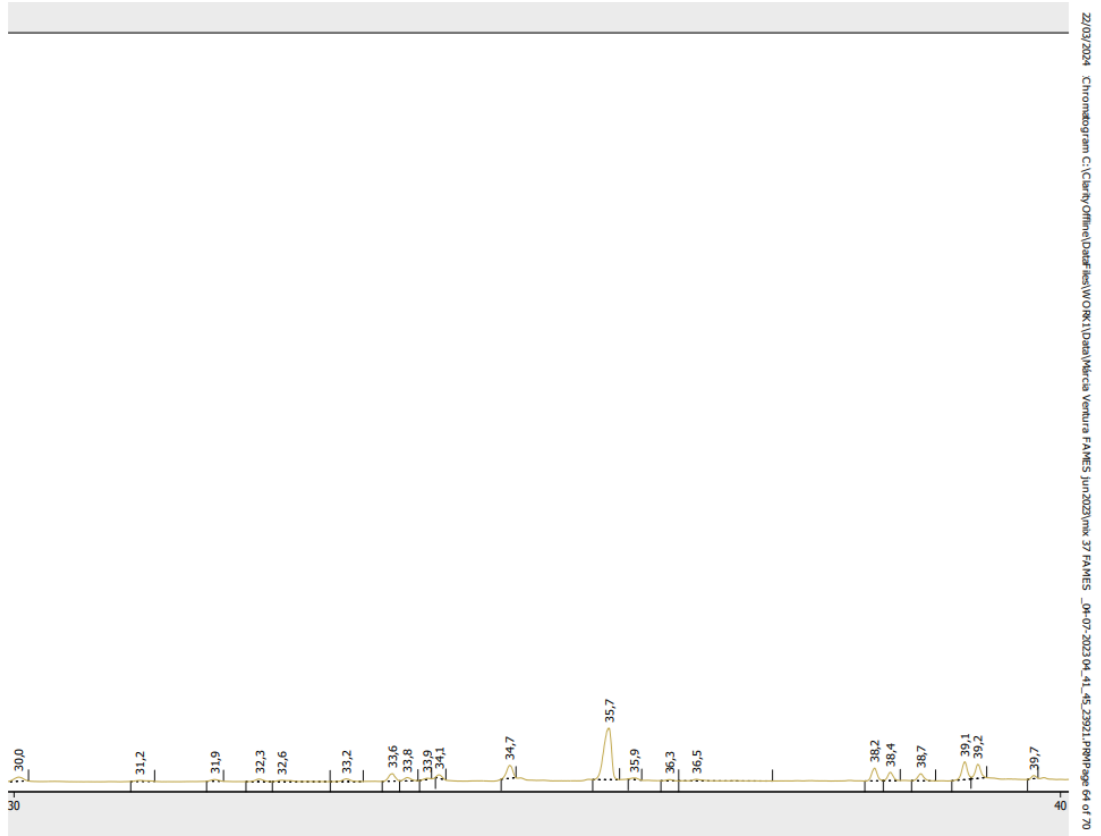




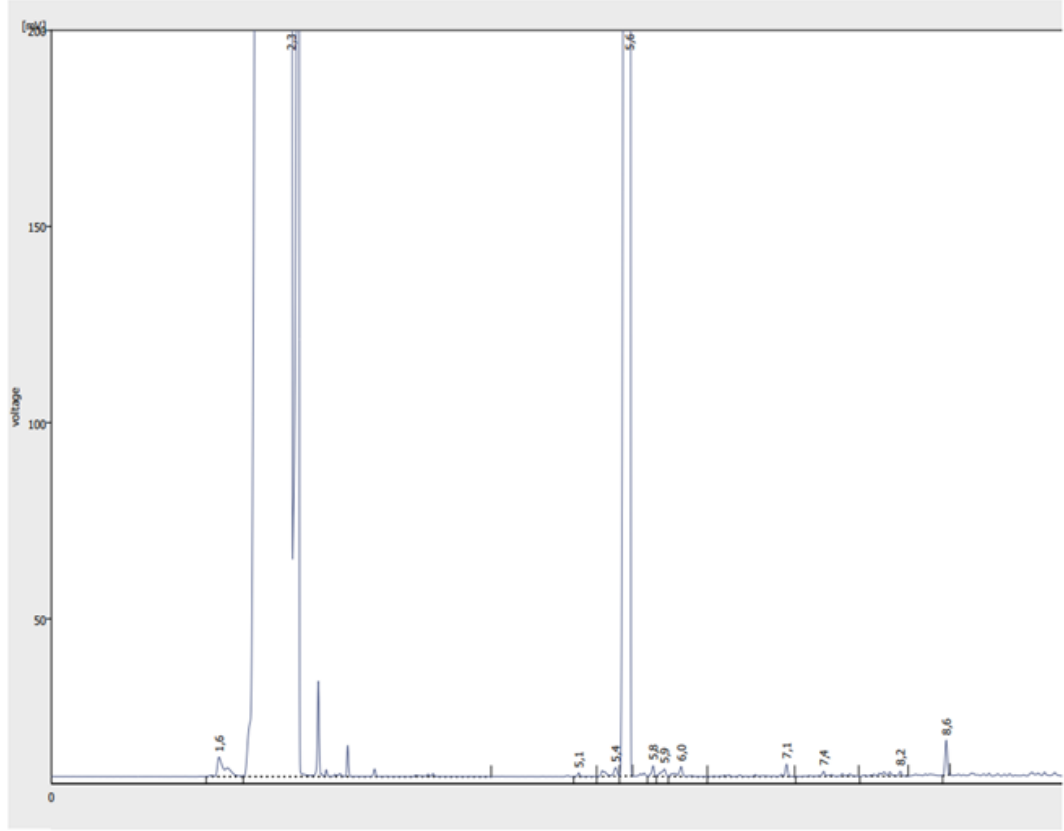
22/03/2024 Chromatogram C:\ChemOffice\DatFiles\WORK1\Data\Marcia Ventura FAMES Jun2023\mk\_37 FAMES \_04-07-2023 04\_41\_45\_2921.PRP Page 62 of 70

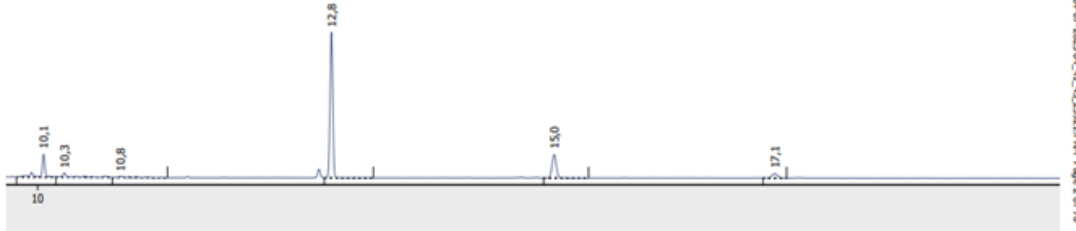


22/03/2024 Chromatogram C:\ChemOffice\DatFiles\WORK1\Data\Marcia Ventura FAMES Jun2023\mk\_37 FAMES \_04-07-2023 04\_41\_45\_2921.PRP Page 63 of 70



Below are the chromatograms of sample B6.

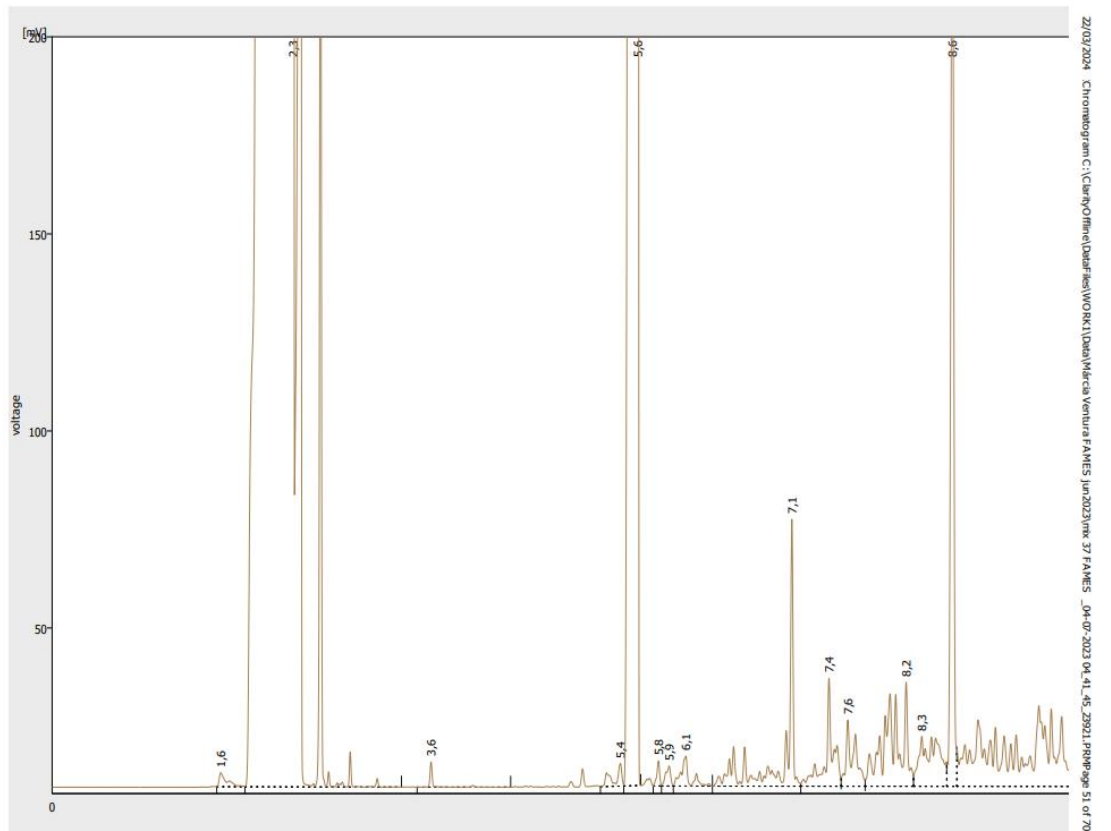


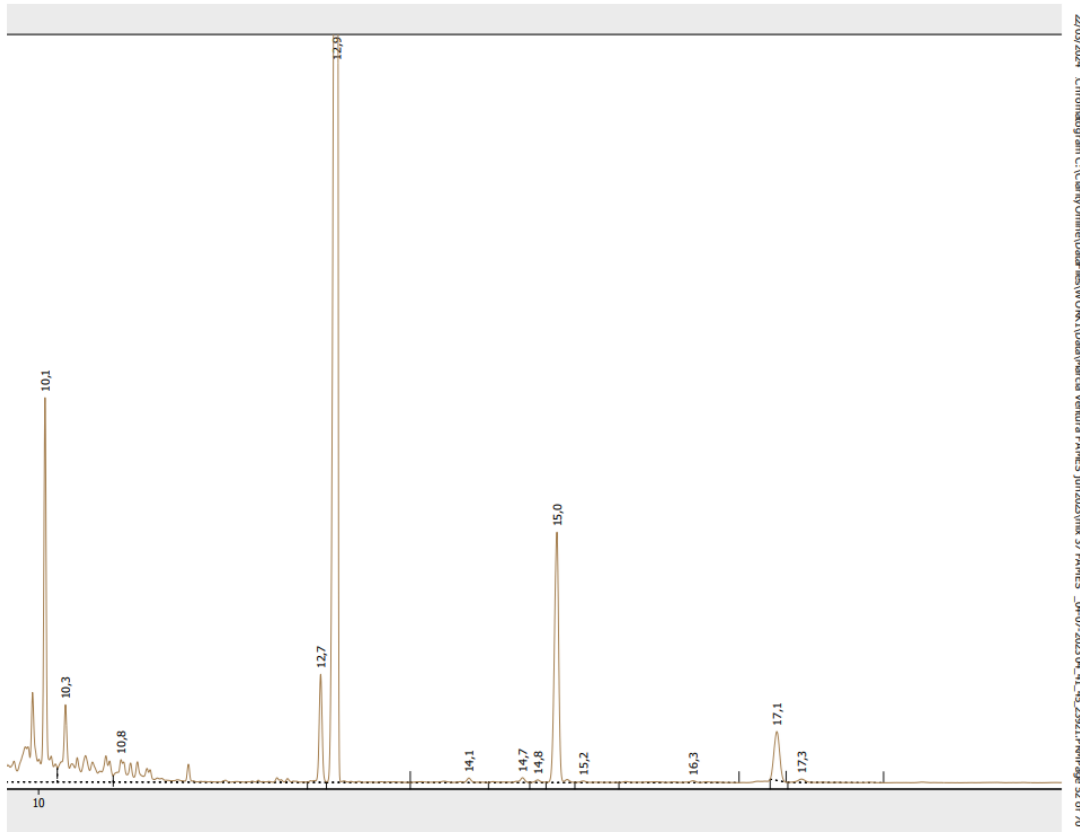




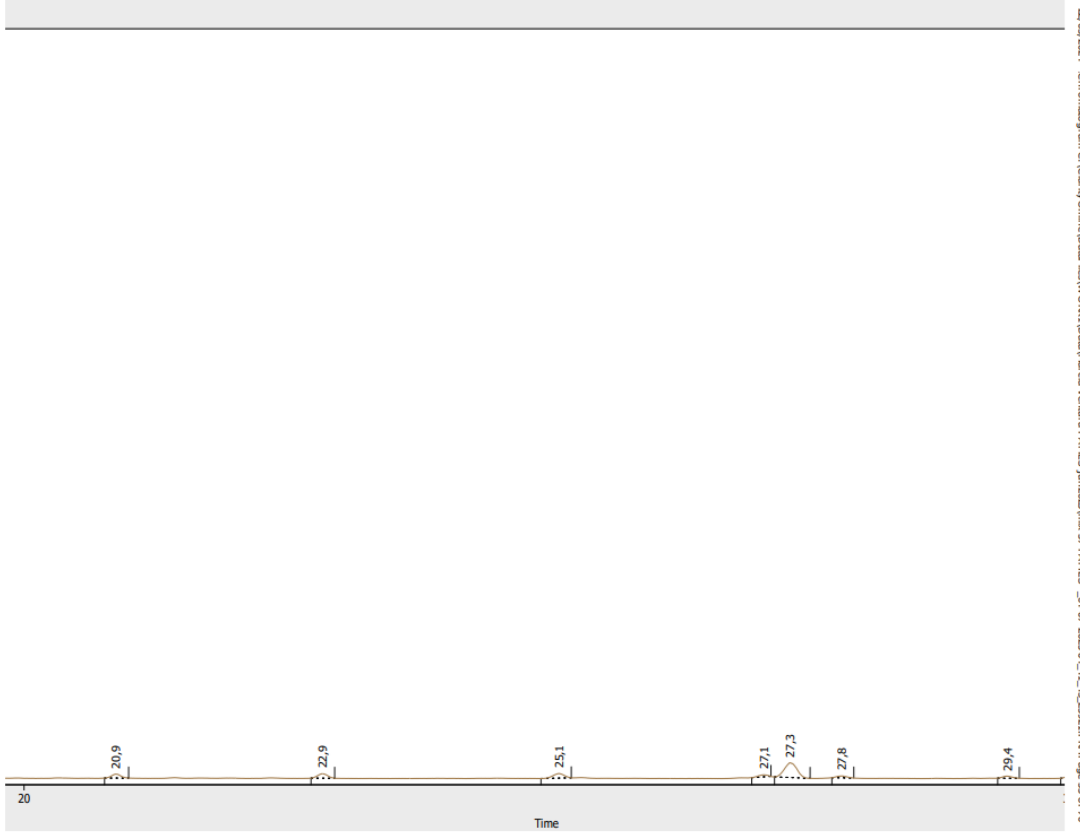


Below are the chromatograms of sample B7.

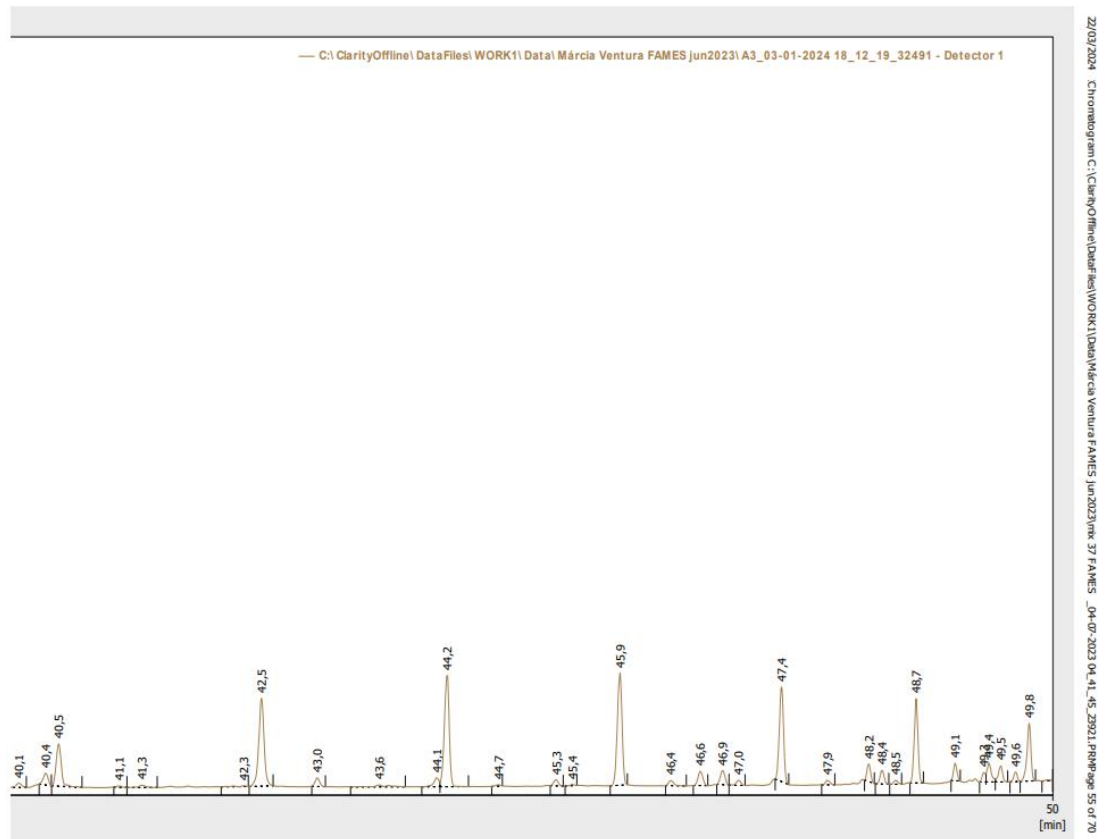
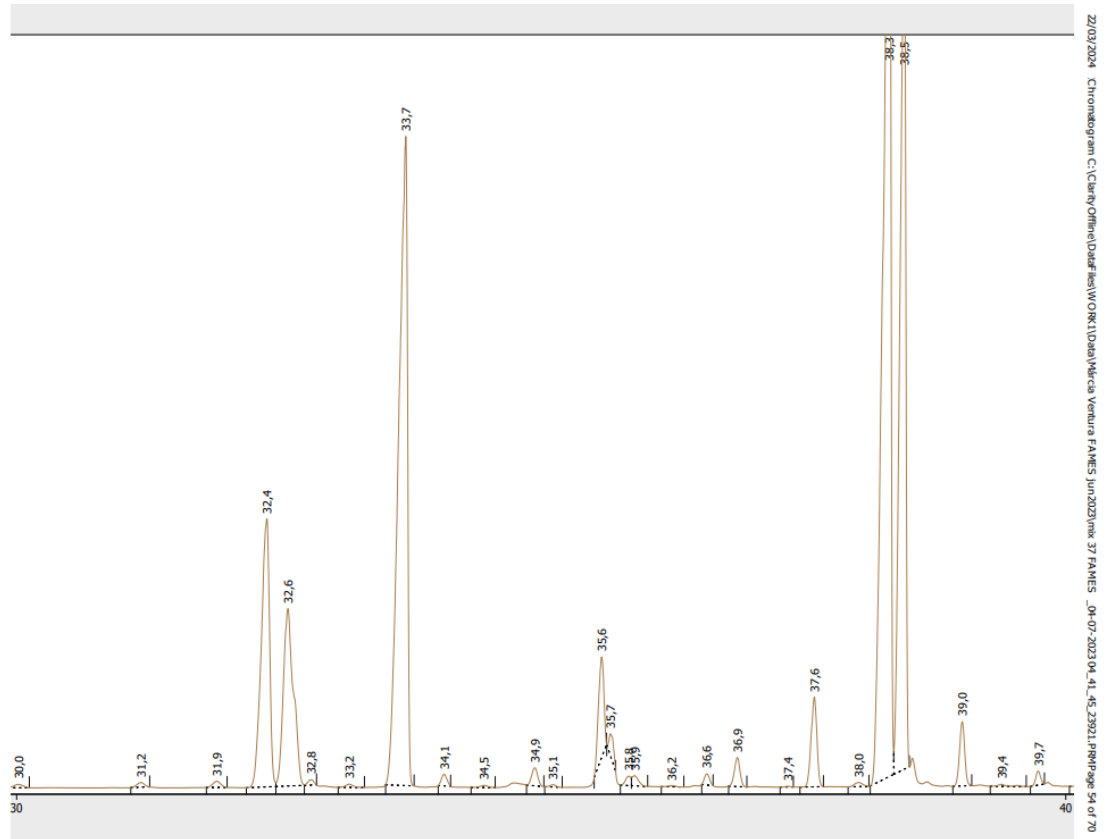




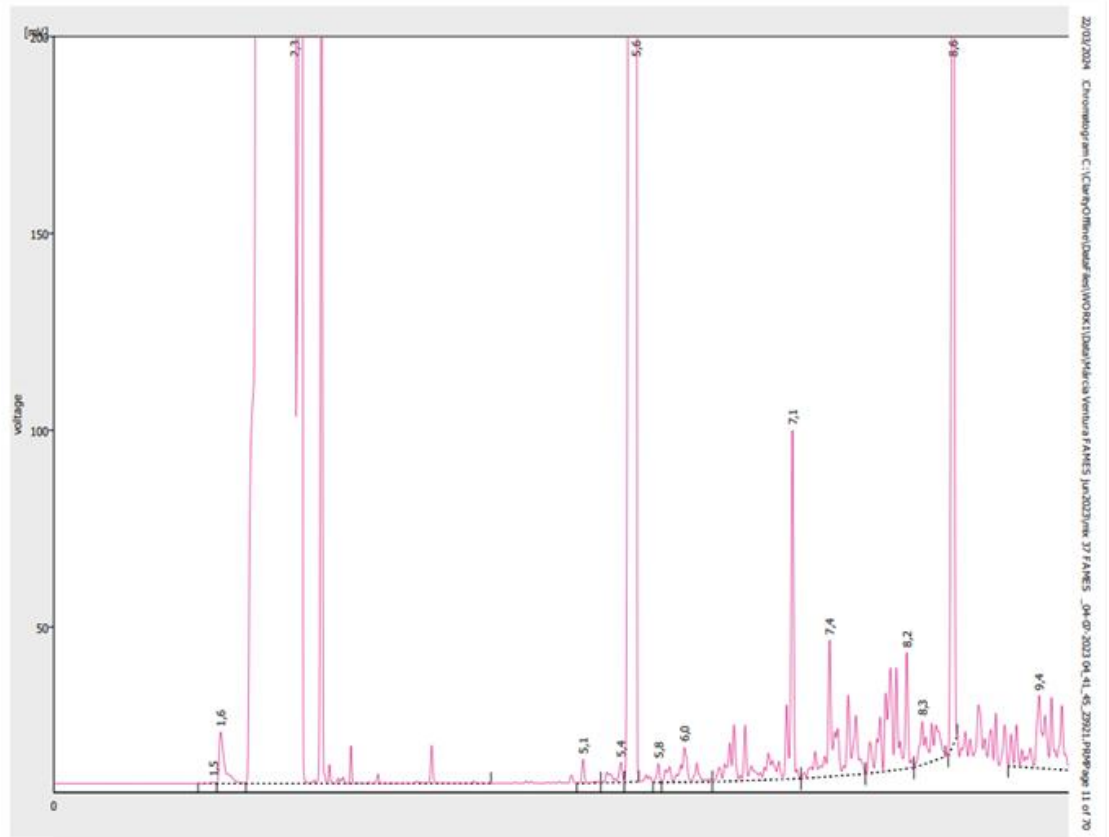
22/03/2024 Chromatogram C:\Client\Offline\Daftar\tes\WORK\1\Daftar\Miscia Ventura FAMES Jun2023\mk\_37 FAMES \_04-07-2023 04\_41\_45\_23921.PRP\Page 52 of 70

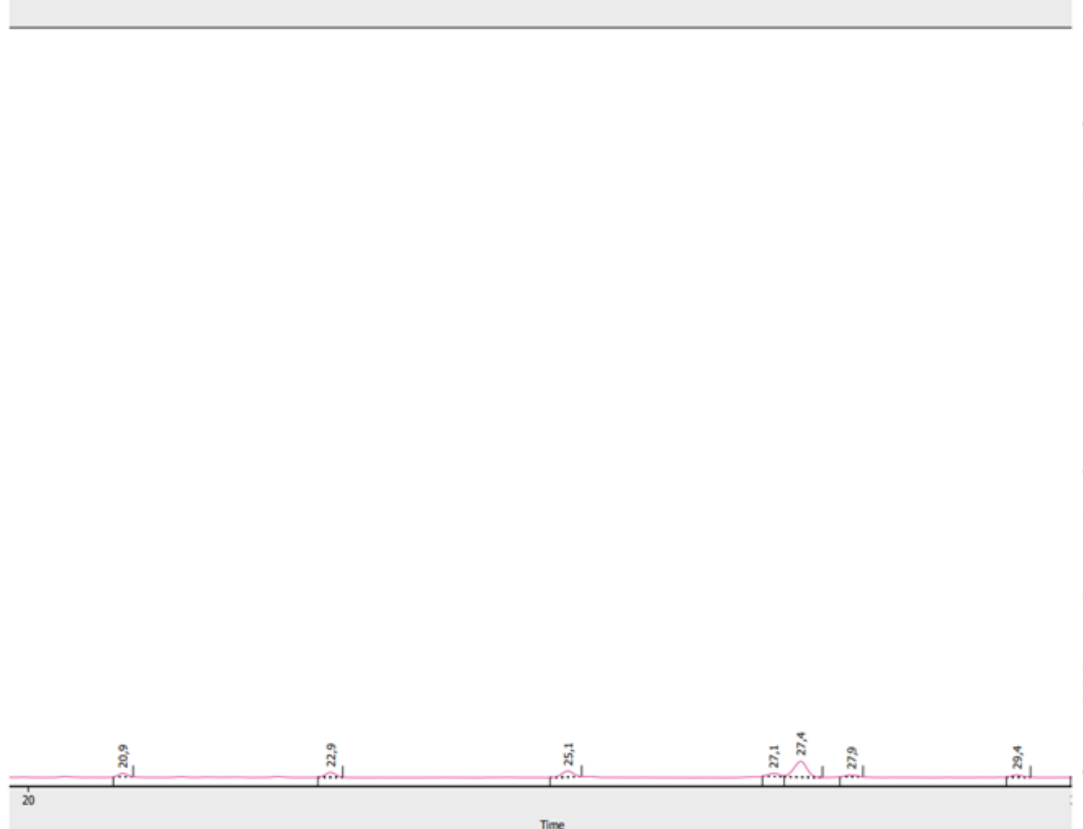
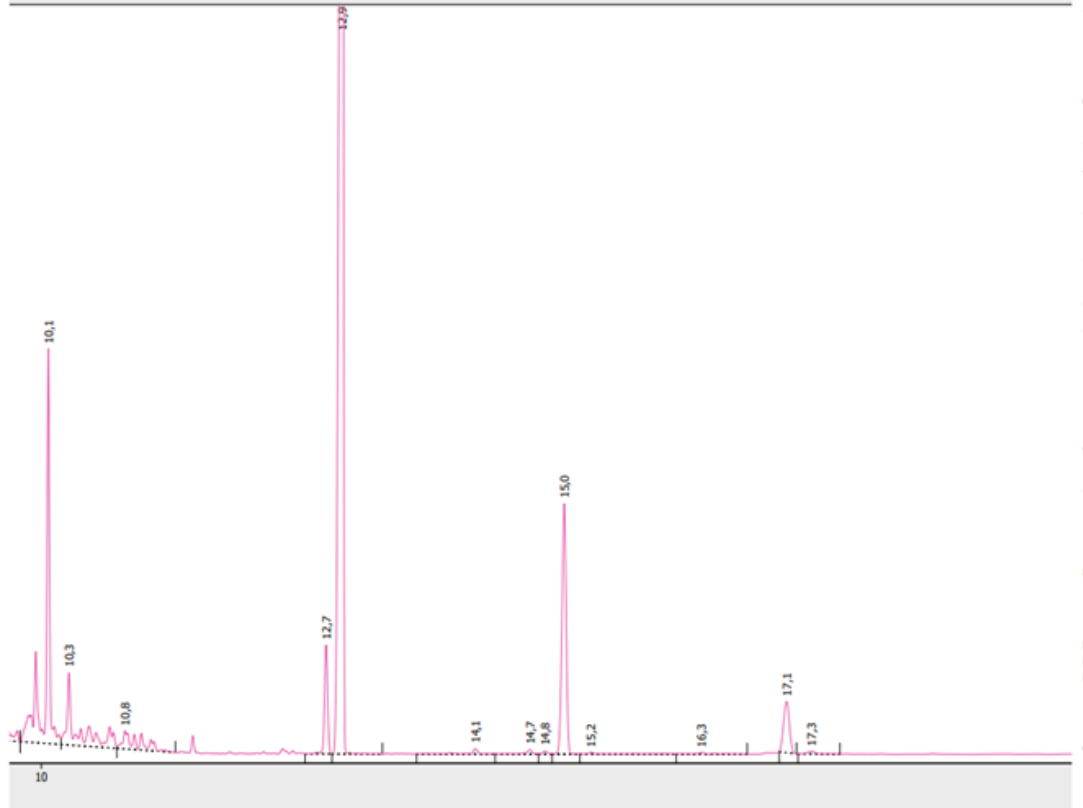


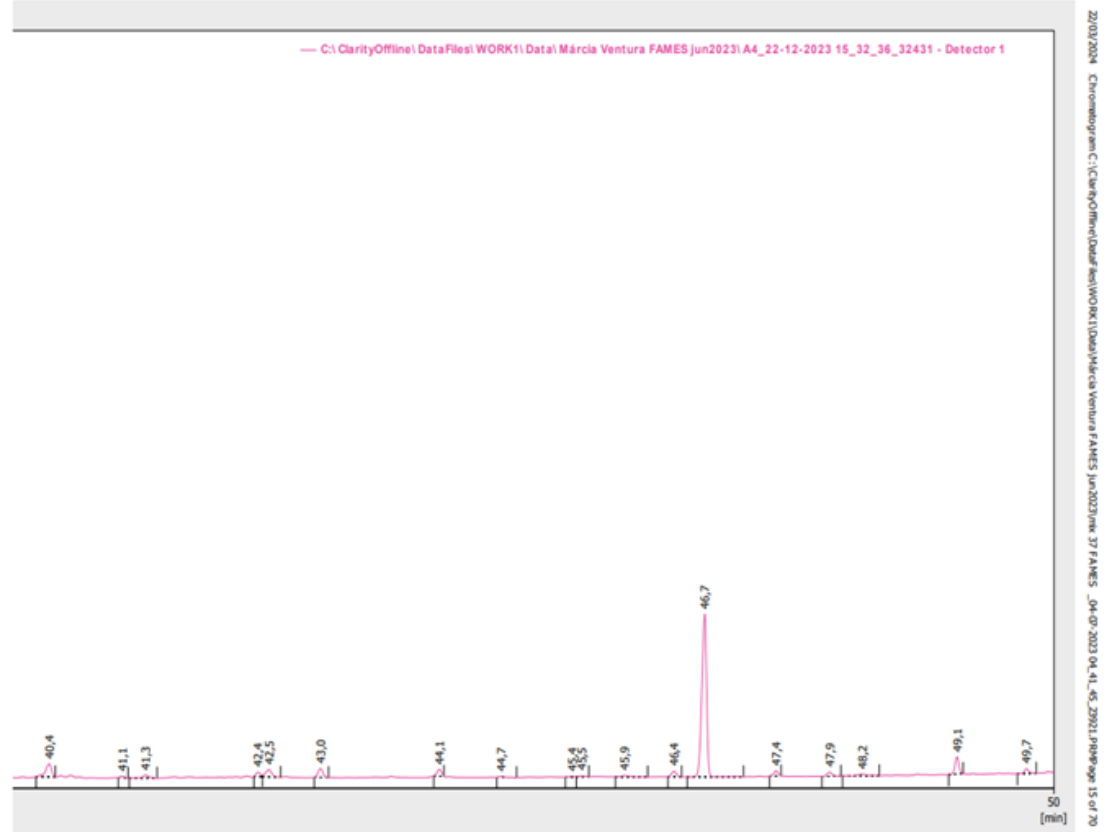
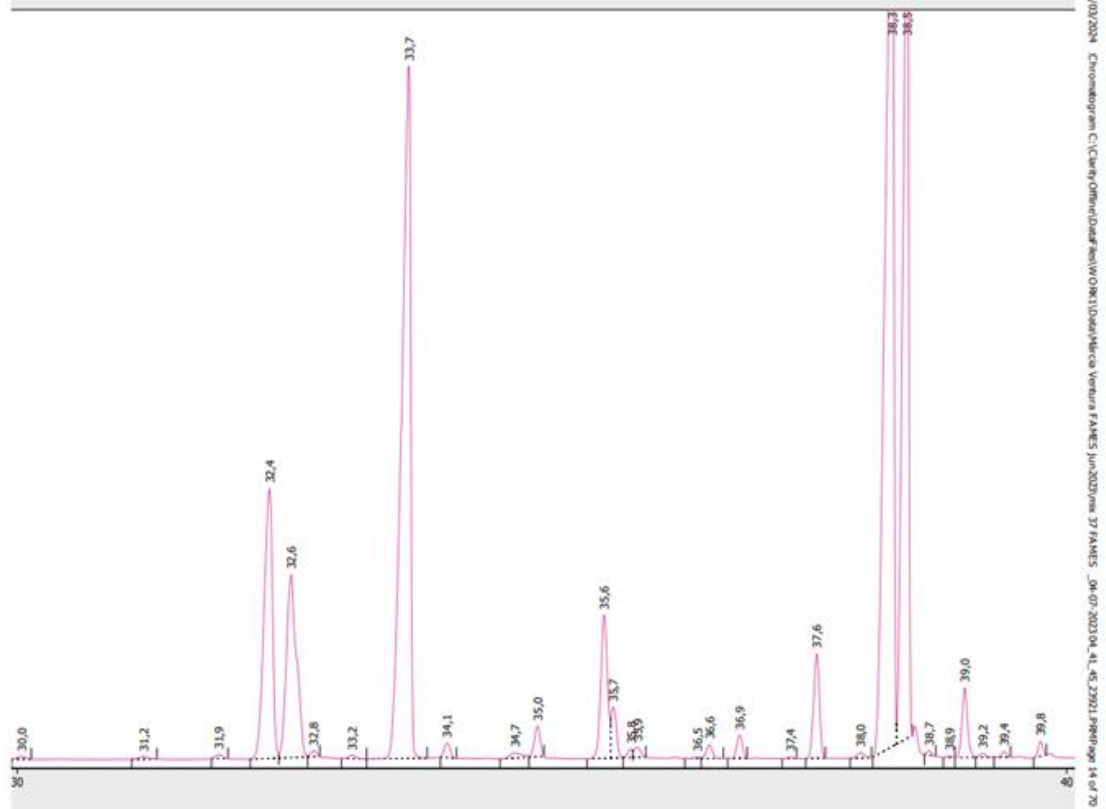
22/03/2024 Chromatogram C:\Client\Offline\Daftar\tes\WORK\1\Daftar\Miscia Ventura FAMES Jun2023\mk\_37 FAMES \_04-07-2023 04\_41\_45\_23921.PRP\Page 53 of 70



Below are the chromatograms of sample B8.























2024

Tiago Martins Rodrigues

Ionic Liquids Assisted Direct Transesterification of Microalgae for Biodiesel